

2023-07

Pushing for Gold On Force Application in Bobsleigh and Cycling

Onasch, Franziska Maren

Onasch, F. M. (2023). Pushing for gold on force application in bobsleigh and cycling (Doctoral thesis, University of Calgary, Calgary, Canada). Retrieved from <https://prism.ucalgary.ca>.
<https://hdl.handle.net/1880/116822>

Downloaded from PRISM Repository, University of Calgary

UNIVERSITY OF CALGARY

Pushing for Gold

On Force Application in Bobsleigh and Cycling

by

Franziska Maren Onasch

A THESIS

SUBMITTED TO THE FACULTY OF GRADUATE STUDIES

IN PARTIAL FULFILMENT OF THE REQUIREMENTS FOR THE

DEGREE OF DOCTOR OF PHILOSOPHY

GRADUATE PROGRAM IN KINESIOLOGY

CALGARY, ALBERTA

JULY, 2023

© Franziska Maren Onasch 2023

Abstract

In many sports, performance is governed by an athlete's ability to produce force paired with a given movement velocity and, thereby, generate power. The 4-man bobsled push start is an event that requires team effort, and its goal is to maximize sled velocity in the shortest possible time. Fractions of a second can decide the outcome of a race, and off-ice tests designed to assess strength and speed are used to identify the athletes that will perform best. However, the actual contributions of the team members during the push start on ice have not been measured. The objective of the first project in this thesis was to better understand the push contributions of the four athletes in a 4-man team by analyzing the components of the push start. A 4-man bobsled was instrumented to record both sled velocity and 2D push forces as applied to the sled by the athletes during the push start. Push force was observed to decrease quickly once the sled picked up speed, and the execution of the loading was discovered to be a crucial component of the push start that can affect overall performance. In project 2, a prowler sled was instrumented to measure sled velocity and push force in an off-ice push force-velocity test to be used as a training and assessment tool in bobsleigh athletes. Greater force results in greater power output – if the force is applied the right way. In project 3 we studied force effectiveness in cycling, where only pedal force directed perpendicular to the crank is effective i.e., results in propulsion, while forces parallel to the crank have been considered wasted. In our study, we aimed to determine the impact of constrained pedal force direction on force output. Constraining static pedal force to be perpendicular to the crank only was counterproductive and resulted in significantly reduced force magnitude. In summary, this thesis work contributes to the applied study of power output in sports, with instrumented devices aiding the study of force and power output in athletes, novel data, and the proposal for a new training method.

Preface

Chapters 3.1, Chapter 4, Chapter 5 and Chapter 6 are based on scientific manuscripts that are in preparation, under review, or have been published.

Chapter 3.1 is based on:

Onasch, F., Sawatsky, A., Stano, A. & Herzog, W. (2023). Development of the Instrumentation of a 4-man Bobsled. *Journal of Biomechanics* 152, 111578. DOI: 10.1016/j.jbiomech.2023.111578

Statement of contribution: FO, ASa, and ASt developed the methodology. ASa and ASt developed/provided the instrumentation (hardware). FO performed the analysis and wrote the manuscript with input from all co-authors. FO and WH acquired funding for the project. WH supervised the project and provided critical feedback.

Chapter 4 is based on:

Onasch, F., Sawatsky, A. & Herzog, W., Functional Sled Push Force-Velocity Profiling for Bobsled Athletes; Like Taking Snow to Canada, or a Pit Stop on the Way to Taking Home Medals? *In preparation for submission.*

Statement of contribution: FO and AS developed the methodology. FO performed the data collection and analysis and wrote the manuscript with input from all co-authors. WH supervised the project and provided critical feedback.

Chapter 5 is an expansion of a manuscript about individual athlete contribution to the 4-man bobsled push start, with a focus in the execution of both the start and the load. *In preparation.*

Chapter 6 is based on:

Onasch, F. & Herzog, W., “Active Control of Static Pedal Force Direction Results in Decreased Maximum Isometric Force Output”. *In revision*; resubmitted (R1) to the *Journal of Biomechanics* on May 12, 2023.

Statement of contribution: FO and WH conceived the experimental protocol. FO collected and analyzed the data and wrote the manuscript with input from WH. WH supervised the research, provided feedback, and helped shape the story.

Ethics Statement: The studies reported in Chapters Chapter 3, Chapter 4, and Chapter 5 had ethics approval under **#REB19-1232**, with the project title: Muscle Properties and Biomechanics of the Bobsled Push Start. The study presented in Chapter 6 had ethics approval under **#REB15-0078** with the project title: In Vivo Skeletal Muscle Fibre Function During Cycling.

Acknowledgements

I would like to express my sincere gratitude to the following people:

My supervisor, *Walter Herzog*: for taking me on as a student in your group, giving me the opportunity to be part of this one-of-a-kind microcosm that is the HPL Calgary, find a second home away from home, and to meet some very amazing people. With that, you have given me so much and I will always remember it.

My supervisory committee members: *Darren Stefanyshyn, Brent -the Hurricane- Edwards, and Matt Jordan*: You may not be aware of it, may not have realized at the time, but for each of you there were moments over the years where you were there for me when I really needed it. Thank you, for your time and for scientific and emotional support. I appreciate it all, and I am glad you were on my team.

My thesis examiners *Rob Thompson and Stuart McErlain-Naylor*: Thank you for your interest and for taking the time to read and discuss my work, it is much appreciated.

Own The Podium: for believing in and funding this research project; it could not have happened without your support.

Bobsleigh Canada Skeleton: Staff and coaches, for supporting this project - through two years of a pandemic, no less. *All the athletes*: for just going with it and donating some of their time in the crunch time of preparation in an Olympic Season; for letting this (comparatively) tiny German hang out during their training sessions and tape sensors to their sleds; for chatting about data; trusting us and our instrumentation; being there when I almost cried seeing them push the sled on the ice for the first time – this thesis would not exist without you.

It is so easy to feel like what you are doing is just not enough and, even worse, that you are on your own. – Which makes it even better when you realize that you are not. To all the lovely people that were part of the journey (here in the lab and outside of it): there are many of you that created special fun and uplifting moments or provided words of support at exactly the right times. I hope you know who you are and what you did; thank you, from the heart.

And especially:

Art Kuo: Thank you for making me an – it seems like maybe nobody should call themselves an honorary anything, but for lack of a better word that's what I'm going with – honorary member of your lab group. Piling in a car with a group of people that I had never met, in a country that I did not really know, to spend a weekend at a conference that had next to nothing to do with my work – still one of my favourites when it comes to little adventures during my time here. And thank you, so much, for all your time and support. You did not have to offer either of them; I am truly grateful.

Our amazing technicians *Andrew Sawatsky and Andrzej Stano*: You know it, I know it, there would not be an instrumented bobsled without you two. Andrew, you find solutions for almost anything; and Andrzej, I am yet to find a cable or an electronic device to break (accidentally!, of course, just in case anyone actually reads this) that you cannot fix. Thank you both, dziękuję, for your friendship and support.

Tim Leonard: I am fortunate to have experienced the HPL in the era of Tim. Thank you for being there, calm, and sarcastic, and hilarious; for sitting with me after my candidacy exam; for a door that was always open, for many fun conversations, for listening and letting me vent, for tissues, mints, and coffee. I wish you a wonderful retirement, you deserve the best time.

The one and only *Alix Westgard (and Osiris)*: Thank you for everything you've done over the years, I do not know how things would have turned out without your tremendous support. And thanks to Osiris for the grumpy faces :)

Dave McCalla: for being the supportive, kind, ever so positive, resourceful, funny human that you are. When you popped up in the picture, it probably could not have come at a better time. You were a game changer for me in this project. Thank you.

Louis Poirier: Just...thank you, so much! You are a wild card in the most positive sense of the word. I doubt that I would have made it to the end without your unexpected and generous help. I hope you know how much it means to me.

Dr. SC and Dr. AS: The rest of us are lucky that people like you choose the M over the Ph. Thank you both very much.

*Eng Kuan Moo**, *Rafael Fortuna*, *Aaron Martinez*, and *Saša Čigoja*: you are true day-ones, the OG's of my time in Canada. Thank you for bike rides, coffee, ice cream, hikes, dinner, birthdays, beers, pep talks, rants, laughs, hugs, muffins, patience, climbing, walks, long evenings at the office, conference trips, vacation, the list goes on and I am thankful forever. *Anja Behling*: for suffering with me, laughing with me, running with me. Already excited to see your thesis, you can do it, and it will be *amaazing! *Philipp Maurus*: for being positive, fun, thoughtful, and supportive, and for miraculously providing candy when times were tough. *Seong-won Han*: for your support and repeatedly reassuring me that I can do it, for burger/pizza/ice cream walks and hours of coffee chats. The next (and first and probably last) maple caramel coconut pumpkin spiced latte with chocolate sprinkles is on me! *Graham MacDonald and Jordyn Vienneau*: for being wonderful office mates; for so much fun, long conversations, sitting with me when I cried. You've seen it all, thank you for being here.

The superhero duo *Jeremy Wong and Rob Griffiths*: two of the most positive and genuinely excited about anything science individuals I know. Rob, thank you for your words of wisdom, as well as all your funny and inspiring anecdotes – except for the giant-spider-on-the-pillow story, that might just haunt me forever now. Jer, thanks for your support and advice, for repeatedly reining in my panicky mind, and for what is hands-down the most constructive way of telling someone to shut up sit down and focus that I have ever experienced. Thank you both for helping me push the bloody trolley. I could not have done this without you two.

Michael -Baggs- Baggaley, Fabian Hoitz, and Leo Martin Alarcon: I am so very lucky you're my friends, simple as that. Thank you for being my gang, for long nights, pool, and beers, for keeping me sane, hydrated, caffeinated, fed, moving, silly, thinking, dancing, and laughing. I think the next step is obvious, really: we need to open that beach-and-mountainside bookstore-café-bar (with a pool table) and hang out together forever.

Last, but never least, *my Family and Friends in Germany:* for supporting me always. While I was far away for a long time and loved it, when I was discouraged and tired and wanted to give up, when I was happy, when I traveled, when you visited, when I cried leaving you, when I missed you; while you continued with your own adventures, when you were happy, when you were sad, when you graduated, retired, made the decision to start a new school year, bought homes, started to send me baby pictures. Knowing that you were rooting for me and that whenever I came back you would be there, you have no idea what that means to me. Danke.

To my parents.

To the other two musketeers.

To Annemarie and Ria

Hoping to someday have just some of your strength, wisdom, and kindness.

Table of Contents

Abstract.....	ii
Preface.....	iii
Acknowledgements.....	v
Dedication.....	ix
Table of Contents.....	x
List of Tables	xiii
List of Illustrations, Figures, Graphics	xiv
List of Symbols, Abbreviations, Nomenclature.....	xxi
Epigraph.....	1
Chapter 1 Introduction	2
1.1 Rationale and Specific Objectives.....	2
1.2 Presentation of the Thesis	4
Chapter 2 Background	5
Part A: Bobsled and Functional Force-Velocity Profiling.....	5
2.1 Bobsleigh 101.....	5
2.2 The (4-man) Push Start	8
2.3 Force-Velocity Relationships.....	16
2.4 Functional force-velocity profiling in sports.....	17
2.5 Why individual athletes may display varying force-velocity properties.....	20
Part B: Force Effectiveness.....	22
2.6 The Concept of Force Effectiveness in Sports	22
2.7 Force Effectiveness in Cycling	24
Summary Chapter 2	25
Chapter 3 Methods: Instrumenting a Prowler (Gym Sled) and a Bobsled	27
3.1 Development of the Instrumentation of a 4-man Bobsled	28
3.1.1 Abstract.....	28

3.1.2 Introduction	28
3.1.3 Methods and Results.....	30
3.1.4 Discussion.....	39
3.1.5 Acknowledgements	41
3.2 Taking a Step Back: The Evolution of the Sensor Set-up for Force Measurements on Prowler and Bobsled	43
3.3 Determining Sled Velocity.....	47
3.4 Summary of Chapter 3	52
Chapter 4 Functional Sled Push Force-Velocity Profiling for Bobsled Athletes; Like Taking Snow to Canada, or a Pit Stop on the Way to Taking Home Medals?	53
4.1 Abstract	53
4.2 Introduction	54
4.3 Methods.....	57
4.4 Results	61
4.5 Discussion	66
4.6 Conclusion.....	72
4.7 Acknowledgements	73
Chapter 5 Force application during the 4-man bobsled push start.....	74
5.1 Introduction	74
5.2 Methods.....	78
5.2.1 The hit.....	83
5.2.2 Across the push start, from hit to load.....	84
5.2.3 A closer look at two sample starts	85
5.2.4 The load	86
5.3 Results	92
5.3.1 The hit.....	92
5.3.2 Across the push start, from hit to load.....	95
5.3.3 A closer look at two sample starts	98
5.3.4 The load	102
5.4 Discussion	106
5.4.1 The hit.....	106
5.4.2 Across the push start, from hit to load.....	108

5.4.3 A closer look at two sample starts	111
5.4.4 The load	112
5.4.5 Limitations.....	115
5.5 Conclusion.....	118
5.6 Acknowledgements	118
Chapter 6 Active Control of Static Pedal Force Direction Results in Decreased Maximum Isometric Force Output	120
6.1 Abstract	120
6.2 Introduction	121
6.3 Methods.....	124
6.4 Results	127
6.5 Discussion	132
6.6 Conclusion.....	138
6.7 Acknowledgements	138
Chapter 7 Discussion and Conclusions.....	139
7.1 Summary	139
7.2 The Utility of force measurements in a sports context.....	143
7.3 Functional Force velocity profiling – a useful tool in bobsleigh?	144
7.4 Should maximal force effectiveness in sports tasks be enforced?	146
7.5 Limitations and Future Directions.....	148
7.6 Conclusions	149
Bibliography	151
Appendix.....	164

List of Tables

Table 2-1: Weight regulations for the bobsleds in Monobob, 2-woman/man and 4-man (IBSF, 2022b, p. 47). 12

Table 3-1: Calibration coefficients to calculate the moment acting about a given sensor (S1 through S4) on the bobsled push bars, based on the voltage output measured in all four sensors for a given loading situation. The moments that were compared to the known moments, as illustrated in **Figure 3-3**, were calculated using the coefficients presented here. 35

Table 3-2: Calibration coefficients to calculate the moment acting about a given sensor (S1 through S3) on the prowler push bars, based on the voltage output measured in all three sensors for a given loading situation. The moments that were compared to the known moments, as illustrated in **Figure 3-7**, were calculated using the coefficients presented here. 45

Table 5-1: Overview of the parameters that were used to determine the efficiency of a team load: (1 & 2) The measured sled speed at the onset and at the end of the load (Start speed and End speed, respectively), (3) the difference between the two speeds (delta s), (4) the distance traveled during the loading process as calculated based on the recorded sled speed (d data), (5) the theoretical distance traveled during the loading process as calculated based the assumption of a constant acceleration from start speed to end speed (d constant acceleration), (6) the difference between the two distances (delta d), and (7), delta d, the distance that theoretically could have been travelled expressed as a time (Time lost). 106

Table 6-1: Overview of the Post-hoc comparisons for effective force (F_{Eff}) and index of effectiveness (IE). This table contains the differences of the means for each group comparison ($a - b$), as well as the corresponding test statistics (t). The top row illustrates the different combinations of crank positions. For F_{Eff} (white background) between angle comparisons were run on data combining both testing conditions. For IE (shaded background) between angle comparisons were performed within testing condition. All the differences shown here were statistically significant with $p \leq .001$ 130

List of Illustrations, Figures, Graphics

Figure 2-1: The current specifications for the profile of the start section of a bobsled track as issued by the International Bobsleigh and Skeleton Federation (IBSF, 2019). 9

Figure 2-2: A 4-man bobsled with the arrows (one for each hand) indicating where the four athletes are in contact with the sled and push it. 11

Figure 3-1: Overview of the force sensor instrumentation. **Panel A** shows a 4-man bobsled, with the arrows indicating the points of push force application by the athletes. Three of the four athletes push on one bar with both hands. The fourth athlete, the brakeman, pushes at the end of the sled with a separate handle for each hand. **Panel B** shows a schematic of the sensor set-up on the push bars. The two grey-shaded boxes depict the strain gauges, with the black rectangles indicating the location of the actual sensor areas. The light grey shaded end of the bar is the part that attaches to brackets on the sled. Push forces are applied to the white part to the right of the sensors. **Panel C** shows the set-up of the brakeman handle instrumentation: The schematic on the left shows the orientation of a set of brakeman handles on our sled, with sensor units on top; the grey-shaded area indicates the body of the bobsled. The right schematic shows the details of one sensor unit: a sandwich of force sensors with rubber disks for equal force distribution between two metal plates. 34

Figure 3-2: The push bars were calibrated by hanging known weights at known distances from the sensors and then relating the output voltage to the calculated moments. Side bars, with their square base could be rotated and clamped to calibrate forces in the horizontal and vertical direction (**panel A**). The pilot bar can only be fixed in one orientation, which led to two different calibration approaches for vertical (**panel B**) and horizontal (**panel C**) sensor pairs. Grey shaded structures are the push bars, with the asterisk indicating roughly where a bar was attached to the sled. White boxes indicate the indented sections where the strain gauges were attached. 35

Figure 3-3: First part of results from the calibration process. The **top panel** shows the agreement of calculated moments based on the sensor calibration with the known moments that were applied to the bars (strain gauges on aluminum). Individual data points are represented by black squares, calibration curves by grey lines. The **bottom panel** shows the calibration curves and equations for the brakeman handles (force sensors). Grey circles represent the sensors' behaviour in loading, black in unloading. Dark grey lines indicate the calibration functions (brakeman handles) and regression lines (push bars). 36

Figure 3-4: Bland-Altman plots (Altman & Bland, 1983) comparing calculated force to known force to illustrate potential measurement error for the different sensor units. For pilot, left and right bar: black circles = horizontal force, grey circles = vertical force. For brakeman handles: black circles = bottom sensor for given hand/side, grey circles = top sensor for the same side. Horizontal dashed lines indicate mean differences in force, solid lines the upper and lower bounds of the 95 % confidence intervals. The deviations of calculated from known force shown above correspond to median errors of 6 %, -7 %, 4 %, and -5 % for **aB** left bottom, top, right bottom and top, respectively, as well as 0 % for **aP** vertical and horizontal, -6 %

and -5 % for **a2** horizontal and vertical, and -5 % and -3 % for **a3** horizontal and vertical, respectively. The shaded regions in each figure mark the ranges of force that were observed for a given sensor during the push phase of the bobsled start (not including the initial push that accelerates the sled from its zero-speed starting position)..... 37

Figure 3-5: Data from a sample trial that were collected from the instrumented push bars (**aP**, **a2**, **a3**) and the brakeman handles (**aB**): horizontal and vertical push force components (solid black and dotted traces, respectively) in the global frame, where the vertical axis is aligned with gravity. For the brakeman, the traces are the sums of the forces measured from left and right hand. The solid vertical lines (orange, if in colour), show the instance of loading/no more push contribution for a given athlete, as we would determine it based on the force recordings. The dashed vertical (blue) lines indicate the (approximate) time of loading based on a video recording. 38

Figure 3-6: Strain gauge set-up on the push bars for the prowler. The part of the bar marked with the letters was clamped to the sled, push forces are applied to the right of the strain gauges (dark grey boxes) with the propulsive push force direction pointing into the page. The sketch on the right represents the bar as it would be unfolded, with the dark grey boxes representing the strain gauges. Sensors on side A and side C pick up deformation due to push force applied in the horizontal direction, while the sensors on sides B and D register strain resulting from force application in the vertical direction. 45

Figure 3-7: Results of the push bar calibration for the prowler. The **top row** shows the agreement of calculated moments, horizontal forces and moment arms based on the sensor calibration with the known moments, horizontal forces, and moment arms for the left bar. Individual data points are represented by black squares, the regression lines by grey lines. The **bottom row** shows the same parameters for the right push bar..... 46

Figure 3-8: Average Peak sled speeds as determined from video recordings compared to calculations based on acceleration data from a 3D accelerometer (left panel) and from an Inertial Measurement Unit (right panel). Each circle represents one push trial (190 total), the regression lines (solid black lines) were forced through zero. The dashed grey lines are unity lines..... 48

Figure 3-9: The profile of the bobsled track at the Ice House Calgary, based on sketches of the track as well as previous measurements of the slope on the same track (Poirier, 2011). The straight sections on grey shaded background were obtained directly from the drawing of the track, the dotted part was derived by modeling a function that fit the two straight sections together. 49

Figure 3-10: The orientation of the Inertial Measurement Unit (IMU) on the bobsled (panel A), which was derived from the data recorded with the gyroscope that is part of the IMU and used as a measure of the slope of the bobsled track. The plot shows the sections that are discussed above: a constant slope section in the beginning (~0 to 11 s), a part where the slope changes (increases, ~11 to 12 s), and then a second (steeper) constant slope section (~12 to 16 s). The remainder of the trace illustrates the particular design of the Ice House track, where the track flattens out again after the last timing light and then turns into a steep upward slope (20 % or ~11.31°) that serves to decelerate the bobsled. To account for the fact that the first

part of the track is not flat (0°) but already has a slight downward slope ($\sim 1.14^\circ$), 1.14° were added to the original trace (panel B). 51

Figure 4-1: Summary of key considerations regarding functional force (or load) velocity (fFv) profiles. fFv profiles have been found (a) to be linear for many performance tests and (b) to differ between individuals. F_0 and v_0 indicate maximum task-specific force and velocity, respectively. 56

Figure 4-2: Force (top panels) and sled speed (bottom panels) for two sample trials of the same participant. On the left, with the lightest sled load, 34 % body mass, on the right, with the heaviest sled load, 195 % body mass. The red dashed lines indicate first and last time points where sled speed was equal to or greater than 95 % of the peak speed. Average speed and average force within that range constitute the velocity and force components that were used to determine a participant's fFv profiles. 60

Figure 4-3: Illustration of the selection of different data points used for determining the fFv profiles; the circles represent real data of one test day. $A_i = 9$ data points, full range, all data points (small circles) were used. $A_{ii} = 5$ data points, full range, points $5_1 - 5_5$ were used. $A_{iii} = B_i = 3$ data points, full range, points $3_1 - 3_3$ were used. The ellipses show the groups of data points used for B_{ii} through B_{iv} (close to v_0 , central, and close to F_0 , respectively). 60

Figure 4-4: Test-retest reliability results for sled speed (left) and horizontal push force (right). 15 participants completed the test protocol on two different days, with the same ten sled push trials on both days. Each individual sled load condition is represented by a circle, comparing data from test day 1 (x axis) to data from day 2 (y axis). The solid black lines are the linear fits through all data points, forced through zero, the dashed lines indicate unity lines. 61

Figure 4-5: Test-retest reliability results for the axis intercepts F_0 (left) and v_0 (right) that were calculated using the linear regression functions of the individual fFv profiles. Each circle represents a day one/day two pair for a participant. The solid black lines are the linear fits through the data points, forced through zero, the dashed lines are unity lines. 62

Figure 4-6: The boxplot on the left shows the distribution of r^2 values for all the individual fFv best fitting linear regression lines. Top and bottom edge of the box indicate the 75th and 25th percentile of the distribution, respectively; the horizontal line inside the box represents the median. The whiskers extend to the furthest points from the median that are not considered outliers, while an outlier is defined as any value more than 1.5 times the interquartile distance from the median. In the plot on the right, you find examples of fFv profiles from different participants. The solid line and circles are associated with the maximum r^2 value, the dashed line and squares with the lowest r^2 . Dotted line and plus signs and dash-dotted line and diamonds are associated with the 75th and 25th percentile of the r^2 distribution, respectively. 63

Figure 4-7: There was no relationship between the extrapolated maximum speed (v_0) and push force (F_0) values. 64

Figure 4-8: Varying constellations of load conditions were used to determine individual functional force-velocity (fFv) profiles. The effects of the varying constellations on the extreme values/axis intercepts of fFv profiles, v_0 (top row) and F_0 (bottom row) are shown. Left column: the number of data points included to fit the fFv profiles was varied (9 vs. 5 vs. 3, always including the lightest, heaviest, and middle load conditions). Centre and Right columns: the proximity of 3 data points to either one of the extreme ends of the relationship changed. i = 3 data points condition from left column, included load conditions that spanned the full range that was tested. ii = lightest load conditions. iii = central load conditions. iv = heaviest load conditions. Asterisks indicate significant differences with $p < .005$. Extreme outliers (greater than 5 times the interquartile range from the median) were excluded from statistical analyses (right column). 65

Figure 5-1: A 4-man bobsled with the arrows (one for each hand) indicating where the four athletes are in contact with the sled and push it. 77

Figure 5-2: Examples of how start of movement (red circle, A) and end of a push start trial (dashed vertical line, B) were determined. 80

Figure 5-3: Schematic of the start section of the bobsled track at the Calgary Ice House. The track profile was derived from building plans and previous measurement (Poirier, 2011). This profile is consistent with the regulations published by the International Bobsled and Skeleton Federation (IBSF, 2019). 81

Figure 5-4: Schematic to define the directions ‘propulsive’ and ‘normal’ in the context of a bobsled on the ice track. 82

Figure 5-5: Visualization of how the instants of hit impulse, 50 %, and 90 % of peak impulse across a trial were determined. 84

Figure 5-6: Exemplar calculation the proposed approach to determine team performance during the load. The data used for this figure are from example push start A (ExS_A). 88

Figure 5-7: Comparing push force at loading to the theoretical critical push force, below which an athlete would contribute more to sled acceleration by sitting inside the bobsled than when pushing. The vertical and horizontal black dashed lines indicate time of last ground contact before loading and average push force for the last second (shaded green bar) prior to this point respectively. The red dotted lines represent the critical forces as calculated for the conditions at the time of loading. To account for potential error in the estimates of the athletes’ body masses, critical force was calculated three times (for estimated body mass and estimated body mass ± 10 kg). Consequently, there are three red dotted lines in each graph but the effect of variation in mass on critical force was so small, that the three lines lie on top of each other. The graphs in the top row show data from example trial A (ExS_A), the bottom row from example trial B (ExS_B). A dashed black line above the red dotted lines means that an athlete loaded before they reached critical force – and may have loaded the sled too early. A dashed black line below the red lines means that an athlete loaded the sled when they already contributed less than the critical force. 91

Figure 5-8: Push force data of all push starts, normalized to total push start duration. The dashed vertical lines correspond to the median time of the occurrence of (1) the end of the hit, (2) the point where 50 % of peak cumulative impulse were achieved, and (3), the point where 90 % of peak cumulative impulse were achieved. The horizontal spread of the dots around each lines indicates the variation in time associated with an event. The horizontal spread in the distribution of the darker red dots indicates the variation in what percentage of peak impulse the hit accounted for in each push start (right y-axis, median = 41 %). 93

Figure 5-9: Box-and-whiskers plots presenting the distributions of peak force (left panel) and impulse (right panel), as produced by the individual athletes during the first hit on the sled across the 13 recorded runs. A red line represents the median. Upper and lower bounds of a box represent 75th and 25th percentile, respectively. Outliers are defined as values that are more than 1.5 times the interquartile distance away from the median; the whiskers extend to the most extreme data points that are not considered outliers. The x axis shows the four positions of athletes. P = Pilot, L = athlete on the left, R = athlete on the right, and B = the brakeman. 94

Figure 5-10: Times of peak propulsive push force on the first hit, relative to the pilot (#relative to the athlete on the left, run 8, as the pilot was not pushing). Time differences are presented for each run, with the athletes represented by different markers. Asterisk = pilot, circle = athlete on the left, square = athlete on the right, diamond = brakeman in the back. Negative values indicate that the associated athlete reached peak force before the pilot did, a positive value means that they reached it later. 94

Figure 5-11: Boxplots of the mean propulsive (left column) and normal (right column) push force for the first 45 % of the start phase. The rows represent from top to bottom: the Pilot (P), Left (L), Brakeman (B), Right (R) athlete. 96

Figure 5-12: Mean force effectiveness for each 5 % interval across the push starts. The top panel contains data for all the pilots (P), middle for the athletes who pushed on the left (L), and bottom for the athletes who pushed on the right (R). Each circle corresponds to the value of force effectiveness for a given interval in a push start trial. 97

Figure 5-13: Push force effectiveness from the time after the first hit to before the start of loading. The top panel contains data for all the pilots (P), middle for the athletes pushing on the left (L), bottom for the athletes pushing on the right (R). Each vertical chain of dots indicates the spread of values for push force effectiveness for a given push position across all trials. The centre dot (blue) indicates the median, bottom (red) the 25th percentile of the distribution, and top (yellow) the 75th percentile. Push force effectiveness was calculated as the mean absolute propulsive force during the 5 % of the push intervals, divided by the mean absolute normal force measured during that same period. 97

Figure 5-14: Time series data of sled speed and propulsive push force for two exemplary trials (ExS_A and ExS_B). Complete time series data are presented in the left column for speed (top) and total propulsive push force (sum of all four athletes; bottom) and zoomed in views of the region of interest (red shaded area) are presented in the right column. A plateau in the speed trace of trial ExS_B corresponds with push a force magnitude near zero. 99

Figure 5-15: Example trial A (ExS_A). The top left panel shows the pilot data, bottom left the ones for the athlete who pushed on the left side of the bobsled behind the pilot. The top right panel shows the data for the athlete who pushed on the right side of the bobsled, bottom right the ones for the brakeman. Solid black traces represent the propulsive push force component, dashed black traces represent the normal push force component. The steadily increasing blue line associated with the right y-axis represents sled speed across the push start. The dashed vertical line near time zero indicates the instant of peak force as determined from the sum of propulsive push force from all four athletes. The solid vertical lines mark certain events in the loading process that can be observed in the video data. The labels (small caps letters) indicate what happened in the specified instant. With **a** = ground contact last step, **b** = toe off to load, **d** = foot on bunk (left or right athlete), **e** = last hand off the push bar or handle(s), **f** = move off bunk into the sled (left or right athlete), **g** = sitting or standing inside the sled, and **h** = brakeman rests on sled before moving inside. 100

Figure 5-16: Example trial B (ExS_B). The top left panel shows the pilot data, bottom left the ones for the athlete who pushed on the left side of the bobsled behind the pilot. The top right panel shows the data for the athlete who pushed on the right side of the bobsled, bottom right the ones for the brakeman. Solid black traces represent the propulsive push force component, dashed black traces represent the normal push force component. The steadily increasing pink line associated with the right y-axis represents sled speed across the push start. The dashed vertical line near time zero indicates the instant of peak force as determined from the sum of propulsive push force from all four athletes. The solid vertical lines mark certain events in the loading process that can be observed in the video data. The labels (small caps letters) indicate what happened in the specified instant. With **a** = ground contact last step, **b** = toe off to load, **c** = pilot moves one hand across the push bar and over onto the cowling – before starting the load, **d** = foot on bunk (left or right athlete), **e** = last hand off the push bar or handle(s), **f** = move off bunk into the sled (left or right athlete), **g** = sitting or standing inside the sled, and **h** = brakeman rests on sled before moving inside. 101

Figure 5-17: Box-and-whiskers plots presenting the estimated sled speed at the instant of loading (toe off the ice), grouped by position. P = Pilot, L = athlete on the left, R = athlete on the right, B = brakeman in the back. 103

Figure 5-18: Estimated sled positions along the track at the instant of loading (toe off the ice), grouped by position: Asterisks and magenta shaded bar (first from the left) = pilots, circles and blue bar (second) = athletes on the left, squares and yellow bar (third) = athletes on the right, diamonds and green bar (rightmost) = brakemen in the back. Note, that the different ‘loading regions are not completely separated. The loading order (pilot, left, right, brakeman) was consistent across starts. However, overall loading timing was earlier in some trials than in others, causing the markers for a given team to shift left relative to others and the bars to overlap. 103

Figure 5-19: Box-and-whiskers plots representing - separated by athlete (**P** = pilot, **L** = left side, **R** = right side) **A**: the force of air drag based velocity of the bobsled measured at the instant of load, **B**: the critical push force at which an athlete would contribute more to sled acceleration by sitting inside the bobsled than by pushing it – calculated for the associated drag conditions, and **C**: the average propulsive push force recorded in the last second prior to the instant of loading. 104

Figure 5-20: Sled acceleration as simulated for push forces ranging from 0 to 100N (circles) The different colours represent different drag magnitudes based on varying sled velocities: blue = 8 ms, red = 10 ms, and yellow = 12 ms. The horizontal lines indicate the acceleration of the sled if the athlete ceased pushing and jumped in the sled instead. The vertical lines indicate the critical forces for the different drag conditions. 105

Figure 6-1: The crank positions that were tested in this study..... 125

Figure 6-2: Effective force (F_{Eff} , top panel) and index of effectiveness (IE, bottom panel), separated by test condition (NC = dark grey boxes, C = light grey) and crank position. An individual box represents the distribution of a batch of data as follows: The horizontal line inside the box indicates the median, top and bottom end of the box stand for 75th and 25th percentile, respectively. The whiskers extend to the most extreme values not considered outliers. An outlier is any value more than 1.5 times the difference between 75th and 25th percentile away from the median. Paired comparisons were made across testing conditions for F_{Eff} , and separately within each testing condition for IE. Letters above the horizontal lines indicate significantly different from: a = 30°, b = 60°, c = 90°, d = 120°, e = 150°, with $p \leq .001$ 129

Figure 6-3: Median muscle activation (as % of maximum activation measured in this test) separated by crank angle and test condition (dark grey = NC, light grey = C). TA = tibialis anterior, RF = rectus femoris, VL = vastus lateralis, SOL = soleus, GMAX = gluteus maximus, MG = medial gastrocnemius, BF = biceps femoris. 131

Figure A- 1: Box-and-whiskers plots representing the extrapolated axis intercepts V0 and F0 as derived from hyperbolic (H) and linear (L) fits of the functional push force-velocity relationships in Chapter 4, as well as the respective coefficients of determination (r^2) as measures of goodness of fit. Wilcoxon's paired group comparisons were run resulting in significant differences ($p < .01$) for all three variables.166

Figure A- 2: Examples of fitting the functional push force-velocity profiles using Matlab's fit function, with a hyperbola based on Hill's equation (Hill, 1938) as the target function, as described above. The black dots are the individual data points for a participant during their test session. The fit of the data points is represented by the red solid lines, and the dashed grey lines are the extrapolated graphs of the fitted functions.167

List of Symbols, Abbreviations, Nomenclature

°	Degree (unit of a geometrical angle)
2-man	Discipline in bobsled, where two male athletes push the sled at the start (pilot and brakeman)
2-woman	Discipline in bobsled, where two female athletes push the sled at the start (pilot and brakewoman)
4-man	Discipline in bobsled, where four male athletes push the sled at the start (pilot - aP, brakeman - aB, and one additional athlete on either side in between - a2 and a3)
a2	Athlete in a 4-man bobsled crew, pushing on the left side, behind the pilot
a3	Athlete in a 4-man bobsled crew, pushing on the right side
aB	Athlete in a 4-man bobsled crew, Brakeman, pushing at the back of the sled
aP	Athlete in a 4-man bobsled crew, Pilot
α	Alpha, level of statistical significance
BF	m. biceps femoris
brakeman	Any athlete on a bobsled team who is not the pilot. Throughout this thesis, the term is used to specifically refer to the athlete who pushes in the position behind the sled
cm	Centimetre

COM	centre of mass
cowling	the shell or casing of a bobsled
DAQ	data acquisition
EMG	Electromyography: a technique to measure muscle activation
exit velocity	The velocity of a bobsled at the end of the push start phase.
ExS_A	Sample trial A picked from all recorded bobsled push starts
ExS_B	Sample trial B picked from all recorded bobsled push starts
F_0	Maximum force as extrapolated from a (functional) force-velocity relationship
F_{Eff}	Effective force; in cycling, the pedal force component that is directed perpendicular to the crank
fFv	Functional force-velocity
Fv	Force-velocity
GMAX	m. gluteus maximus
Hz	Hertz
IBSF/FIBT	International Bobsled and Skeleton Federation/Federation International de Bobsleigh et Tobogganing
IE	Index of force effectiveness

IMU	Inertial Measurement Unit, a sensor unit containing a 3D accelerometer, a 3D gyroscope, and a magnetometer.
kg	Kilogram
km/h	Kilometres per hour
L	Athlete in a 4-man bobsled crew, pushing on the left side, behind the pilot
m.	muscle/musculus
m	Metre
MG	m. gastrocnemius medialis
$\frac{m}{s}$	Metres per second
$m\ s^{-1}$	Metres per second
Monobob	Discipline in bobsled, where one female athlete pushes the sled at the start (pilot and brakewoman in the same person)
N	Newton
Nm	Newton meter
prowler	A sled-like frame that is typically used at gyms for power workouts. It can be pushed (or sometimes pulled) across various tracks/surfaces and, if need be, made heavier by loading it with weight plates.

r	Pearson's correlation coefficient
r^2	Coefficient of determination
R	Athlete in a 4-man bobsled crew, pushing on the right side, behind the pilot
RF	m. rectus femoris
runners	The blades on which a bobsled runs/ the sled's point of contact with the ice
run time	The time it takes a bobsled team to complete a run or heat in a competition, from start line to finish line.
s	Second
SD	Standard Deviation
SOL	m. soleus
start time	The time it takes a bobsled team to complete the officially timed start portion of the track i.e., the first 50m from the start line.
TA	m. tibialis anterior
v_0	Maximum velocity as extrapolated from a (functional) force-velocity relationship.
VL	m. vastus lateralis
W	Watt

It was the best of times it was the worst of times.

from A Tale of Two Cities ~ by Charles Dickens

Chapter 1

Introduction

1.1 Rationale and Specific Objectives

“Citius. Altius. Fortius.”, that was the original motto of the Olympics (IOC, 2022a). Faster, Higher, Stronger. Probably at least one part of this motto is the mantra for any competitive athlete, be it in comparison to others or simply to oneself the day before. But how to achieve this goal? This question is not new and to this day, athletes, coaches, and researchers work to improve performance in their sport.

Faster, Higher, Stronger. The common denominator behind all three of those aims is that athletes need to generate force and apply it to a piece of equipment or against the ground (or water). One could argue that both moving faster and higher really boil down to just being stronger, but this may not paint the full picture. What does stronger mean anyway? Or rather, what does it depend on? Being stronger is a multi-faceted problem: Any external force that we produce, depends on (i) the forces that are produced within, by our muscles, (ii) the coordination of/between those muscles, and (iii) the technique on the outside, exactly how the resulting force is applied to the target. This general problem of force production and delivery in different sport contexts is the overarching theme of this thesis. The projects presented below were focused on functional force-velocity relationships, timing of force application, force delivery in a team, and force effectiveness in bobsleigh and cycling.

We developed an instrumented 4-man bobsled, which allowed us to measure individual push forces from the athletes, as well as the velocity of the sled throughout the start phase. We were fortunate to have National Team athletes perform starts with the instrumented sled and used the data that were collected to evaluate our measurement system, as well as gather information to better characterize the 4-man push start and the individual athletes' contributions. Although we encountered some challenges with the sensor set-up for the brakeman handles, our system is a valuable product that can provide novel information about team push performance. We describe the 4-man push start from hit (the very first push) to load (when the athletes jump into the bobsled). We found that the propulsive push force seemed to decline quickly and at times long before the end of the push and before loading. This observation fits with our view of the athletes' contribution during bobsleigh push start as a force-velocity problem. During the push start, the athletes' task is to accelerate the sled from rest to maximum velocity at the end of the start phase. In other words, start performance depends on the athletes' abilities to continuously apply push force while running at increasing speeds. Therefore, in addition to the bobsled, we also instrumented a prowler (gym sled), which might be used as a training and assessment tool for bobsled athletes. First, however, the instrumented prowler was used to assess functional sled push force-velocity (fFv) relationships in recreationally active individuals. Measures of peak speed and associated horizontal push force were reliable between two test days (one week apart), and linear regressions were found to provide good fits of the resulting fFv profiles.

In cycling, only the pedal force component that is perpendicular to the crank (= effective force) results in propulsion, while force acting parallel to the crank does not contribute to propulsion and thus might be considered wasted. Therefore, the question of whether it makes sense to try to change pedaling technique to be perfectly effective has been an ongoing discussion for decades. We

assumed that perfect force effectiveness might be desirable from a mechanical standpoint but a disadvantage to the biological musculoskeletal system and conducted a study exploring the effect of constrained pedal force direction on pedal force magnitude. When individuals tried to direct static pedal forces perpendicular to the crank only, their force effectiveness was improved, but it came at the cost of substantial reductions in effective pedal force. This finding suggests that encouraging individuals to modify their cycling technique to achieve 100 % force effectiveness can come with serious drawbacks and should be avoided.

1.2 Presentation of the Thesis

Please note, that this thesis is manuscript-based. Some paragraphs in this document will therefore contain repeating information, particularly where the background is discussed i.e., Chapter 2 and the introduction sections of Chapters 3.1, Chapter 4, Chapter 5, and Chapter 6.

Chapter 2 of this thesis provides relevant background information about the sport of bobsleigh and functional force-velocity profiling, and the concept of force effectiveness in sports. The objectives of the individual studies that were completed as parts of this thesis work are presented. *Chapter 3* contains the description of the instrumentation that was developed for the two sleds (proowler gym sled and 4-man bobsled) and were used for the studies outlined in *ChaptersChapter 4 and Chapter 5*, respectively. *Chapter 4* is about the first study conducted as part of the bigger bobsled project, investigating functional force-velocity profiling for sled pushes. In *Chapter 5*, I discuss the data that were collected from the instrumented 4-man bobsled. In *Chapter 6*, the topic is pedal force application and force effectiveness in cycling. *Chapter 7* contains a comprehensive discussion of the findings presented in this thesis, including concluding thoughts and ideas for future research.

Chapter 2

Background

Even though under the umbrella of force application in sports, the research projects presented in this thesis were focused on two very different examples. First, the push start in bobsleigh, where we aimed to measure and analyze athlete push contribution and investigate the utility of functional force-velocity profiling in the sport. Second, cycling, with a focus on pedal force effectiveness. Therefore, this background chapter is structured in two parts, A (sections 2.1 – 2.5): bobsleigh and force-velocity profiling, and B (sections 2.6 – 2.7): force effectiveness in sports, and specifically in cycling; concluding with a brief summary of both parts and an outlook on the following chapters.

Part A: Bobsled and Functional Force-Velocity Profiling

2.1 Bobsleigh 101

If you have ever traveled by air, you will have experienced this: your plane slowly turns on the runway and comes to a halt. The pilot waits for the green light from the tower – and then the machine comes to life. The ignition of the engines results in an acceleration that you can feel as it pushes you back in your seat and, within a few seconds, you are in the air, flying. This feeling is what I was reminded of when I stood next to the track at the start of a 4-man bobsled World Cup competition for the first time. Naturally, these two scenarios are not actually the same (and not only because in bobsleigh the goal is definitely not to fly), but watching a bobsled start from up close is impressive, nonetheless.

Bobsleigh is one of the fastest Winter sports with recorded top speeds of up to 150 km/h and the athletes experiencing forces of 5 g and more in some turns. The sole performance measure is the time it takes a team to complete their run and fractions of a second can decide the outcome of a race. In the 2-man competition at the 2018 Olympic Games (PyeongChang), two 2-man teams tied for the gold medal with run times identical to the hundredths of a second, and at the most recent Games, Beijing 2022, the top 5 teams in the 4-man event all finished within just 1 second, with bronze medal and 4th place separated by only 6/100ths of a second (IBSF, 2023a; IOC, 2018, 2022b). Bobsleigh competitions have been part of the Olympic program since day one. The first bobsleds were built in the early 1900s, the International Bobsled and Skeleton Federation (IBSF) was founded in 1923 and, only one year later, 4-man teams competed in the first Winter Olympic Games in Chamonix, France. At that time, the athletes would all sit in the sled at the start and rock – or bob – back and forth to get the sled going (faster) – hence the name, bobsled. Several years later, around the 1950s, this strategy at the start changed into the characteristic push start that is used today (IBSF, 2022a).

The execution of the start is not the only aspect that has changed since the early days of bobsleigh. The sleds, which used to be essentially metal frames with a steering mechanism and seats, have developed into streamline racing capsules worth several tens of thousands of dollars, and anecdotal evidence suggests that the preparation of the runners before a race is a secret science perfected by athletes and mechanics over years in the sport. The cowlings are now made of carbon fibre and their shapes keep changing, aiming to perfect the aerodynamics and allow the teams to speed down the tracks even faster. Finally, from its origins in Switzerland, the bobsled has also made its way across the globe. There are currently 15 operational tracks in the world, eight of which are in Europe, four in Asia, and three in North America. Track lengths range from 1,330 to 1,975m, with

vertical drops between 95 and 148 m, featuring an average of 16 curves (IBSF, 2023b) and, despite the limited number of bobsled tracks, athletes from 48 nations participate in the sport (IBSF, 2023c).

As of today, there are four different disciplines in bobsleigh, named after the number of athletes pushing the sled at the start: The *4-man*, where the team consists of a pilot, a brakeman¹ in the back and two additional athletes, one pushing on the left and one on the right side of the sled. The *2-man* and *2-woman* teams, with a pilot and a brakeman/woman. And finally, the latest addition, the *Monobob*, where a female athlete is pilot and brakewoman in one person. For all of them, there are three main components that influence the outcome of a race and which a team can control: (1) material, (2) the pilot, and (3) the team and their push performance. Material, that is the sled and its runners, is very important – and very expensive. Previous calls for equal conditions among contestants have led to rule changes in the past (IBSF, 2022a) yet, there has been ongoing discussion in the bobsled community about whether some particularly successful nations simply have material advantages over the others. The build of the sled aside, a pilot's skill certainly matters. Driving errors can, in the best case, make the sled lose velocity and, in the worst case, result in accidents, some of which have been fatal. At the same time, seemingly small mistakes made during the push at the start can mean that, even with flawless pilot work, the podium is out of reach – which is where it gets interesting from a human athletic point of view. The push-start is human-powered, no mechanically induced propulsion, which means performance depends on the athletic abilities of the team members, as well as the coordination between them. Moreover, there

¹ It is common practice in the bobsleigh community to refer to any athlete who is not a pilot as brakeman (or brakewoman), even when they are pushing on the side in a 4-man and are not actually in the position to pull the brakes at the end of the run. However, since the positions matter for the work presented here, and to make it clear which is being discussed, the term 'brakeman' will be used specifically for the athlete who pushes at the back of the bobsled.

is a strong positive relationship between start times (measured over a 50 m distance from the start line) and the total run times in all bobsled events (Brüggemann et al., 1997; Harrison, 2017; Morlock & Zatsiorsky, 1989; Smith et al., 2006), and a rule of thumb in the sport is that 1/10th of a second lost at the start turns into a 3/10ths of a second deficit at the finish line. Environmental factors like weather or ice conditions may affect this relationship, but the fact remains that without a good performance at the start, a team cannot win their race, and even small improvements at the start can have a big impact on total race time.

2.2 The (4-man) Push Start

Before discussion the athletes' actions during the push start, I want to briefly describe what the start section of a bobsled track looks like. The design of the start section is regulated by the International Bobsled and Skeleton Federation (IBSF), the international governing body of the sport, and the key parameters are outlined below.

First, there is the so-called *push-off stretch*, 15 m long, with a downhill slope of 2 % (approx. 1.1°). It is bordered by a start block in the beginning, and the official start line at the end. The start line marks the location of the first official timing light, which means that the first 15m of the push-off stretch are not included in the official run time. The teams have a “flying” start into the race. After passing the start line, the sled is in the *starting area*, 60 m long, with a slope of 12 % (6.8°). The first split time of the race is taken at 50 m from the start line, and counts as the official start time (IBSF, 2019; **Figure 2-1**). The track where we collected the data for this research project was built according to these specifications, but not all the tracks in the world are. However, even with deviations from the profile described above, the following important elements remain consistent for all tracks and races: (1) The flying start into the race, and (2) the athletes pushing the bobsled

on an increasing downhill slope. Additionally, throughout the official start portion, the bobsled runs in grooves, which guide the sled in that first section of the race. Depending on the track, a bobsled run takes approximately 50 to 60 seconds, the push start (the part of it that is officially timed) lasts about 5 seconds for elite teams, or about 8 to 10 % of the total race time. The untimed section before the start line adds another 2-3 seconds to the entire duration of the event.

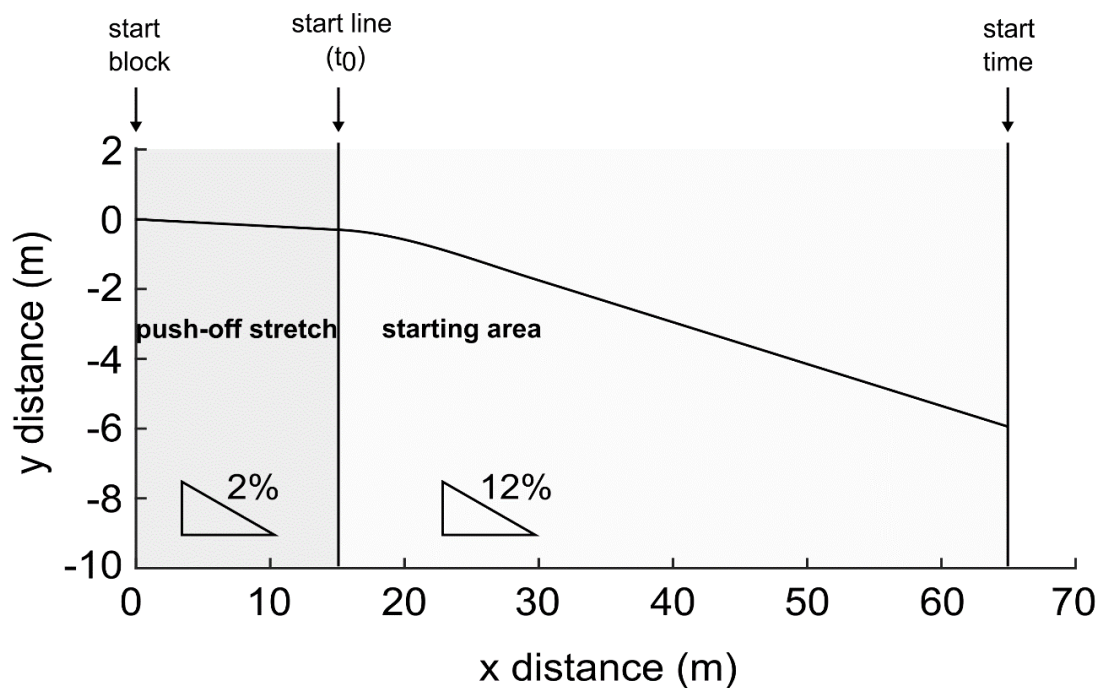


Figure 2-1: The current specifications for the profile of the start section of a bobsled track as issued by the International Bobsleigh and Skeleton Federation (IBSF, 2019).

Regardless of the track profile or bobsled discipline (4-man, 2-man/woman, Monobob), the athletes' task during the push start is to accelerate the sled from a zero-speed starting position to a maximal exit speed at the end of the start phase in the shortest time possible.

In detail, the process for the 4-man (**Figure 2-2**) looks like this²:

- The four athletes take their positions around the sled: the brakeman with both feet on the start block, athletes on the left and right in contact with the start block as well, the pilot in front – each of them holding on to their push bars or handles. (The pilot might also stand back on the starting block and run to his push bar when the others first hit the sled. However, starting this way can be risky, particularly in the 4-man event, and in the bobsled starts that we recorded none of the pilots chose this option.)
- Each team has a signal on which the athletes start pushing the sled and accelerate it as much as possible before loading (i.e., jumping into the sled).
- The empty sled at the start must meet a certain minimum mass requirement, which changes depending on the discipline. For the 4-man, the minimum empty sled mass is 210 kg, the maximum permitted mass with the crew inside the bobsled is 630 kg (**Table 2-1**).
- The loading is initiated by the pilot, followed by – in the starts that we recorded – the athlete pushing behind the pilot on the left, then the athlete on the right. (Note, there is no rule specifying the order of athlete loading and some teams load differently compared to what we recorded). The brakeman in the back loads the sled last. Loading the sled is an important part of the push start, and one that requires practice. In competition, loading of

² For a visual, use the link below to see a video of the last heat in the 4-man World Championship competition 2019 in Whistler (credit and rights: International Bobsleigh and Skeleton Federation).

<https://www.youtube.com/live/UEaWQ8byTnc?feature=share&t=2642>

all four athletes happens within about 3 seconds. Such quick loading is particularly impressive considering that bobsled athletes are, fitting for the task, tall and trained to be strong – while the sleds are not exactly spacious. Imagine gathering three friends and the four of you trying to elegantly and quickly slide into a 12-foot-long box that is about the width of your desk chair. This pattern of loading the sled means that, one by one, the athletes stop actively contributing to sled propulsion. Moreover, the driver runs the shortest distance and enters the sled at the slowest speeds, whereas the brakeman, who loads last, covers the greatest distance, and enters the sled at the highest speeds.

- Once inside the bobsled, the pilot takes over and steers it down the remainder of the track to the finish line.

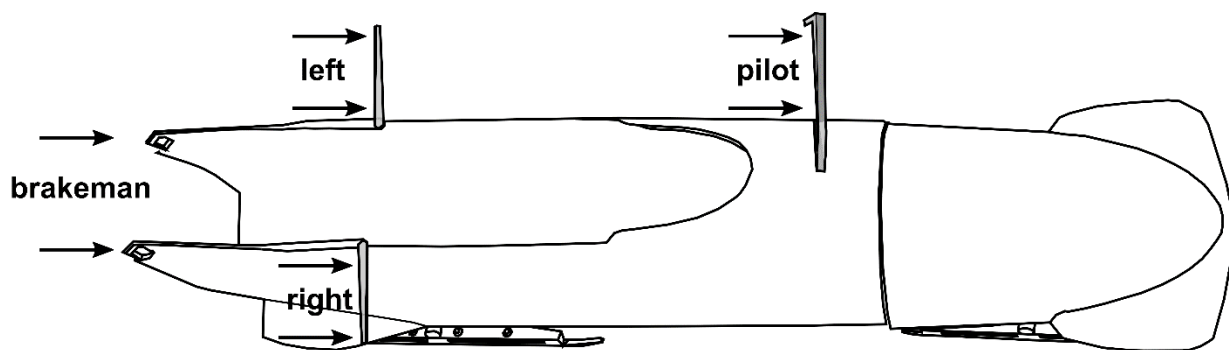


Figure 2-2: A 4-man bobsled with the arrows (one for each hand) indicating where the four athletes are in contact with the sled and push it.

Table 2-1: *Weight regulations for the bobsleds in Monobob, 2-woman/man and 4-man (IBSF, 2022b, p. 47).*

	Minimum mass - without crew - (kg)	Maximum mass - with crew - (kg)
Monobob	163	248
2-woman	170	330
2-man	170	390
4-man (men and/or women)	210	630

Even though the importance of the push start for the outcome of a bobsled race is recognized, the literature on the subject is scarce. Morlock and Zatsiorsky's (1989) investigation of the relationship between start time and run time was one of the first research projects on bobsleigh, and most of the work in the field since then has been published within the last decade.

In previous publications, the authors discussed three broad topics: (1) External conditions i.e., bobsled design and aerodynamics (Braghin et al., 2011; Dabnichki & Avital, 2006) or ice properties (Poirier, Lozowski, Maw, et al., 2011; Poirier, Lozowski, & Thompson, 2011). (2) Recruitment and team selection tests and athletic characterization of the typical bobsled athlete (Challis et al., 2015; DeWeese, 2012; Harrison, 2017; Osbeck et al., 1996; Tomasevich et al., 2020). And (3) The human contribution to race performance, with research groups investigating athletes' kinematics during the push start (Leonardi et al., 1985; Lopes & Alouche, 2016; Park et al., 2017a, 2017b; Smith et al., 2006), their muscle activity (Park et al., 2019), or the effects of footwear (Park et al., 2017b). Since the work presented in this thesis targeted the individual athletes' push force contributions to propulsion during the push start phase of a run, the following discussion of the literature is focused on thematic groups (2) and (3).

Recruitment and Team Selection: Bobsleigh coaches repeatedly face the challenge of recruiting the right athletes for the team, as well as choosing the best team composition and loading order for a given race. The latter is important because it affects what exactly is required from each athlete during the push start, but the general points are valid for all starts and all positions: In the beginning of the start phase, athletes need to be able to produce great force at slow velocities but then, as sled velocity increases, they also need to be able to continue contributing push force while running fast. Loading later means being required to run further and to keep up with increasing sled velocity for longer. Coaches seek to recruit individuals who are both fast and strong (DeWeese, 2012; Morlock & Zatsiorsky, 1989), with sprints (15-60 m), broad jumps, and underhand throws (shot or medicine ball) as typical recruitment tests (Bobsleigh Canada Skeleton, 2022; Team USA, 2022). Additional athlete screening items may include squats and power cleans (Tomasevicz et al., 2020). However, the validity of these tests has been questioned, as strength and power assessments were found appropriate to detect differences in high-level athletes, while speed assessments proved more useful in discriminating between lower level athletes (Harrison, 2017, p. 290). An important final team selection test is the so-called single push test (on ice or dry land, depending on what is available for team). In this test, individual athletes perform push starts, and the time it takes to complete the task is often the deciding factor for who is chosen to join a crew. Here, too, it has been suggested that common recruitment tests results do not correlate well with athletes' on-ice single push times. Instead, it was proposed that (a) the extrapolated take-off speed for a load equivalent to the mass of the single push test sled as derived from a loaded jump force-velocity test and (b) an athlete's one-repetition maximum for the bench press exercise correlated well with single push test performance (Challis et al., 2015). In addition, there is anecdotal evidence suggesting that single on-ice push results do not necessarily translate well to an athlete's

performance in a team push. These observations of occasional mismatches between team selection test results and performance in the actual bobsled start suggest that the contributions of the individual athletes during the push start itself needs to be better understood.

The push start with a focus on the athletes: Lopes and Alouche (2016) studied the kinematics of pilots and brakemen during the hit (the very first push of the push start) in the 2-man competition at the 2004 World Championships. No significant differences in pushing technique were found between athletes in different performance groups. Conversely, Park et al. (2017a) reported significant differences in similar kinematics variables between performance groups, suggesting that the faster starters prioritized horizontal (forward) movement rather than vertical displacement, as well as longer stride lengths, compared to the slower group. Breaking up the top 15 finishing teams into three performance groups, the authors reported that no significant differences were found between the groups. Smith et al. (2006) measured step parameters (length, frequency, and ground contact time), as well as centre of mass velocity, trunk, knee, and elbow angle for brakemen over the first 3 to 4 steps of the 2-man push start. Mean step frequency was found to increase from 3.31 to 4.22 steps per second, with mean contact times decreasing (from 0.28 to 0.21 seconds). The observed combinations of frequency and time also suggests very short (average) flight times of ~0.02 to 0.03 seconds. The authors further highlighted a significant moderate negative relationship between start time and centre of mass velocity measured at toe-off of the second step, which was interpreted as an indicator of the importance of explosive strength in the athletes for good performance. Leading up to the 2018 Olympic Winter Games in Pyeongchang, several research projects were completed around the South Korean Bobsleigh team. Aside from joint angle kinematics, the researchers were interested in athletes' footwear (Park et al., 2017b, 2017c), as well as their muscle activity during the push start (Park et al., 2019). Significantly greater

activation of the gluteus maximus was found in the stronger one of two performance groups, as well as a significant but weak relationship between biceps femoris activation and start time.

And what about the kinetics of the push start and the athletes' push force contributions to sled acceleration? Decades ago, Leonardi et al. (1985) published an abstract emphasizing the need to determine the forces acting on the bobsled during the push start in order to be able to improve start performance. The authors allude to a simulation approach that they developed but, unfortunately, the results are not available. Since then, three articles were published in which the authors discussed continuous push force and/or sled speed data from bobsled athletes in the 2-man configuration: Lee et al. (2015) described the instrumentation that they developed for a 2-man sled on wheels and presented exemplar data, push forces recorded from both the brakeman and the pilot, as well as sled speed. Dabnichki (2016) discussed the instrumentation of a 2-man bobsled that was pushed on ice but reported sled acceleration and velocity only. Based on the results of a computer simulation, the author suggested that adjusting the timing of loading may increase sled exit speed at the end of the start phase. Lastly, Peeters et al. (2019) instrumented a sled-like frame on wheels that was pushed by non-athlete participants. The authors assessed how synchronized two individuals were on the first hit. Good synchronization (a time difference between the occurrence of force peaks of less than 100 ms) was (not significantly) associated with reduced start time and increased sled speeds. These three studies support the idea that there is useful information to be gained from a closer look at the actual forces applied during the bobsled push start, regardless of the discipline, and the more athletes are involved the more important such information might be. Additionally, the number of starts a team gets to perform during a season is limited. There were only 8 competition days (with two starts per day) for 4-man teams during the 2022/2023 world cup season, which means that there is little to no room for experiments with different team

makeups during that time. Consequently, the more information that can be gathered in training, the easier it might be for coaches to make decisions on race day. Previously, in-race velocity measurements were obtained on a straightaway section of the Calgary bobsled track during a 2-man World Cup competition (Poirier, 2011) but, to the best of our knowledge, no push force or continuous velocity measurements currently exist for the 4-man bobsled.

2.3 Force-Velocity Relationships

While the term *force-velocity relationship* is familiar to researchers studying muscles mechanics and sports practitioners alike, it is not necessarily used to describe the same phenomenon. In the following, I discuss the difference between the two different perspectives, as well as the significance of the concept of force-velocity profiling in a sports context.

The ‘classic’ force-velocity (Fv) relationship describes an important property of isolated skeletal muscle. First systematically studied by Fenn and Marsh (1935), the force-velocity relationship of muscle was first mathematically described by and has since been primarily associated with A.V. Hill (1938). In experiments with isolated frog muscle, Hill observed the characteristic increase in maximum contraction velocity with decreasing resistance i.e., decreasing work done and decreasing force produced by the muscle during the contraction. This result was obtained under perfect testing conditions where the muscle was set up at its optimal operating length, maximally activated in isometric contraction, and then released to contract concentrically. In this concentric muscle action, the Fv relationship was found to be of hyperbolic shape where calculating instantaneous power as the product of force and velocity results in a curve resembling a distorted inverted U with its peak occurring at approximately one third of the maximum contraction velocity

(Hill, 1938). Skeletal muscle force-velocity characteristics were later attributed to the cycling of the cross-bridges inside the sarcomeres of the muscle fibres (Huxley, 1957).

In a sports context, force-velocity relationships are typically associated with specific exercises. Instead of exploring the relationship between muscle force and contraction velocity the question might be, for example, what are the take-off velocities an athlete can achieve in squat jumps as a function of varying loads that they need to move in excess of their own body mass (Samozino et al., 2012). For a clear distinction between the two types of force-velocity relationships, any such relationship that is obtained for either the movement of a muscle group (e.g., for a knee-extension task in a dynamometer) or for a multi-joint or full-body movement (e.g., leg press, cycling, or sprints) are referred to as *functional force-velocity (fFv) relationship* throughout this thesis and discussed in more detail below.

2.4 Functional force-velocity profiling in sports

In many sports, performance is determined by an athlete's or a team's ability to produce power (Adams et al., 1992; Baker, 2001; Coyle et al., 1991; Cronin & Hansen, 2005; Hawley et al., 1992). Power is defined as the product of force and velocity, which makes fFv profiling an excellent tool for assessing an individual's power generation capacity. fFv relationships have been determined for a variety of exercises such as cycling (Dorel et al., 2010; Dunst et al., 2022; Dwyer et al., 2022; Rudsits et al., 2018; Vandewalle et al., 1987), cross-country skiing (Herzog et al., 2015; Østerås et al., 2002), skating (Perez et al., 2022; Stenroth et al., 2020), sprinting (Cross et al., 2017; Rabita et al., 2015; Samozino et al., 2016), jumping (Challis et al., 2015; Janicijevic et al., 2020; Jimenez-Reyes et al., 2014; Samozino et al., 2012), squats (Rahmani et al., 2001), and the leg press exercise (Bobbert, 2012), and it has been shown that individuals display different task-specific fFv

capabilities (Samozino et al., 2012). However, in addition to characterizing athletes' force-velocity and power properties and comparing individuals, functional force-velocity profiling is also applied to predict performance. fFv relationships have been utilized to predict performance within the same sport (Dorel et al., 2010; Dunst et al., 2022; Dwyer et al., 2022; Perez et al., 2022; Rabita et al., 2015; Rudsits et al., 2018; Samozino et al., 2016; Stenroth et al., 2020; Vandewalle et al., 1987), as well as across disciplines i.e., in exercises that were not the ones assessed in the fFv profiling test (Challis et al., 2015; Nikolaidis & Knechtle, 2020; Vandewalle et al., 1987). Functional force-velocity profiles across movement tasks have been determined to show the same general relationship between force and velocity that has been observed in muscle force-velocity profiles. The typical pattern is a decrease in force production with increasing movement velocity or, vice versa, decreasing velocity with increasing force. In contrast to Fv profiles, however, most functional force-velocity relationships have been described as linear rather than hyperbolic. This finding, aside from a few exceptions (Herzog et al., 2015; Rudsits et al., 2018), has been confirmed empirically (Challis et al., 2015; Janicijevic et al., 2020; Jaric, 2016; Jimenez-Reyes et al., 2014; McMaster et al., 2016; Rahmani et al., 2001; Samozino et al., 2016), as well as in a modeling project ('quasi-linear'; Bobbert, 2012). Across fFv tasks, we can speculate that the conditions are unlike the ones in Hill's experiment (Hill, 1938) in many ways. There are several muscles working, instead of just one, and they are not isolated but surrounded by connective tissue and connected to the bone via an elastic tendon (Herzog & Loitz, 1994, pp. 148–150). The muscles are likely neither maximally activated throughout the movement, nor operating at their optimum lengths and, moreover, they need to move (i.e., accelerate) not just their own mass but the body segments that they are attached to (Bobbert, 2012). Finally, the velocity that is considered in fFv profiling is the externally measured movement velocity that cannot be assumed to be equal to the contraction

velocity of muscles and fibres. The apparent linearity of fFv profiles comes with two advantages: (1) It is generally preferable to keep a testing protocol as short as possible and even more so in an elite sports environment where time can be a limited resource. Regarding fFv profiles as linear functions means that they can be obtained based on just a few velocity or load conditions and, subsequently, extrapolated to any other force-velocity pair of interest (Challis et al., 2015; Janicijevic et al., 2020; Jaric, 2016; Nikolaidis & Knechtle, 2020). (2) Testing near an individual's maximum force or maximum speed extremes is difficult, for some functional tasks maybe even impossible. For example, a push sled can never have zero resistance, thus the maximal velocity/zero resistance condition cannot be tested practically. Similarly, it would be hard to test for maximum (isometric) force in many functional tasks. Specifically, it has been argued that higher loads for example in jumping or sprinting tests can alter the participants' movement patterns and thus change the movement under investigation (Cahill et al., 2019; Lockie et al., 2003; Markovic & Jaric, 2007). With a linear fFv relationship, the profiles can easily be extrapolated to lighter or heavier loads (or faster and slower velocities) that could not be tested.

Aside from the study by Challis et al. (2015), where the authors correlated take-off velocities from a loaded jump fFv profiling test with athletes' start times in a single push test, there are no reports about fFv profiling being applied to the bobsled (team) push-start. As indicated above, the 4-man push-start comes with position-specific demands for athletes' strength and speed capabilities, which is why we believe that determining functional force-velocity relationships for the athletes on a team (i.e., how much push force they can produce with increasing sled velocity) will be a useful tool and provide an objective basis for selecting and placing the athletes in the optimal position for the 4-man push-start.

2.5 Why individual athletes may display varying force-velocity properties

Functional force-velocity profiling is utilized in various sports because it can help to determine an athlete's capacity to generate power – and to compare their force-velocity-power characteristics to others. But *why* might athletes' individual functional force-velocity profiles differ? What determines an individual's capacity to produce force and move fast?

On the isolated muscle level, one of the main determinants of maximum force capacity is the physiological cross-sectional area (PCSA), where a greater PCSA i.e., more sarcomeres in parallel, is associated with a proportional increase in maximum muscle force (Lieber, 2002, p. 31; Wickiewicz et al., 1983). While the general relationship between PCSA and muscle force is widely accepted, it needs to be acknowledged that it can be more complex in practice, which can be attributed to the fact that there are other factors, beyond the PCSA, that influence a muscle's force production capacity (Jones et al., 2008). First, the *active force-length relationship* of a muscle describes how much maximum isometric force the contractile elements of a muscle can generate as a function of its length (Herzog, 1994, p. 168). Similar to the results from the classic study by Gordon, Huxley, and Julian (1966), which were based on isolated frog muscle fibres, it has been observed that human muscles have individual optimal operating lengths, at which their isometric force is maximized (Lieber, 2002, pp. 51–52; Winters et al., 2011). Second, the *fibre type distribution* in a muscle is an important determinant of the muscle's force capacity. It can be distinguished between fast- and slow-twitch fibres, and fast-twitch fibres have been suggested to be able to produce greater force than the slow fibres (Lieber, 2002, pp. 86–87). Third, in dynamic muscle contraction, the muscle's *force-velocity relationship* (Hill, 1938) needs to be considered, as well, which also marks the transition zone from the factors influencing maximum force

production to the determinants of maximum contraction velocity. How much force a muscle or muscle fibre can produce as a function of contraction velocity is, again, influenced by the *fibre type*. The greater force production capacity in fast twitch fibres compared to slow twitch fibres is paired with higher maximum shortening velocities than can be observed in slow twitch fibres (Herzog, 1994, pp. 174–175). This combination suggests that at a given contraction velocity the capacity for force production in fast twitch fibres is greater than in their slow counterparts. Finally, a second important parameter to determine maximum shortening velocity is *fibre length*, where longer fibres (or muscles with longer fibres i.e., with more sarcomeres in series) can contract at higher maximum velocities than shorter fibres or muscles (Lieber, 2002, pp. 72–73; Wickiewicz et al., 1983).

While it may be feasible to estimate the force to be produced by a fibre or muscle based on its configuration in an isometric situation, the dynamic case is more complex and, moving to an in-vivo setting, perhaps a task like the bobsleigh push start, complicates matters more. Not only does the number of muscles involved increase, each one also now acts in muscle-tendon units. The connection to the bone via an elastic tendon can alter the force produced by a muscle, as well as the moment created about an associated joint (Herzog & Loitz, 1994). Due to multiple muscles working together in groups, the resulting force (or the moment about a joint), will be the product of all the individual architectures (fibre lengths and pennation angles), fibre type compositions, force-length, and force-velocity relationships.

Given that sled pushes are considered a useful training tool to improve sprinting performance (Cahill et al., 2019), it appears reasonable to assume that most of the force produced when pushing the sled is generated in the lower limbs, like in sprinting (Mero et al., 1992; Park et al., 2019; Schache et al., 2015; Wiemann & Tidow, 1995), and then needs to be transferred to the bobsled,

which introduces pushing technique as an additional variable. Finally, in vivo, neural factors play an important role in force production, as well. Instantaneous force production in a muscle can be modulated with varying *activation level*, specifically through modifications of fibre recruitment and stimulation frequency, where an increase in either one of these parameters is associated with an increased force output (Herzog, 1994, pp. 165–166; Mero et al., 1992)

In summary, functional force-velocity profiles have been shown to differ between individuals (Samozino et al., 2012) and there are many different factors that influence an individual's maximum force and velocity capacities for a given task. Due to potential differences in muscle architecture, fibre type distribution, tendon properties or neural control of their muscles, as well as in how accomplished their technique is, different athletes may perform differently – for example in a functional force-velocity test, or when pushing a bobsled down the track. As these variations and their specific consequences are not identifiable purely by observing an individual, testing is required to predict and improve performance.

Part B: Force Effectiveness

2.6 The Concept of Force Effectiveness in Sports

An important aspect in many sports is not only how much force is applied, for example, to a bobsled, a shot, a bicycle, or the ground, but how effectively that force is applied. Approaching the execution of different movement tasks from a purely mechanical perspective may naturally lead to considerations of force effectiveness. The effectiveness of a force depends much on the direction of application. For example, cyclists push against the pedals in a general downward

direction (Cavanagh & Sanderson, 1986; Gruben et al., 2003a). However, only the component of the applied force that is directed perpendicular to the crank will result in propulsion. In sprinting, only the ground reaction force associated with the horizontal component of the resultant force that an athlete applies to the ground will move them forward. In bobsled, athletes want to apply force in the direction of the bobsled track. Consequently, to improve performance in a given task, it may seem reasonable to consider focusing on maximizing those effective force components and to reduce the amount of force lost in unbeneficial directions, thereby increasing force effectiveness. The concept of force effectiveness has been discussed in various settings, for example, in swimming (Toussaint & Beek, 1992), wheelchair propulsion (Bregman et al., 2009; De Groot et al., 2002; Roeleveld et al., 1994; Vanlandewijck et al., 2001; Veeger et al., 1992; Veeger & van der Woude, 1994), sprinting (Hicks et al., 2020; Lockie et al., 2013; Morin et al., 2011; Morris et al., 2022; Samozino et al., 2016), hand cycling (Hettinga et al., 2010) and, probably most extensively, conventional bicycling (Bini et al., 2013; Bini et al., 2014; Cavanagh & Sanderson, 1986; Ericson & Nisell, 1988; Ettema et al., 2009; Gregor et al., 1991; Hasson et al., 2008; Henke, 1998; Kamba et al., 2023; Kautz et al., 1991; Kautz & Hull, 1993; Kistemaker et al., 2023; Korff et al., 2007; Leirdal & Ettema, 2011; Mornieux et al., 2008; Rossato et al., 2008; Zameziati et al., 2006). Efforts to modify technique with the aim to improve force effectiveness have been suggested to be desirable to enhance sprinting performance (Hicks et al., 2020; Lockie et al., 2013; Morin et al., 2011). Conversely, the utility of such an intervention has been found to be debatable, for example, in wheelchair propulsion (Rankin et al., 2010; Vanlandewijck et al., 2001; Veeger & van der Woude, 1994) or bicycling where it has been a topic of research for decades, as can be seen in the examples of references above and is discussed in more detail below.

2.7 Force Effectiveness in Cycling

In pedaling, only the force component perpendicular to the crank causes propulsion and is therefore referred to as effective force. Forces along the crank that do not contribute to propulsion have been considered wasted (Bini et al., 2013; Bini et al., 2014). Force effectiveness is commonly expressed as an ‘index of force effectiveness’, the ratio of the effective force component to the total or resultant pedal force (Bini et al., 2013; Lafortune & Cavanagh, 1983; Zameziati et al., 2006), with a value of 1 indicating perfect effectiveness. It has been shown that cyclists can adapt their pedaling technique to improve force effectiveness (Hasson et al., 2008; Henke, 1998; Korff et al., 2007; Mornieux et al., 2008). However, whether improved cycling effectiveness is associated with improved racing performance has not been demonstrated. Neither recreational nor elite cyclists naturally produce forces purely perpendicular to the crank throughout the pedaling cycle and, for some sections, the resultant pedal force direction deviates substantially from perpendicular (Cavanagh & Sanderson, 1986; Ericson & Nisell, 1988; Ettema et al., 2009; Gruben et al., 2003b; Hasson et al., 2008; Kautz & Hull, 1993; Mornieux et al., 2008; Rossato et al., 2008; Zameziati et al., 2006). Moreover, Coyle et al. (1991) showed that in experienced cyclists those who achieved the greatest power output and largest pedal forces in the downstroke also displayed lower force effectiveness compared to the others. The authors attribute this pattern to the better performing athletes’ ability to recruit their muscles differently (specifically to recruit more muscles), compared to the athletes in the lower performing group. In addition to this mechanical observation, previous work provides evidence that increased force effectiveness may be associated with decreased muscular and metabolic efficiency and, thus, might not be beneficial for performance (Korff et al., 2007; Mornieux et al., 2008). When it comes to modifying specific parameters like, for example, seat height or cadence, the literature provides conflicting evidence regarding the effects of such

modifications on pedal force effectiveness. While the majority of studies suggest decreasing force effectiveness with increasing cadence (Bini et al., 2013; Ettema et al., 2009; Kautz & Hull, 1993; Leirdal & Ettema, 2011), it has also been reported that a freely chosen cadence resulted in the greatest index of force effectiveness, compared to both higher and lower cadence conditions (Rossato et al., 2008), or that there was no effect of cadence (Ericson & Nisell, 1988). Seat position (towards or away from the handlebars) has been found to increase force effectiveness (Menard et al., 2016), as well to have no effect on it (Leirdal & Ettema, 2011). Lower seat height was found to decrease effectiveness (Bini et al., 2011) or to not have any effect on it (Ericson & Nisell, 1988). Finally, the latest addition to this line of research is a recently published study by Kistemaker et al. (2023), in which the authors used a musculoskeletal modeling approach to show that constrained pedal force direction would result in dramatically increased power output, due to suboptimal utilisation of the muscles involved.

Summary Chapter 2

The 4-man bobsled push start is an intricate choreography and proper execution is crucial for a successful run down the track and fractions of a second differences in run time can make a team win or lose a medal. Literature discussing individual push contributions in this team sport is scarce, particularly when it comes to the discipline of the 4-man. The first part of the work presented in this thesis investigates individual push forces and sled speed throughout the 4-man bobsled push start. Furthermore, we explore a dry-land sled push testing and its potential to be used as a training and/or recruitment tool for bobsleigh teams in the future. The second part of this thesis work was focused on the effects of constrained pedal force direction (with the aim to achieve complete force effectiveness) on pedal force output i.e., magnitude. Various ways to increase pedal force

effectiveness have been explored over the years. And while cyclists can learn how to pedal more effectively, there is strong evidence suggesting that focusing on maximizing pedal force effectiveness is not desirable. Our study aimed to provide empirical evidence for this notion. The data in the following chapters are important additions to the literature in both fields, will provide new insights for athletes and coaches in both sports and can inform future training and assessment protocols.

Chapter 3

Methods: Instrumenting a Prowler (Gym Sled) and a Bobsled

As indicated in the introduction, our Bobsled project consisted of two parts: (i) gaining insights into the kinematics during the 4-man bobsled push start, and (ii) investigating functional force-velocity profiles determined using sled pushes using a prowler (gym sled). The main outcome variables in both cases were the individual athletes' push forces and sled velocity, and since there was no off-the-shelf system available for this purpose, we had to develop our own. The process of the design and development of the instrumentations for both a bobsled and a prowler, as well as the final set-ups, are presented in this chapter.

Chapter outline:

Chapter 3.1 is based on a short communication, currently in review for publication in the Journal of Biomechanics. It focused on the instrumentation that was used to measure push forces on the bobsled. *Chapter 3.2* contains information about how the instrumentation for the prowler differs from the instrumentation used in the bobsled. *Chapter 3.3* describes the instrumentation used to measure the velocity of both the bobsled and the prowler. Lastly, *Chapter 3.4* is a summary of 3.1 through 3.3 and an introduction for the next few sections of the thesis.

3.1 Development of the Instrumentation of a 4-man Bobsled

This chapter is based on: Onasch, F., Sawatsky, A., Stano, A. & Herzog, W. (2023). Development of the Instrumentation of a 4-man Bobsled. *Journal of Biomechanics* 152, 111578. DOI: 10.1016/j.jbiomech.2023.111578.

Individual contributions: Franziska Onasch, Andrew Sawatsky, and Andrzej Stano developed the methodology. ASa and ASt developed/provided the instrumentation. FO performed the analysis and wrote the manuscript with input from all co-authors. FO and Walter Herzog acquired funding for the project. WH supervised the project and provided critical feedback.

3.1.1 Abstract

A bobsled race can be won or lost at the start, and the contribution of the athletes during the start phase is crucial. Nevertheless, the details of that contribution are not well understood, and we believe that, to improve team performance, it is necessary to determine the contributions of the individual athletes to the bobsled's speed throughout the start phase. The goal of this project was to develop the instrumentation for a 4-man bobsled that allows for measuring the propulsive forces of each athlete during the bobsled push start. We describe the final set-up and discuss potential applications. The instrumented bobsled can be used to provide novel and important information about individual athlete and team performance during the start phase of bobsledding.

3.1.2 Introduction

A bobsled run can be divided into two sections, the push start, and the driving phase. There is a strong positive relationship between start times (measured over a 50 m distance from the start line) and the total run times in all bobsled events (Morlock & Zatsiorsky, 1989), and a rule of thumb in the sport is that 1/10 of a second lost at the start turns into a 3/10 s deficit at the finish line.

Moreover, at the 2018 Olympics, two teams tied for the gold medal with the same time to the 100th of a second, indicating that even small improvements at the start can have a great impact on placing in international competitions.

Except for the Monobob, bobsled requires a team effort, with two (2-man/-woman) or four (4-man) athletes accelerating the sled from a zero-speed starting position. The objectives of the start phase are to cover the start distance as quickly as possible, and to maximize the exit speed at the end of the start phase. The bobsled start may be divided into two sections. The first part consists of a 15 m run up to the start line, during which the athletes try to achieve the highest possible speed from a still start, before officially entering the race. In this first phase, the track has a downhill slope of about 2 %. The second section, and the official timing, start at the 15 m mark. All four athletes continue to push and accelerate the sled until, one by one, they board the sled. In this second phase, the slope of the track gradually increases to and then remains constant at about 12 %. The official start time is measured at the end of the second section, 50 m from the start line (IBSF, 2019).

Although the contribution of athletes to start performance is a crucial aspect of the sport, there are only few scientific publications discussing the push contribution of each athlete. Among the first to mention the importance of understanding individual push contributions was a short abstract by Leonardi and colleagues (1985). Since that work, push force contributions to the bobsled start have been investigated by three groups. Using a simulation approach, Dabnichki (2015) concluded that optimized timing of loading (when the athletes jump into the sled) can increase the start exit speed by up to 1 km/h. Lee and colleagues (2015) instrumented a 2-man bobsled with load cells to determine the contributions of the two athletes during the start phase, and Peeters et al. (2018)

instrumented a sled-like 2-man frame on wheels, pushed by recreationally active individuals, and related how well participants synchronised peak force in the first push to exit speed and start time.

Compared to a 2-man bobsled, the start phase of a 4-man bobsled is more complex and technically more difficult because two more athletes need to load the sled from the side. The timing of the four athletes pushing and entering the sled requires precise coordination that is not required to the same extent in the 2-man event. The contributions of athletes to the start in the 4-man sled, the optimal coordination between athletes, and the assignment of push positions remain unknown. We hypothesize that the instantaneous contributions of each athlete to the propulsion of the bobsled throughout the start phase, the coordination among the athletes, and the timing of loading the sled may provide important information in the selection of athletes, the assignment of positions to the athletes, and the effectiveness of the 4-man team relative to the crew members' individual capacities. Therefore, the objective of this study was to design and build a 4-man bobsled that allows for simultaneous measurement of the contribution of each athlete to the acceleration of the sled, as well as determination of the acceleration, speed, and displacement of the sled during the start phase. The report by Lee et al. (2015) was used as a guide for the design of our sensor set-up.

3.1.3 Methods and Results

A 4-man crew consists of the pilot (**aP**), who pushes on the bar in the front, one athlete pushing on the left side (**a2**), one pushing on the right side (**a3**), and the brakeman (**aB**), who pushes at the back of the sled (**Figure 3-1A**). **aP**, **a2**, and **a3** place both hands on their push bars, while **aB** uses two handles, one for each hand. While the location of the brakeman's hands is well defined during the push, the hand positioning of the remaining three team members is not. The bars for **a2** and **a3** are about 30 cm long, the pilot's bar up to 50 cm. There are no rules that regulate hand placement,

which allows athletes to find their preferred grip positions. Therefore, it was necessary to design the instrumentation for unknown hand positioning.

Our push bar instrumentation is shown schematically in **Figure 3-1B**, which shows the side push bar used by **a2** or **a3**. The bars are solid aluminum, and an indentation was added on all four sides of the bar to create an area of strain concentration, where the strain sensors were placed. Two pairs of resistive strain gauges (Micro-Measurements, Raleigh, NC, USA) were placed on opposite sides of the bar in a half-bridge arrangement for recording the horizontal and vertical components of the push force. The sensors were paired on each side of the bar because push forces had to be calculated without knowing the location of an athlete's hands. If sensor 1 (S_1) is at a greater distance from an applied force than sensor 2 (S_2), the following applies:

$$M_1 = d_1 \cdot F \quad [3.1]$$

and

$$M_2 = (d_1 - x) \cdot F \quad [3.2]$$

where M_1 and M_2 are the moments produced by the resultant push force (F) about S_1 and S_2 , respectively, d_1 is the perpendicular distance between force and S_1 , and x (measured with calipers) is the known distance between sensors S_1 and S_2 . Since F - the resultant force of both hands - is the same in both equations and M_1 and M_2 are known through appropriate calibration experiments, we can solve for the only unknown, the resultant push force, F , using:

$$F = \frac{M_1 - M_2}{x} \quad [3.3]$$

While the pilot's bar is longer than the side bars for **a2** and **a3**, the sensor working principle and placement are the same as those used for **a2** and **a3**. Signals from the push bars were filtered using a cable-integrated 50Hz lowpass Butterworth filter.

For the brakeman handles, FlexiForce force sensors (Tekscan, Boston, MA, USA) were used. There is one handle for each hand, and each handle consists of two parts. During the start phase, the athlete will start with their hands on the lower parts of the handles, and then, after the first big push, move them up to the upper part of the handles. Therefore, each handle was instrumented with two independent sensor units. One unit consists of three force sensors, capable of measuring up to 445 N each. FlexiForce force sensors are small, with a circular sensing area of 0.9 cm in diameter and by using three sensors for one unit, we were able to reach the desired force capacity. To cover the entire area of the handles and distribute the brakeman's push force across the sensors, we fixed them to a base plate, added a rubber disk on top of each sensor, and a metal plate on top of the three rubber disks (**Figure 3-1C**).

Calibration of the push bars was performed by hanging known weights from different locations of the bar (**Figure 3-2**) and then relating the known moment to the voltage output of the sensors. To account for crosstalk between sensors, each sensor was calibrated based on the output of all four (horizontal and vertical) sensors.

$$\begin{bmatrix} V_1 & V_2 & V_3 & V_4 \\ \vdots & \vdots & \vdots & \vdots \end{bmatrix} \cdot \begin{bmatrix} c_{11} & \cdots & c_{14} \\ \vdots & \vdots & \vdots \\ c_{41} & \cdots & c_{44} \end{bmatrix} = \begin{bmatrix} M_1 & M_2 & M_S & M_4 \\ \vdots & \vdots & \vdots & \vdots \end{bmatrix} \quad [3.4]$$

with M_1 = the moment acting about S_1 , V_1 = the voltage output of S_1 , etc., and the c-matrix representing the calibration coefficients (**Table 3-1**). The moment calibration function for the second horizontal sensor, for example, looks like this:

$$M_{S2} = V_{S1} \cdot c_{12} + V_{S2} \cdot c_{22} + V_{S3} \cdot c_{32} + V_{S4} \cdot c_{42} \quad [3.5]$$

The resulting moments (**Figure 3-3**, for agreement with the known values) were used to calculate push force in each direction (**Equation [3.3]**). The brakeman handles were calibrated using a

material testing machine (MTS, 858 Mini Bionix II, Eden Prairie, MN), with the following compression protocol: 3 conditioning ramps to 1500 N, hold for 10 s, release, at $2 \frac{\text{mm}}{\text{s}}$, followed by 20 cycles from 0 to 1500 N at $2 \frac{\text{mm}}{\text{s}}$. The voltage output from the sensors was then related to the known force from the MTS machine. Initially, the full range from 0-1500 N was used to determine the sensors' calibration coefficients. The first data collection, however, showed that push forces applied by the brakemen were much smaller than we had anticipated. Therefore, calibration coefficients were recalculated, based on forces from 0 to 700 N (**Figure 3-3**). Force error estimates for both push bars and brakeman handles are shown in **Figure 3-4**.

To obtain sled acceleration and velocity, an Inertial Measurement Unit (OPAL, APDM, Portland, USA) was placed on the cowling near the tip of the bobsled. Using a modified version of code by Rebula and colleagues (2013), 3D acceleration and 3-axial gyroscope data were integrated to calculate sled velocity.

The system was tested with elite bobsled athletes on a training replica of the start ramp of the Calgary Olympic bobsled track. Push forces were recorded at 400 Hz per channel with a NI USB-621x DAQ-box (National Instruments, Austin, TX, USA). Sample results for push force are shown in **Figure 3-5**.

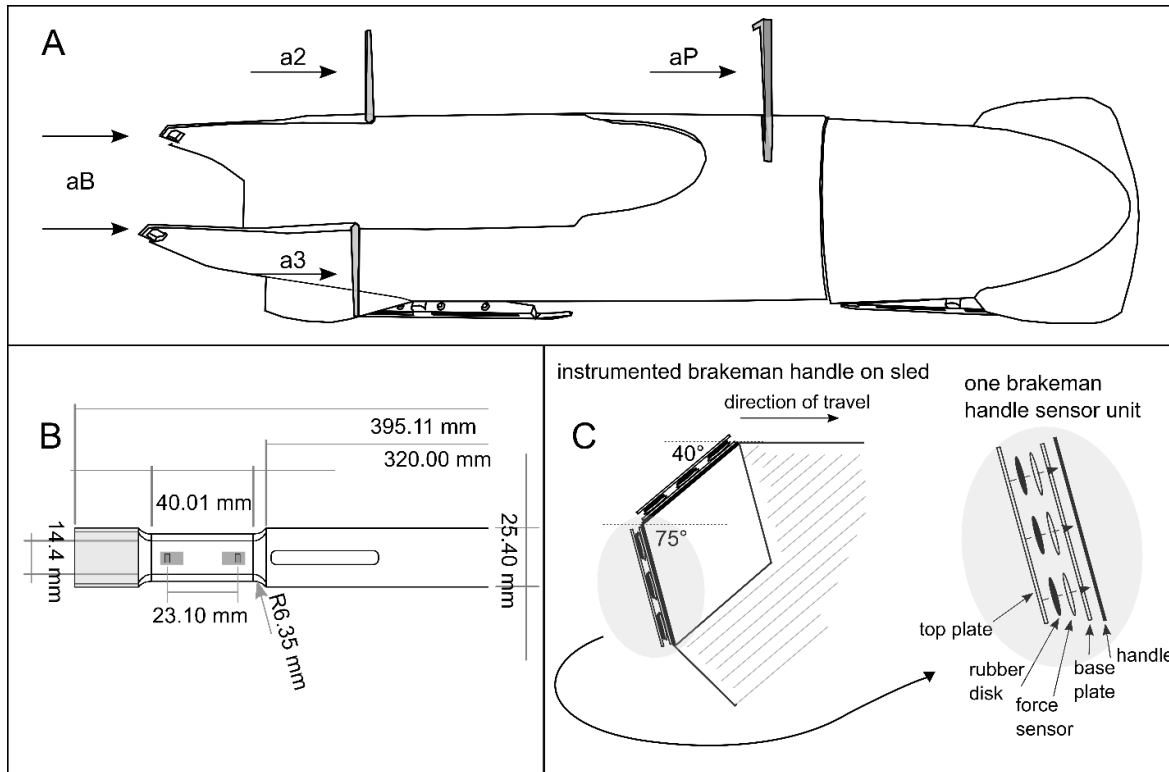


Figure 3-1: Overview of the force sensor instrumentation. **Panel A** shows a 4-man bobsled, with the arrows indicating the points of push force application by the athletes. Three of the four athletes push on one bar with both hands. The fourth athlete, the brakeman, pushes at the end of the sled with a separate handle for each hand. **Panel B** shows a schematic of the sensor set-up on the push bars. The two grey-shaded boxes depict the strain gauges, with the black rectangles indicating the location of the actual sensor areas. The light grey shaded end of the bar is the part that attaches to brackets on the sled. Push forces are applied to the white part to the right of the sensors. **Panel C** shows the set-up of the brakeman handle instrumentation: The schematic on the left shows the orientation of a set of brakeman handles on our sled, with sensor units on top; the grey-shaded area indicates the body of the bobsled. The right schematic shows the details of one sensor unit: a sandwich of force sensors with rubber disks for equal force distribution between two metal plates.

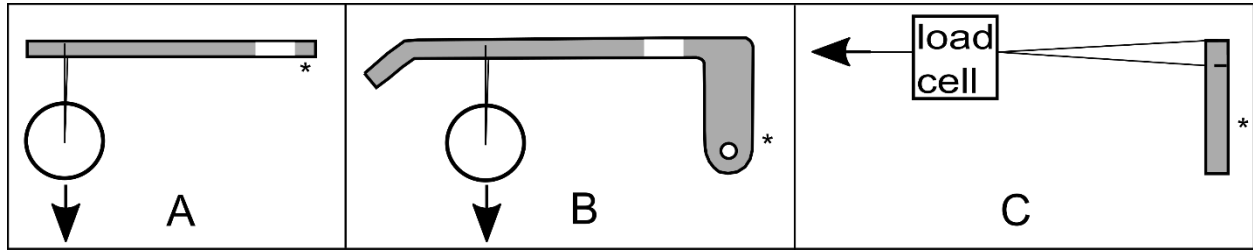


Figure 3-2: The push bars were calibrated by hanging known weights at known distances from the sensors and then relating the output voltage to the calculated moments. Side bars, with their square base could be rotated and clamped to calibrate forces in the horizontal and vertical direction (**panel A**). The pilot bar can only be fixed in one orientation, which led to two different calibration approaches for vertical (**panel B**) and horizontal (**panel C**) sensor pairs. Grey shaded structures are the push bars, with the asterisk indicating roughly where a bar was attached to the sled. White boxes indicate the indented sections where the strain gauges were attached.

Table 3-1: Calibration coefficients $\left(\frac{Nm}{V}\right)$ to calculate the moment acting about a given sensor (S1 through S4) on the bobsled push bars, based on the voltage output measured in all four sensors for a given loading situation. The moments that were compared to the known moments, as illustrated in **Figure 3-3**, were calculated using the coefficients presented here.

PILOT	S1 (horizontal)	S2 (horizontal)	S3 (vertical)	S4 (vertical)
	64.845	-27.975	47.240	41.863
	90.278	181.243	-52.648	-44.91
	3.253	2.033	175.503	10.392
	-4.155	-2.956	14.605	177.748
LEFT	S1 (horizontal)	S2 (horizontal)	S3 (vertical)	S4 (vertical)
	103.226	5.538	8.381	5.637
	-9.650	88.249	-8.302	-6.733
	-2.862	-2.913	96.264	6.064
	4.850	2.785	-2.298	93.249
RIGHT	S1 (horizontal)	S2 (horizontal)	S3 (vertical)	S4 (vertical)
	87.47101	-7.0018	-6.18213	-3.06955
	7.640577	101.9783	6.074275	3.27631
	7.813098	5.819703	89.33273	-2.39296
	-7.81895	-5.6525	5.941662	102.8443

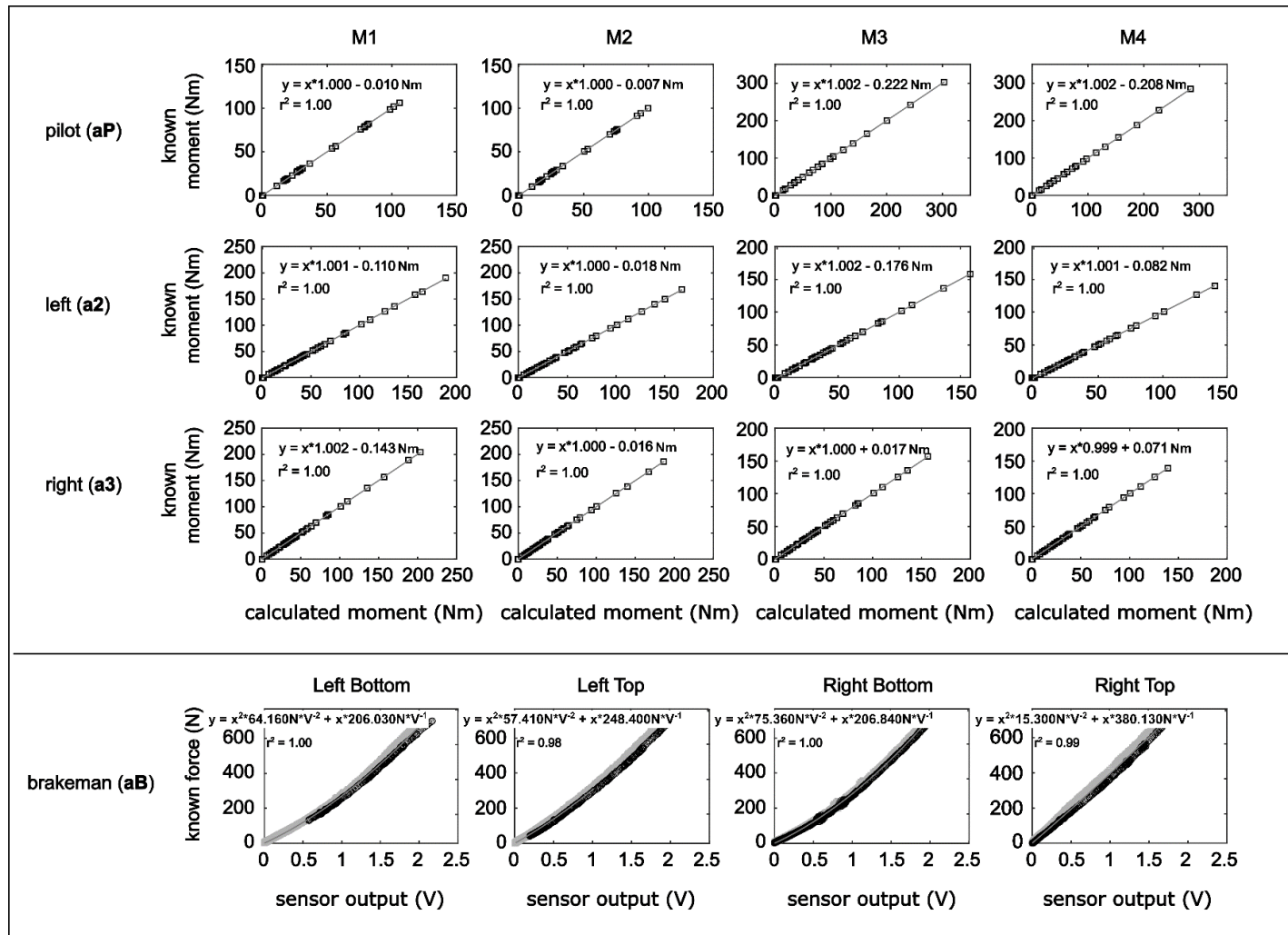


Figure 3-3: First part of results from the calibration process. The **top panel** shows the agreement of calculated moments based on the sensor calibration with the known moments that were applied to the bars (strain gauges on aluminum). Individual data points are represented by black squares, calibration curves by grey lines. The **bottom panel** shows the calibration curves and equations for the brakeman handles (force sensors). Grey circles represent the sensors' behaviour in loading, black in unloading. Dark grey lines indicate the calibration functions (brakeman handles) and regression lines (push bars).

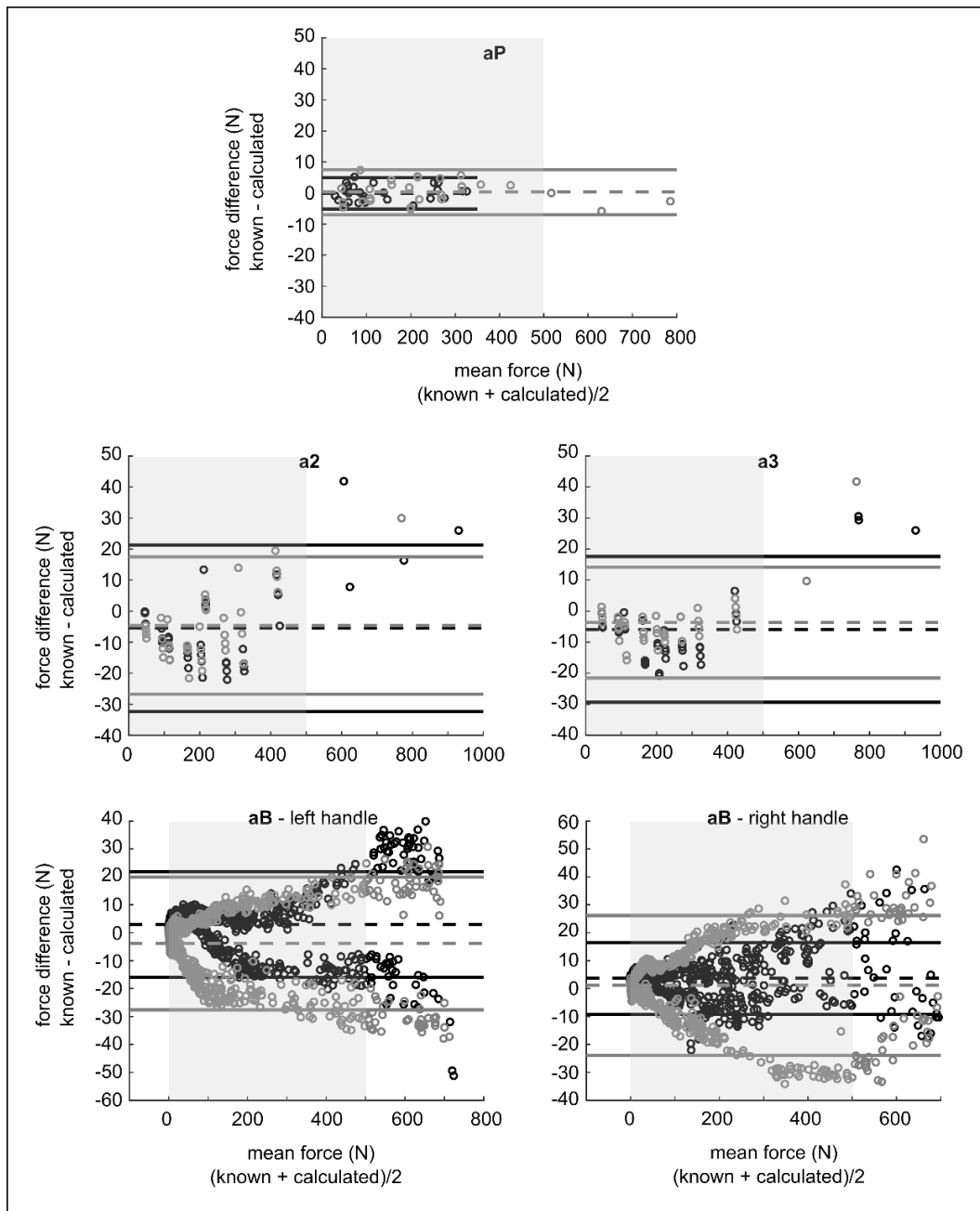


Figure 3-4: Bland-Altman plots (Altman & Bland, 1983) comparing calculated force to known force to illustrate potential measurement error for the different sensor units. For pilot, left and right bar: black circles = horizontal force, grey circles = vertical force. For brakeman handles: black circles = bottom sensor for given hand/side, grey circles = top sensor for the same side. Horizontal dashed lines indicate mean differences in force, solid lines the upper and lower bounds of the 95 % confidence intervals. The deviations of calculated from known force shown above correspond to median errors of 6 %, -7 %, 4 %, and -5 % for **aB** left bottom, top, right bottom and top, respectively, as well as 0 % for **aP** vertical and horizontal, -6 % and -5 % for **a2** horizontal and vertical, and -5 % and -3 % for **a3** horizontal and vertical, respectively. The shaded regions in each figure mark the ranges of force that were observed for a given sensor during the push phase of the bobsled start (not including the initial push that accelerates the sled from its zero-speed starting position).

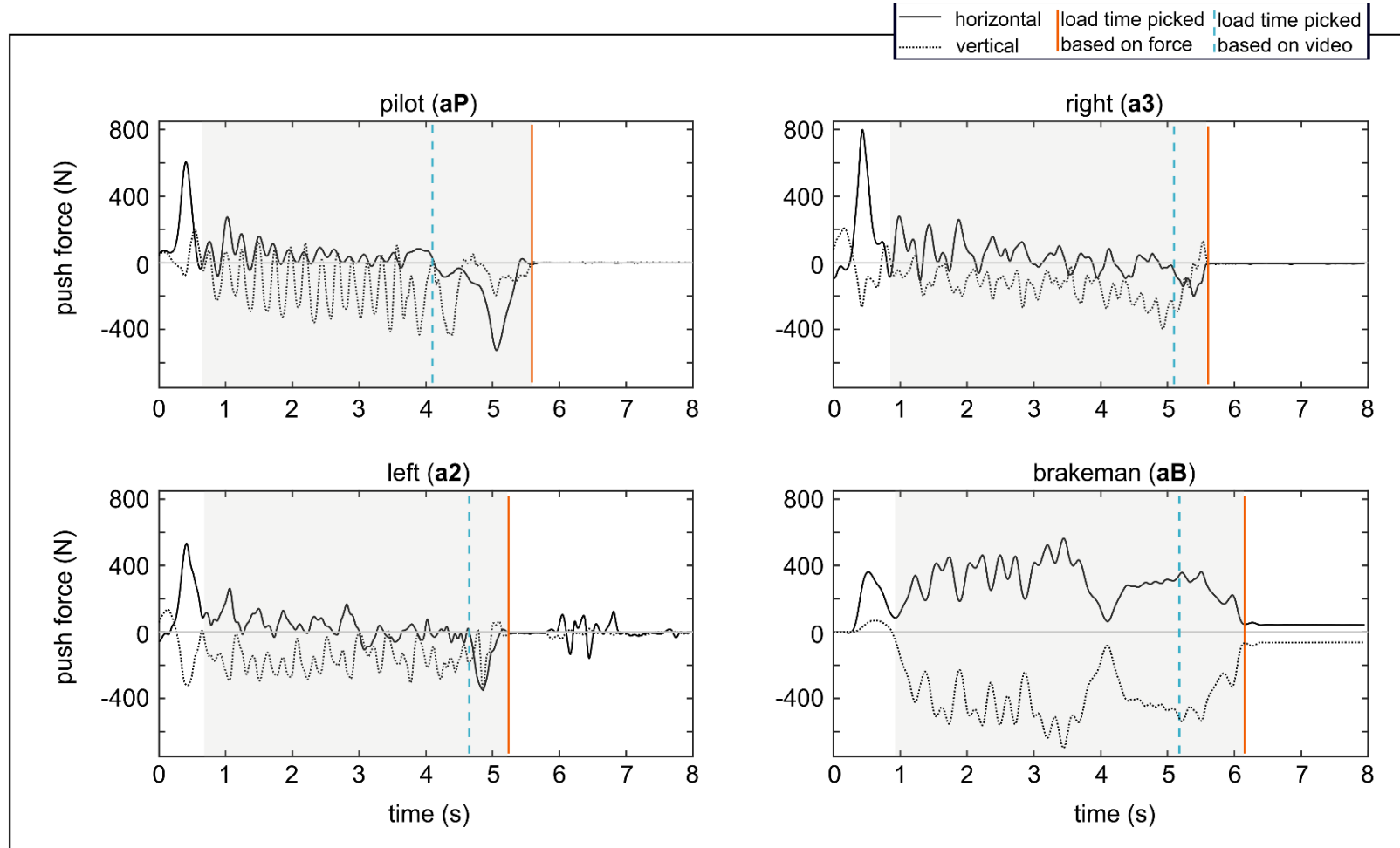


Figure 3-5: Data from a sample trial that were collected from the instrumented push bars (**aP**, **a2**, **a3**) and the brakeman handles (**aB**): horizontal and vertical push force components (solid black and dotted traces, respectively) in the global frame, where the vertical axis is aligned with gravity. For the brakeman, the traces are the sums of the forces measured from left and right hand. The solid vertical lines (orange, if in colour), show the instance of loading/no more push contribution for a given athlete, as we would determine it based on the force recordings. The dashed vertical (blue) lines indicate the (approximate) time of loading based on a video recording.

3.1.4 Discussion

We built a measurement system to assess individual push force contributions in a 4-man bobsled start. While the system is not perfect, it can be used to provide novel and important information about individual athlete and team performance during the start phase of bobsledding.

Potential sources of error in force measurement: (i) Two strain gauges used to measure the variable push force were placed close to each other. This arrangement had the advantage that athletes had complete freedom of where to place their hands. The disadvantage is that even small errors in the inter-sensor distance “ x ” (Equations [3.2] & [3.3]) affect both the accuracy of the calibration of the instrumented force bars and the push force calculation. (ii) When designing the instrumentation, we did not know what push force magnitudes to expect. Aiming to avoid signal clipping, we chose sensors and amplification settings that would allow for measuring high forces and big strains. A bigger measuring range, however, results in reduced resolution. Our expectations for the push forces were generally appropriate, but optimization of the system would now be possible. The brakeman handles were designed to measure forces up to 1500 N each, which is roughly three times more than the actual peak forces applied. (iii) Another concern is that the forces from the brakeman do not show the same fluctuation around zero that is produced by the **aP**, **a2** and **a3** athletes. One possible explanation is that the brakemen squeezed the handles while pushing the sled, which cannot be teased out with the current set-up but would add a baseline force that does not have a propulsive effect. However, while squeezing of the handles could explain part of the brakeman force patterns, it likely cannot account for the several hundred Newtons of force that we see throughout the pushes. Other reasons might be: (I) a slow dynamic response of the sensors that results in a delayed response in unloading. (II) The brakemen can put all their body

weight on the handles when loading the sled, therefore, it seems possible that they might lean on the sled handles more than the other team members between steps, potentially as a strategy to better keep up with the increasing sled speed. (III) the force sensors for the brakeman are meant to be loaded in compression only. However, the athletes may have produced shear forces, thereby potentially affecting the performance of the sensors.

The timing of athletes loading the sled was not readily visible from the force traces. Video data helped to identify this crucial part of the start phase and will be required for future analyses aimed at studying the start and loading phase of bobsledding.

Recommendations: The issue of small differences in strains recorded between the two strain gauges on the push bars could be resolved by increasing the distance between them. However, the length of the push bars is regulated, thus leaving little space for the force sensor placement without affecting the hand position of the athletes and, thereby, potentially performance. Alternatively, the material or the design of the bar could be altered to maximize the strain differential between the sensors while keeping the sensor placement as is.

The brakeman handles could be designed for lower maximum force capacity, which would increase sensitivity at lower forces. Lastly, while we can register and measure when **aP**, **a2** and **a3** pull the sled back instead of pushing forward, pulling forces applied by the brakeman cannot be measured with the current design. When loading the sled, athletes may produce pulling (breaking) forces and, if so, this would be important to quantify as it could have a considerable negative effect on propulsion.

Application: Continuous measurement of the push forces for each athlete throughout the start phase can be used to establish basic information that is largely unknown. For example, how much

propulsive force is applied by each athlete? How synchronous are the athletes in pushing, and what is the timing of loading the sled? What are running speed and propulsive force for each athlete just before boarding the sled?

Furthermore, the sled should prove useful for determining a variety of performance criteria valuable to scientists, coaches, and athletes. The following is just a small list of possible applications:

Identifying

- (i) the factors that contribute to a good/bad start of a given team by comparing the force-time profiles of the athletes between starts resulting in different performances (start time, exit velocity).
- (ii) the contributions of individual athletes to the speed of the sled at various phases of the start: at the beginning when sled velocity is low and acceleration high vs. the end of the start phase when sled velocity is high, and acceleration is low.
- (iii) optimal timing of loading for each athlete.
- (iv) optimal placement of the athletes by rotating push positions.
- (v) the best team composition when more than three athletes compete for the three push positions.

3.1.5 Acknowledgements

We would like to thank *Own The Podium* for financial support, *Bobsleigh Canada Skeleton* for support in the data collection, and the members of the *Science Workshop at the University of*

Calgary for technical support. We would also like to thank our anonymous reviewers for their invaluable feedback.

3.2 Taking a Step Back: The Evolution of the Sensor Set-up for Force

Measurements on Prowler and Bobsled

As mentioned in the introduction to this chapter, developing the force instrumentation was a process, and the first set of push bars that we made were the ones that were eventually used for the prowler. From the beginning, and just as described above for the bobsled, we aimed for a sensor design that would allow for the measurement of push forces without knowing the points of force application. The solution that we chose for this problem was to place pairs of strain gauges on the bars. Push force (F) could then be calculated as $F = (M_1 - M_2)/x$ (**Equation [3.3]**), with x = the known distance between the two strain gauges in a pair, and M_1 and M_2 = the moments acting about the two sensors, which were calculated based on a previous calibration procedure. The bars for the prowler are solid aluminum with a 2.5 cm * 2.5 cm cross section, and the strain gauge placement is illustrated in the schematic in **Figure 3-6**. All four sides of a bar were instrumented, with the sensors on opposite sides (A-I & C-I, A-II & C-II, B & D, **Figure 3-6**) wired together, to sum and thereby amplify their signals. Sensor calibration was performed by hanging known weights at different locations across the bars, as described for the bobsled above (**Figure 3-2; Equations [3.4] & [3.5]**). The resulting calibration coefficients for the individual sensors (2 horizontal and 1 vertical per bar), based on the output from the sensors during loading, are presented in **Table 3-2**. **Figure 3-7** shows (based on the calibration data) the agreement between known and calculated moments, forces, and moment arms.

For the vertical direction, only one strain gauge was placed on each side of the bar, instead of a pair. The rationale for this arrangement was that the signals from the horizontal sensors could be used not only to determine the push force in the horizontal direction, but also the corresponding

moment arms (d_1 or d_2 , associated with A-I/C-I or A-II/C-II, respectively). Since the vertical (B and D) and the proximal horizontal sensors (A-I and C-I, **Figure 3-6**) were aligned, the moment arm $d_2 + x = d_1$ would have to be the same in both the horizontal and the vertical direction. Therefore, one vertical strain sensor should have been enough to calculate the force applied in the vertical direction based on

$$\frac{M_{vertical}}{(d_2+x)} \quad [3.6]$$

Unfortunately, it turned out that the strain differentials in a pair of strain gauges (A-I/C-I vs. A-II/C-II) were small, and the signals noisier than expected. This combination affected the calculations of force and moment arm and, therefore, led to the following modifications of both the system and part of the processing protocol:

- (i) To reduce the noise in the raw signal, we integrated a physical 50 Hz low-pass Butterworth filter into the cables leading from the sensors to the data acquisition box.
- (ii) In the study in which the prowler with this first set of push bars was used (Chapter 4), hand position was controlled by two stripes of tape between which participants were asked to place their hands. When calculating the moment arm length, any value that would be greater or smaller than what was possible within the constraints of the dimensions of the bar was forced to the maximum or minimum possible value, respectively. Then, assuming that once someone was running and pushing the sled, they would not move their hands on the bars, an average moment arm length was calculated across an entire trial and was then used to determine the vertical push force component for that trial.

- (iii) Finally, closing the loop to Chapter 3.1, a second set of bars (pilot, left, and right) was manufactured for the bobsled, and their instrumentation was informed by our experiences with the initial design for the prowler. In short, pairs of strain gauges were now placed on all four sides of each push bar and the cable-integrated filter was applied to the bobsled set-up. For a more detailed description and an outline of the instrumentation of the brakeman handles, please refer to Chapter 3.1.

Table 3-2: Calibration coefficients $\left(\frac{Nm}{V}\right)$ to calculate the moment acting about a given sensor (S1 through S3) on the prowler push bars, based on the voltage output measured in all three sensors for a given loading situation. The moments that were compared to the known moments, as illustrated in **Figure 3-7**, were calculated using the coefficients presented here.

LEFT			RIGHT		
S1 (horizontal)	S2 (horizontal)	S3 (vertical)	S1 (horizontal)	S2 (horizontal)	S3 (vertical)
82.418	2.493	10.469	76.676	-6.478	3.717
12.028	90.087	-9.915	20.574	101.798	-3.052
-1.105	-0.422	92.615	-2.739	-2.116	93.583

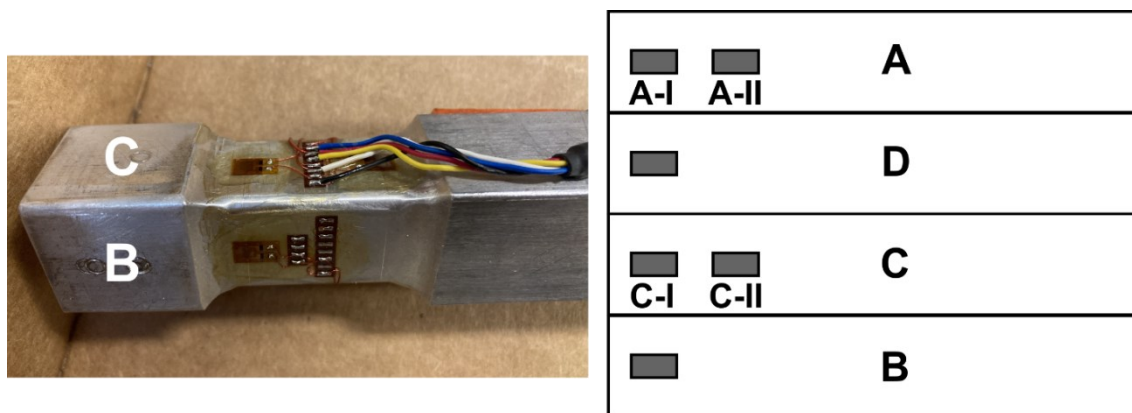


Figure 3-6: Strain gauge set-up on the push bars for the prowler. The part of the bar marked with the letters was clamped to the sled, push forces are applied to the right of the strain gauges (dark grey boxes) with the propulsive push force direction pointing into the page. The sketch on the right represents the bar as it would be unfolded, with the dark grey boxes representing the strain gauges. Sensors on side A and side C pick up deformation due to push force applied in the horizontal direction, while the sensors on sides B and D register strain resulting from force application in the vertical direction.

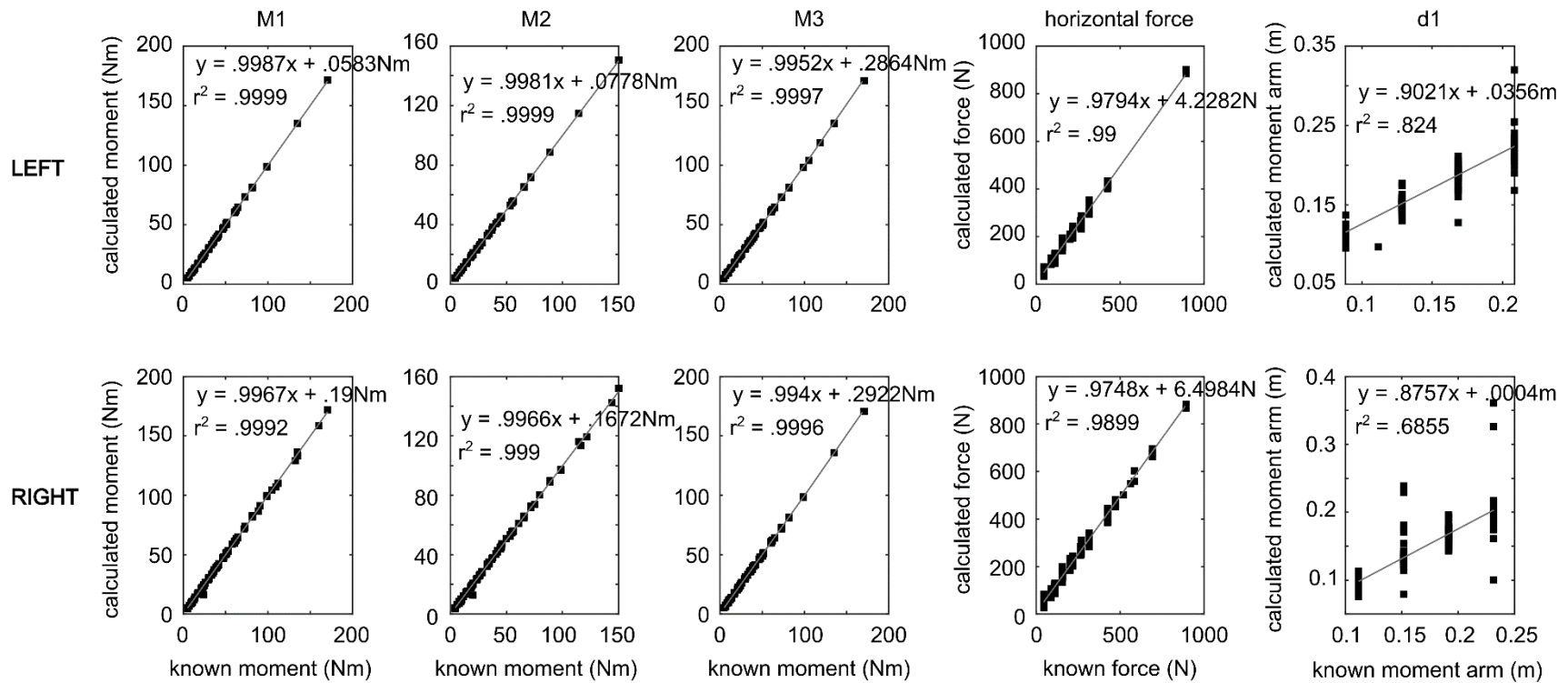


Figure 3-7: Results of the push bar calibration for the prowler. The **top row** shows the agreement of calculated moments, horizontal forces and moment arms based on the sensor calibration with the known moments, horizontal forces, and moment arms for the left bar. Individual data points are represented by black squares, the regression lines by grey lines. The **bottom row** shows the same parameters for the right push bar.

3.3 Determining Sled Velocity

Just like for the force measurement, two slightly different approaches for measuring velocity were chosen for the two sleds (prowler vs. bobsled). An intuitive choice of tools when it comes to determining movement speeds is to record video. However, there are a few things to be considered with this approach: tracking the object of interest in videos can be time intensive, and the camera needs to be set up parallel to the plane of movement of the object. If an object (or person) moves across a great distance, the camera either needs to be placed further away, or multiple cameras may be required, which then also means that an appropriate synchronizing system needs to be in place. For the prowler push project, it was possible to set up a camera (120 Hz, HS EX-ZR700, Casio, Tokyo) and to install a 3D accelerometer on the sled, with the goal to compare the sled velocity calculated from the two systems. Advantages of the accelerometer approach were that (i) its data could be recorded in the same data acquisition box as the force data and thereby be inherently synchronized, and (ii) data processing times were faster than video processing. Velocity was calculated from the acceleration signal as follows: the sensor was attached to the sled such that one axis (z) was aligned with the main direction of movement of the sled, parallel to the ground, the second axis (x) was oriented along the medio-lateral axis, and the third axis (y) was aligned vertically. We integrated the acceleration with respect to time to obtain the velocity for each sensor axis individually and then, after detrending the data, calculated sled speed as the magnitude of the x- z-velocity vector. As is outlined in more detail in Chapter 5, the main outcome variables of the prowler push study were push force and the sled's peak average velocity. This value was calculated as the average of the region of the data $\geq 95\%$ of peak speed for a given trial. Comparison between the video- and accelerometer derived peak speeds was very good, with

$r^2 = 0.994$ and mean difference in measurements (speed from accelerometer minus speed from video) = $-0.12 (\pm 0.25) \frac{m}{s}$ (Figure 3-8).

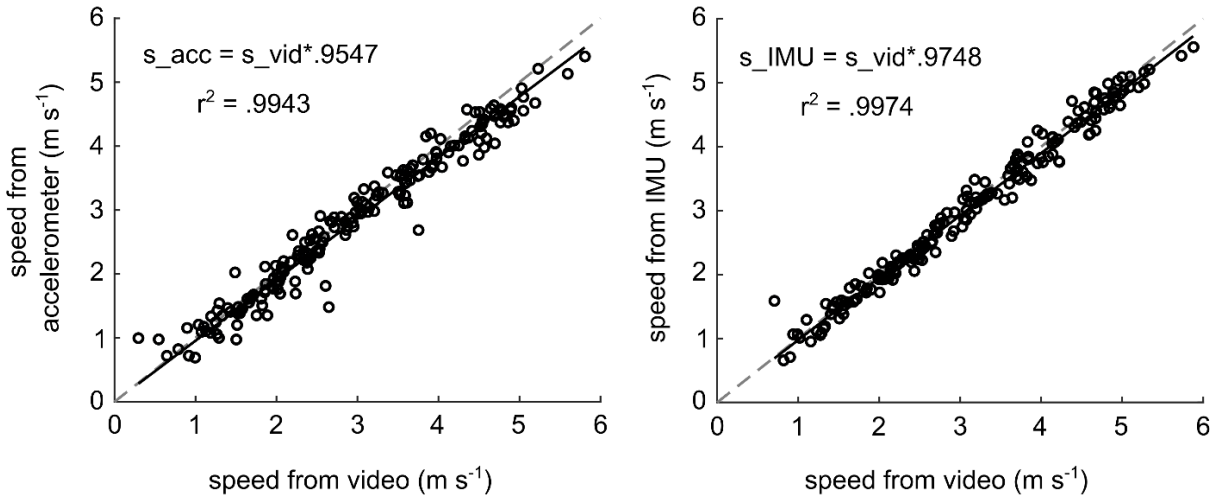


Figure 3-8: Average Peak sled speeds as determined from video recordings compared to calculations based on acceleration data from a 3D accelerometer (left panel) and from an Inertial Measurement Unit (right panel). Each circle represents one push trial (190 total), the regression lines (solid black lines) were forced through zero. The dashed grey lines are unity lines.

For the bobsled, the situation was more difficult than for the prowler. The ice track is built indoors, without much room on the side for cameras and the start portion of the track is about 60 m long and of downward slope. To cover the entire start phase, multiple cameras (and a system to synchronize them) would have been required. Such a system, even though possible for research would likely never be used by coaches and athletes for training purposes. The same type of 3D accelerometer that was used on the prowler was installed on the bobsled. However, the variable slope of the track could not be captured by measuring linear acceleration only, which meant that it was not possible to accurately derive sled velocity from the accelerometer data either. In the

following, I outline the steps that we took to account for the variable incline of the track and to incorporate the information about the track profile when determining the velocity of the bobsled.

First, we were provided with a copy of the plan of the track, and the schematic in **Figure 3-9** was derived from the drawing as follows: The straight sections were taken from the sketch and the profile of the part with changing slope was determined by modeling a function that fit the other two parts together. The slopes of the straight sections matched what we had expected based on the IBSF specifications (IBSF, 2019), namely 2 % (or 1.14°) and 12 % (or 6.80°) and were further confirmed by previous measurements done on the same track (Poirier, 2011).

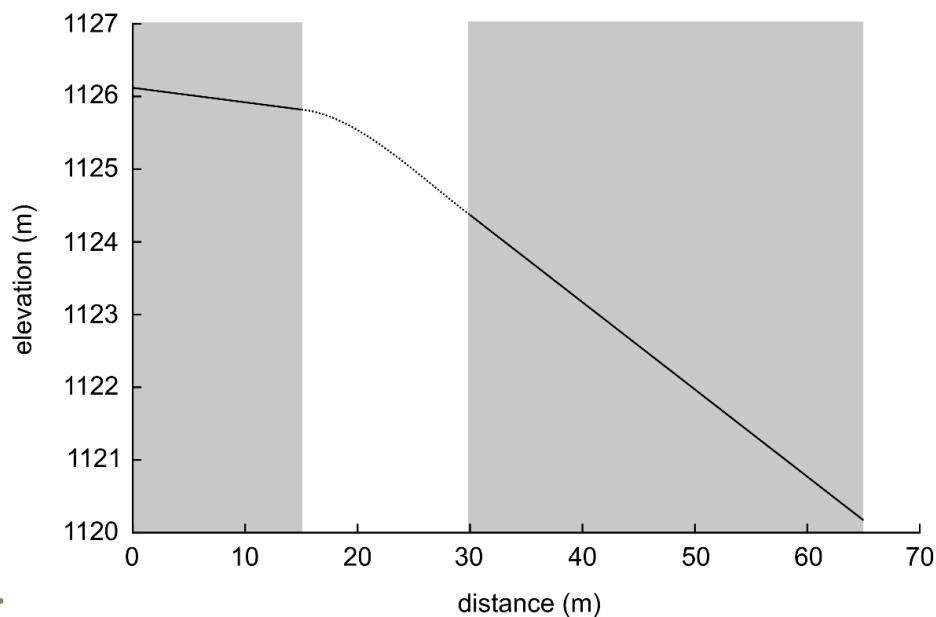


Figure 3-9: The profile of the bobsled track at the Ice House Calgary, based on sketches of the track as well as previous measurements of the slope on the same track (Poirier, 2011). The straight sections on grey shaded background were obtained directly from the drawing of the track, the dotted part was derived by modeling a function that fit the two straight sections together.

While the track profile is the same for each push start, a team's position on the track and the associated slope at a given time vary between trials, depending on how fast the athletes move

during their push start. Therefore, to account for both slope and time, we used an **Inertial Measurement Unit (IMU)**, a device that measures 3D linear acceleration, as well as 3D angular velocity. One Opal IMU (APDM Wearable Technologies Inc., Portland, OR) was attached to the cowling of the bobsled, near the front tip, in a location that was parallel to the floor. Subsequent calculation of the velocity of the bobsled was based on the assumption that the change in orientation of the IMU would be a good representation of the change in orientation of the sled. Using a modified version of code developed by Rebula and colleagues (2013), the orientation of the IMU throughout a trial was determined: first, the angular velocity data were zeroed by subtracting the means of a static period in the beginning from the data for the three axes. The orientation of the sensor in the first frame of a trial was chosen as the sensor reference frame orientation and expressed as a quaternion. Frame by frame, the recorded angular velocities were then converted into a rotation matrix that was applied to the previous quaternion representation of the sensor's orientation, which resulted in a time series of the rotation of the IMU about its three axes in the sensor reference frame throughout a push start trial. The quaternions were converted into Euler angles, allowing us to plot the track profile as measured by the IMU in degrees (**Figure 3-10A**). The change in sensor orientation was registered in the sensor reference frame i.e., relative to the orientation of the sensor at time zero, which is why the resulting pitch angle started at 0° for a given trial (**Figure 3-10A**). Since the bobsled sits on a small slope already when the athletes first start pushing, the calculated pitch angle was adjusted by adding 1.14° , which is (approximately) the arc tangent of the 2 % slope that was determined for the first straight section of the track as described above (**Figure 3-10B**).

To derive the velocity of the bobsled from the acceleration data, the quaternion time series describing the sensor orientation during a push start trial was converted into a series of rotation

matrices, which were then applied to the 3D linear acceleration data. This step resulted in the acceleration data being converted into the initial sensor reference frame. The measured acceleration in the first frame was then used to determine the IMU's initial orientation relative to gravity and to rotate the linear acceleration data into a global reference frame where the vertical axis was aligned with gravity (elevation axis in **Figure 3-9**). Finally, the linear acceleration data were integrated with respect to time and the resulting 3D linear velocity detrended (using the Matlab function “`detrend`”) to account for integration error due to potential bias in the signal. The time window of interest for integration was about 10 seconds, from a point of zero velocity at the beginning of the start phase until the loading of all four athletes into the sled was completed.

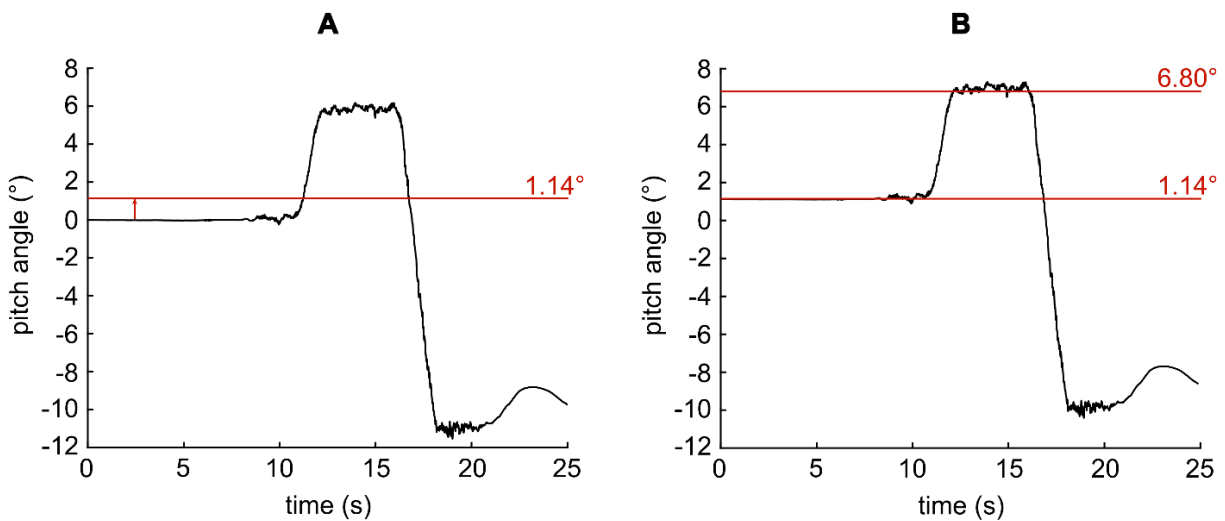


Figure 3-10: The orientation of the Inertial Measurement Unit (IMU) on the bobsled (panel A), which was derived from the data recorded with the gyroscope that is part of the IMU and used as a measure of the slope of the bobsled track. The plot shows the sections that are discussed above: a constant slope section in the beginning (~0 to 11 s), a part where the slope changes (increases, ~11 to 12 s), and then a second (steeper) constant slope section (~12 to 16 s). The remainder of the trace illustrates the particular design of the Ice House track, where the track flattens out again after the last timing light and then turns into a steep upward slope (20 % or ~11.31°) that serves to decelerate the bobsled. To account for the fact that the first part of the track is not flat (0°) but already has a slight downward slope (~1.14°), 1.14° were added to the original trace (panel B).

With bobsled velocity in the global reference frame and push forces initially registered in the sled reference frame (where the x-axis is oriented along the track and the y-axis normal to the track), trigonometry and the information about the track profile i.e., the orientation of the bobsled (**Figure 3-10**), were used to move from one coordinate system to the other.

Finally, similarly to the accelerometer (no integrated gyroscope = no information about changes in orientation), the study with the prowler push was an opportunity to validate the speed calculated based on the IMU data. For 190 trials performed with the prowler, where the sled was pushed on flat ground (Chapter 4), all three modalities i.e., video, accelerometer and IMU were used. The resulting peak speeds, calculated from the IMU acceleration (integrated with gyroscope information) were compared to the peak speeds identified from the video recordings, with excellent agreement between both modalities; $r^2 = 0.997$ and mean difference in measurements (speed from IMU minus speed from video) = $-0.08 (\pm 0.17) \frac{m}{s}$ (**Figure 3-8**).

3.4 Summary of Chapter 3

We instrumented two different sleds, a prowler, and a 4-man bobsled, to measure the push forces, for individual athletes and sled velocities. The prowler was instrumented first and used as (i) proof of concept for the instrumentation of the bobsled push bars and (ii) to validate 3D accelerometry, for determination of bobsled velocity in a field setting. Results from the prowler experiment are discussed in Chapter 4, results from the bobsled experiment are presented in Chapter 5.

Chapter 4

Functional Sled Push Force-Velocity Profiling for Bobsled Athletes; Like Taking Snow to Canada, or a Pit Stop on the Way to Taking Home Medals?

This chapter is based on: Onasch, F., Sawatsky, A. & Herzog, W., Functional Sled Push Force-Velocity Profiling for Bobsled Athletes; Like Taking Snow to Canada, or a Pit Stop on the Way to Taking Home Medals? *In preparation for submission.*

Individual contributions: Franziska Onasch and Andrew Sawatsky developed the methodology. FO performed the data collection and analysis and wrote the manuscript with input from all co-authors. Walter Herzog supervised the project and provided critical feedback.

4.1 Abstract

We designed a new set-up and protocol for a functional sled push force-velocity (fFv) profiling test as a tool for recruitment and assessment for bobsleigh athletes. The goals of this study were (i) to assess test-retest reliability, (ii) to evaluate if linear best fit approximations capture the individual fFv profiles, and (iii) to determine how the choice of load conditions affects the fFv relationships. Recreationally active individuals ($n = 19$) participated in this study, and 15 of them completed the same test twice. Participants performed 10 push trials with loads ranging from the empty sled to up to two times body weight. The main outcome variables were peak sled speed and the corresponding push force. Test-retest reliability was good, with $r^2 = 0.91$ and 0.96 for speed and push force, respectively. Linear approximations fit the experimentally determined fFv

relationships well, with $r^2 > 0.85$ for all but one of the individual profiles. Determining the fFv profiles based on load conditions close to either the maximum speed or the maximum push force capacity changed the profiles significantly compared to when data points spanned the entire testing range. We concluded that the test set-up works well and can, in a next step, be used to evaluate performance aspects with an athlete population.

4.2 Introduction

During the bobsled push start, teams of four or two (*4-man, 2-woman, or 2-man*), or a single athlete (*Monobob*; one female athlete), push the sled from a resting start position, trying to accelerate it as much as possible before loading (i.e., jumping into the bobsled). The goal of the start phase in bobsledding is twofold: to complete it in the shortest time possible and to achieve the highest possible sled velocity at the end. At the beginning of the start phase, athletes need to be able to produce great force at slow speeds, but then, as sled velocity increases, they also need to be able to contribute push forces while running fast. As a result, coaches seek to recruit individuals who are fast and strong (DeWeese, 2012; Morlock & Zatsiorsky, 1989), with sprints (15-60m), broad jumps, and underhand throws (shot or medicine ball) as typical recruitment tests (Bobsleigh Canada Skeleton, 2022; Team USA, 2022). Additional athlete screening exercises may include squats and power cleans (Tomasevich et al., 2020). The final recruitment test is the so-called single push test (on ice or dry land, depending on what is available for a given team), where individual athletes perform push starts, and the time it takes to complete the start is often the deciding factor for who is chosen to join a team. There is little scientific literature on the start phase of bobsledding, but a study performed by Challis et al. (2015) suggests that classic recruitment test results do not correlate well with athletes' single on ice push times. Moreover, there is anecdotal evidence

suggesting that single on ice push results also do not necessarily translate well to an athlete's performance in a team push. These observations suggest that some essential part of performance in the sport might be missing from the screening tests, and we propose that, by testing strength and speed separately, the performance capacity of an athlete in bobsledding cannot be well predicted. Assessing speed and strength simultaneously could be done, for example, through a functional sled push force-velocity³ (fFv) test. fFv profiling is a common approach to determining athletes' capabilities that has been applied in various sports, for example cycling (Dorel et al., 2010; Dunst et al., 2022; Dwyer et al., 2022; Rudsits et al., 2018; Vandewalle et al., 1987), cross-country skiing (Herzog et al., 2015; Østerås et al., 2002), skating (Perez et al., 2022; Stenroth et al., 2020), or recreational marathon runners (Nikolaidis & Knechtle, 2020). One variant of fFv profiling has also been applied in bobsledding before. Challis et al. (2015) found fFv profiles derived from loaded jump tests useful to predict athletes' performance in the single push test.

We instrumented a prowler (gym sled) to measure sled velocity and push forces while participants performed maximum effort pushes with varying loads/resistances. We chose this task because a) the movement is similar to the task of pushing a bobsled and b) it is possible to measure a wide variety of loads that encompass what an athlete might encounter at the different phases of the bobsled start. The primary objective of this study was to determine if the sled push test can be used to determine the functional force-velocity characteristics of bobsled athletes.

To answer this question, we needed to test the reliability of the measurements and determine the shape of the fFv profiles. The main feature of (functional) force-velocity profiles is the general

³ We use the term functional force-velocity for any such relationship that is associated with a specific in-vivo task or movement that involves at least multiple muscles (like a biceps curl) or multiple joints and segments (e.g., a jump), as apposed to force-velocity relationships of isolated muscles, fascicles, or fibres.

observation of a negative relationship i.e., a greater resistance is associated with slower movement or contraction velocity, and vice versa (**Figure 4-1**), and it has been shown that fFv profiles differ between individuals (Samozino et al., 2012; Stavridis et al., 2019). In contrast to the pronounced non-linear force-velocity relationships found for individual muscles and muscle groups (Andersen et al., 2005; Edman, 1988; Edman et al., 1976; Fenn, 1938; Hill, 1938; Katz, 1939) and some functional force-velocity relationships (Herzog et al., 2015; Rudsits et al., 2018), fFv relationships for many exercises have been found to be close to linear (Challis et al., 2015; Hill, 1922; Hill et al., 1924; Jiménez-Reyes et al., 2014; McMaster et al., 2016; Rahmani et al., 2001; Samozino et al., 2012, 2016; Vandewalle et al., 1987), and modelled as ‘quasi-linear’ (Bobbert, 2012).

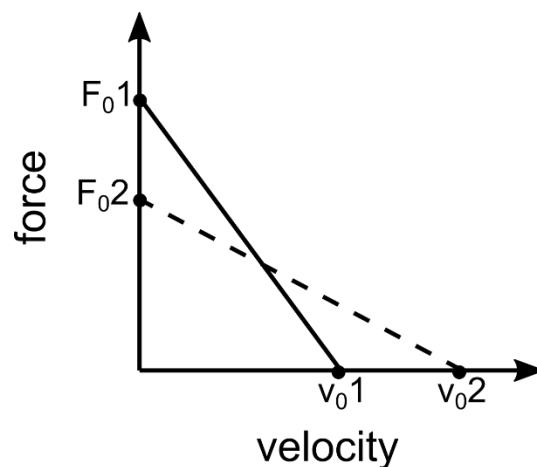


Figure 4-1: Summary of key considerations regarding functional force (or load) velocity (fFv) profiles. fFv profiles have been found (a) to be linear for many performance tests and (b) to differ between individuals. F_0 and v_0 indicate maximum task-specific force and velocity, respectively.

Additionally, we were interested in how reducing the number of independent data points i.e., experimental load conditions, alters the fFv profiles. In practice, it is common to derive fFv profiles with just 3 or 4 load conditions (e.g. Challis et al., 2015; Janicijevic et al., 2020; Nikolaidis & Knechtle, 2020), and Jaric (2016) discussed reducing the number of load conditions from 3 to 2 as

a feasible option. In the present study, we determined fFv profiles based on 9 independent load/speed conditions and then systematically reduced the number of conditions in the theoretical derivation of the fFv relationships to test how the number of observations impacts the fFv profiles.

We hypothesized that:

- (i) push force and velocity measurements are repeatable, with $r^2 \geq 0.9$.
- (ii) linear models are good fits for the individual fFv profiles, with $r^2 \geq 0.8$.
- (iii) the choice of the number of data points might significantly affect the fFv profiles as represented by the extreme values v_0 and F_0 (**Figure 4-1**).

4.3 Methods

Data acquisition: This study was approved by the Conjoint Health Research Ethics Board of the University of Calgary (#REB19-1232). Recreationally active individuals ($n = 19$, 174 ± 7 cm, 70 ± 12 kg, 5 female) gave free, informed, written consent to participate. Fifteen out of the nineteen participants completed the protocol twice, with test days one week apart. After a self-directed warm up, participants first performed two maximal speed 15-meter sprints. The sprints were followed by ten sled push trials against varying resistances. The first and last trials were unloaded (i.e., an empty sled + data acquisition equipment = 197 N). Trials 2-9 were semi-randomized, with a maximum load (including the mass of the sled) of up to two times a participant's body weight, and the maximum sprint or push distance was 15 m. The sled's supports were fit with felt lining to reduce friction with the gym floor and allow for a wide range of load conditions. The target

variables were peak speed and the corresponding push force. For heavy sleds (which led to slow velocities and early peak speed occurrence), participants pushed the sled for 10 m only. Two strain-gauge instrumented push bars (one for each hand) allowed for measurement of the horizontal and vertical push forces. A 3-axis accelerometer was used to determine sled velocity throughout testing, with y in the vertical direction, z in the main direction of movement of the sled, and any sideways movement would have been picked up in the x-axis. Accelerometer data (400 Hz) were recorded and synchronized with the push force data (400 Hz) using Windaq data acquisition software (data acquisition box: DI-710-UHS, Dataq, Acron, OH).

Data processing: Data processing and analysis were performed using Matlab R2020b (Mathworks, Natic, MA) and Excel (Office365, Microsoft, Redmond, WA). Kinovea (Version 0.9.5; Free Software Foundation, Inc., Boston, MA) was used for video tracking. Force and acceleration data were low pass filtered (2nd order recursive Butterworth) with a cut-off frequency of 20 Hz. The 3D acceleration signal was integrated with respect to time, for x and z-axis individually. The resulting linear velocity data were then detrended (by subtracting a linear fit through the beginning and end of the movement, which were both known to have zero velocity). Finally, resultant sled speed was calculated as the magnitude of the xz-velocity vector. Peak speed for a given trial was defined as the mean sled speed determined for a period where speed was greater or equal to 95 % of the actual peak speed value. Push force was determined as the average value for that same time window (Figure 4-2).

Data from participants who completed two full tests were used for reliability assessment. Test-retest reliability was evaluated for push force and velocity separately: All participants' data points from day one were correlated with those from day two and fit with linear regressions. With the regression lines forced through zero, coefficients of determination (r^2) and slopes of the functions

were determined. fFv profiles were approximated using best fit linear regression. As it is common to extrapolate fFv profiles to determine the axis intercepts F_0 and v_0 (**Figure 4-1**), we used the process described above to also assess the reliability of F_0 and v_0 from test day one to day two.

To test the effect of choosing a variable number of data points on the resulting fFv profiles, we used the data collected in this study and changed the number of data points used to derive the fFv profiles (**Figure 4-3**): **(A)** by keeping the full range information i.e., including the lightest and heaviest sled conditions, but with a varying number of points in between these two extreme measurements: 7 vs. 3 vs. 1 and **(B)** by choosing only three data points and changing their location within the full range: (i) spread across (lightest, heaviest, one in the middle), (ii) close to v_0 (the three lightest loads), (iii) centred around mid-range, or (iv) close to F_0 (the three heaviest loads). We used the extrapolated axis intercepts (maximum velocity, v_0 , and maximum push force, F_0) to compare the different approaches. Data points that were more than 5 times the interquartile distance from the median were considered extreme outliers and were excluded from the analysis. Wilcoxon tests were used for individual group comparisons with a Bonferroni correction for multiple comparisons, which resulted in an α level of significance of 0.005 for the individual tests. Cohen's d was calculated to quantify the effect sizes of any significant differences between groups. Effect sizes from 0 - 0.2 were considered small, 0.2 - 0.8 moderate, and $d > 0.8$ large.

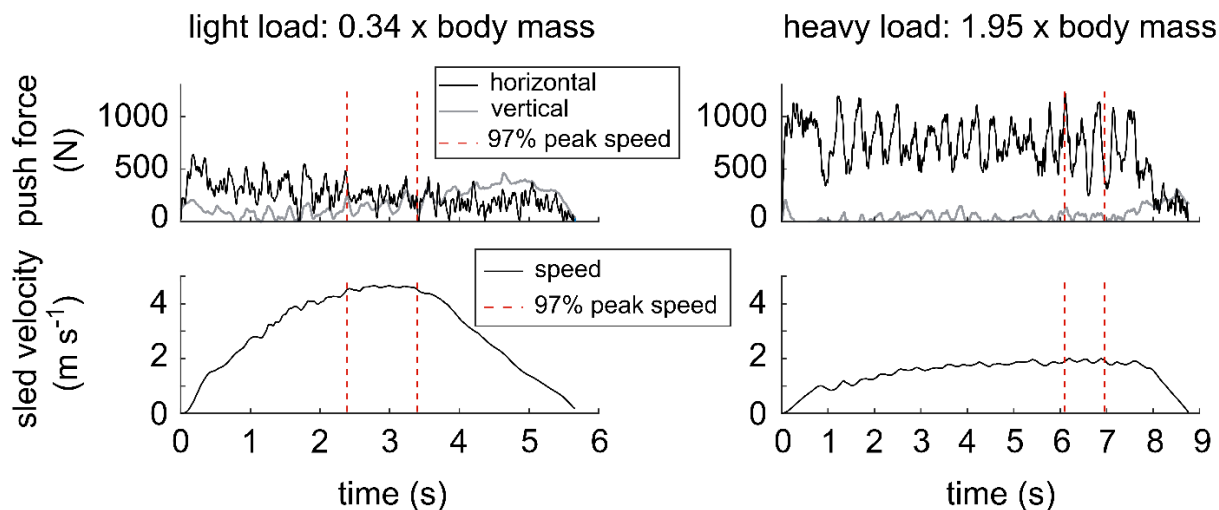


Figure 4-2: Force (top panels) and sled speed (bottom panels) for two sample trials of the same participant. On the left, with the lightest sled load, 34 % body mass, on the right, with the heaviest sled load, 195 % body mass. The red dashed lines indicate first and last time points where sled speed was equal to or greater than 95 % of the peak speed. Average speed and average force within that range constitute the velocity and force components that were used to determine a participant's fFv profiles.

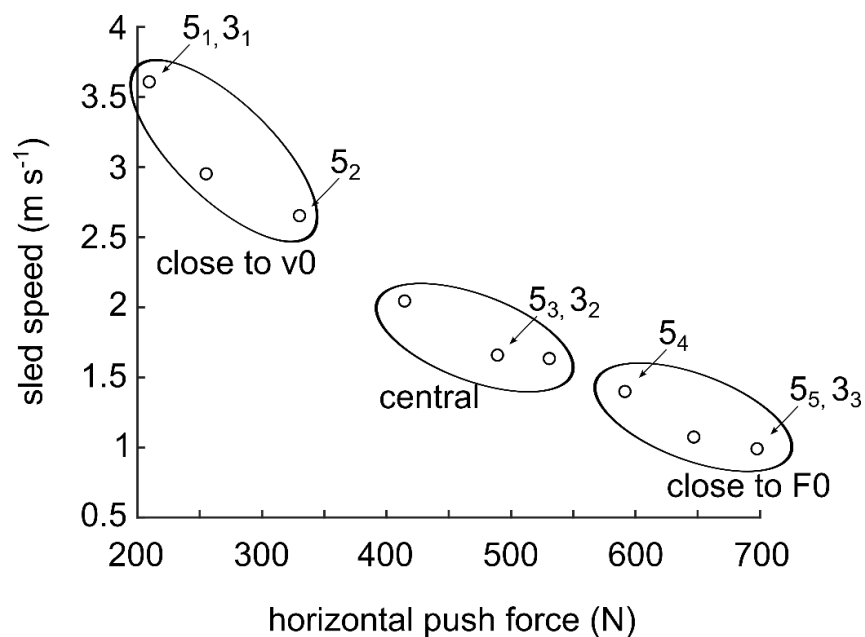


Figure 4-3: Illustration of the selection of different data points used for determining the fFv profiles; the circles represent real data of one test day. A_i = 9 data points, full range, all data points (small circles) were used. A_{ii} = 5 data points, full range, points 5₁ – 5₅ were used. A_{iii} = B_i = 3 data points, full range, points 3₁ – 3₃ were used. The ellipses show the groups of data points used for B_{ii} through B_{iv} (close to v₀, central, and close to F₀, respectively).

4.4 Results

Test-retest reliability and shape of the fFv profiles:

Mean absolute differences between test days were 32 (± 26) N for horizontal push force, and -0.25 (± 0.22) $\frac{\text{m}}{\text{s}}$ for peak sled speed. These differences correspond to about 3 (± 3) % of maximum recorded force and 5 (± 4) % of maximum recorded speed, respectively. Linear regressions of day 1 data versus day 2 data revealed coefficients of determination of 0.91 and 0.96, respectively, as well as a slope of 0.98 for sled velocity and 1.02 for horizontal push force (**Figure 4-4**).

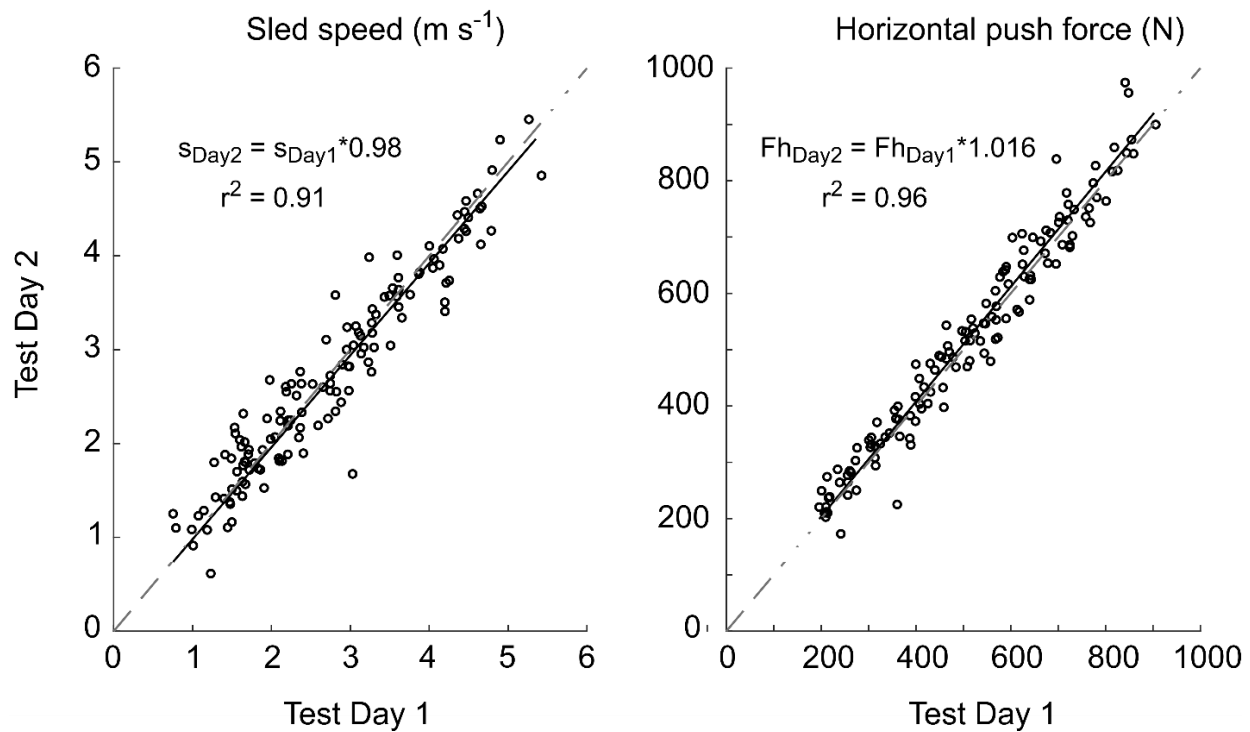


Figure 4-4: Test-retest reliability results for sled speed (left) and horizontal push force (right). 15 participants completed the test protocol on two different days, with the same ten sled push trials on both days. Each individual sled load condition is represented by a circle, comparing data from test day 1 (x axis) to data from day 2 (y axis). The solid black lines are the linear fits through all data points, forced through zero, the dashed lines indicate unity lines.

The test-retest reliability assessment for the axis intercepts of the fFv profiles revealed mean absolute differences between test days of 48 (± 63) N for F_0 , and -0.20 (± 0.34) $\frac{m}{s}$ for v_0 . These differences correspond to about 4 (± 5) % of the largest calculated value for F_0 and 3 (± 5) % of the largest calculated value for v_0 , respectively. Linear regressions of day one data versus day two data revealed coefficients of determination of 0.997 for both parameters, as well as a slope of 0.96 for v_0 and 1.05 for F_0 (Figure 4-5).

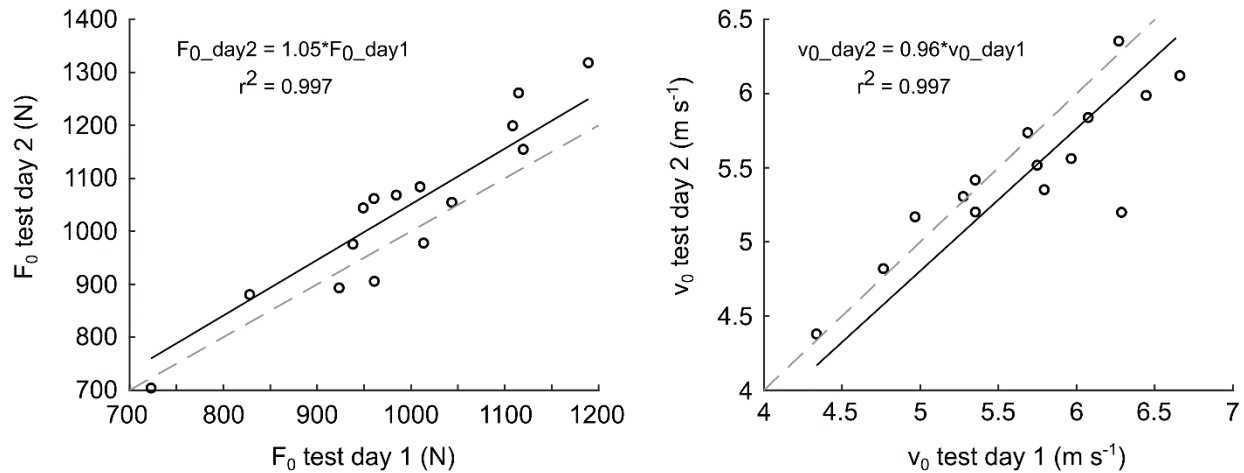


Figure 4-5: Test-retest reliability results for the axis intercepts F_0 (left) and v_0 (right) that were calculated using the linear regression functions of the individual fFv profiles. Each circle represents a day one/day two pair for a participant. The solid black lines are the linear fits through the data points, forced through zero, the dashed lines are unity lines.

Linear functions were good fits for the individual fFv profiles, with $r^2 > 0.85$ for 33 out of 34 cases (including two test days for 15 participants and the data from the additional 4 participants who completed only one test day; **Figure 4-6**). The resulting fFv profiles differed between people with extrapolated maximum push force (F_0) and speed (v_0) values ranging from 575 N to 1189 N and $4.34 \frac{\text{m}}{\text{s}}$ to $6.66 \frac{\text{m}}{\text{s}}$, respectively (for all first test days, including the four participants who only completed day one testing). Moreover, there was no relationship between F_0 and v_0 . When correlating F_0 and v_0 for all participants on day 1, we found a (not significant, $p = 0.28$) correlation coefficient of 0.26 (corresponding to a coefficient of determination of 0.07; **Figure 4-7**).

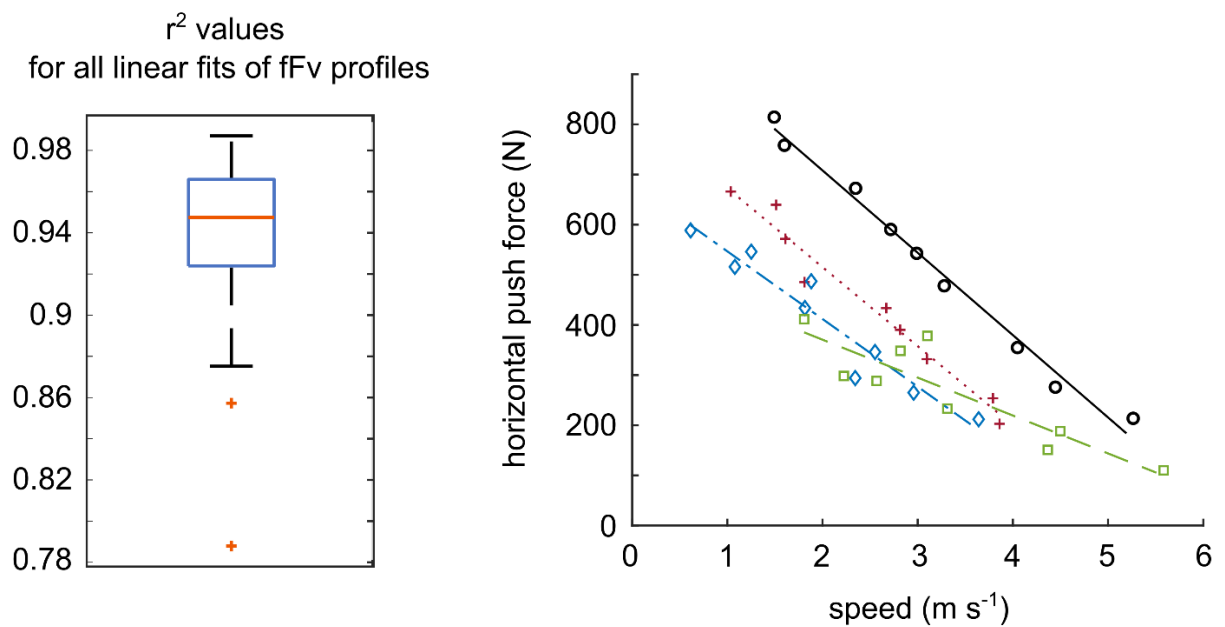


Figure 4-6: The boxplot on the left shows the distribution of r^2 values for all the individual fFv best fitting linear regression lines. Top and bottom edge of the box indicate the 75th and 25th percentile of the distribution, respectively; the horizontal line inside the box represents the median. The whiskers extend to the furthest points from the median that are not considered outliers, while an outlier is defined as any value more than 1.5 times the interquartile distance from the median. In the plot on the right, you find examples of fFv profiles from different participants. The solid line and circles are associated with the maximum r^2 value, the dashed line and squares with the lowest r^2 . Dotted line and plus signs and dash-dotted line and diamonds are associated with the 75th and 25th percentile of the r^2 distribution, respectively.

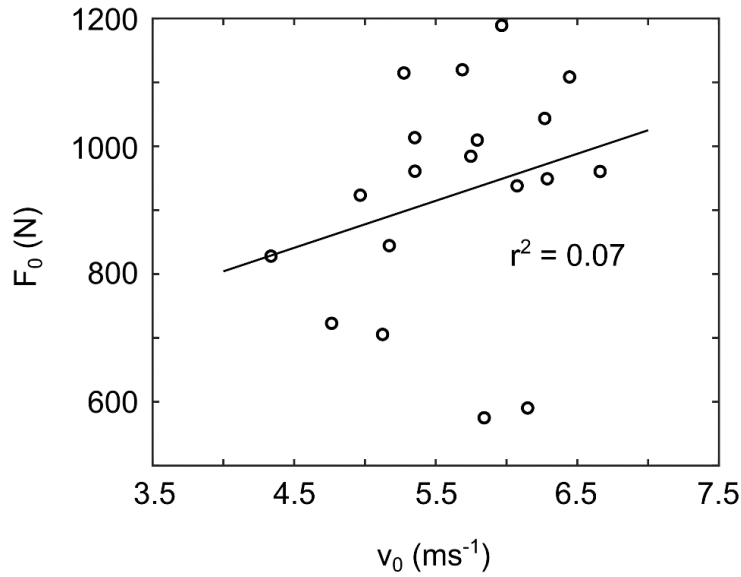


Figure 4-7: There was no relationship between the extrapolated maximum speed (v_0) and push force (F_0) values.

Varying the number and location of data points that were used to calculate the linear fits:

Reducing the number of data points from 9 to 3 while including the heaviest and lightest load condition did not cause statistically significant differences in either v_0 or F_0 . Using only three data points across the range of tested load conditions to derive the fFv relationships, we found the following: Neither F_0 nor v_0 changed significantly when central data points were chosen, compared to when the data points spanned the full range of test conditions. Choosing three data points close to v_0 resulted in statistically significant changes to both F_0 (median: -146 N; 25th percentile: -276 N; 75th percentile: -48 N; $d = 0.71$) and v_0 (median: $0.38 \frac{\text{m}}{\text{s}}$; 25th percentile: $0.17 \frac{\text{m}}{\text{s}}$; 75th percentile: $0.84 \frac{\text{m}}{\text{s}}$; $d = 0.70$). Choosing three data points close to F_0 , too, led to significant changes in both v_0 (median: $-1.36 \frac{\text{m}}{\text{s}}$; 25th percentile: $-2.37 \frac{\text{m}}{\text{s}}$; 75th percentile: $-0.51 \frac{\text{m}}{\text{s}}$; $d = 1.03$), and F_0 (median: 140 N; 25th percentile: 7 N; 75th percentile: 298 N; $d = 0.11$; **Figure 4-8**).

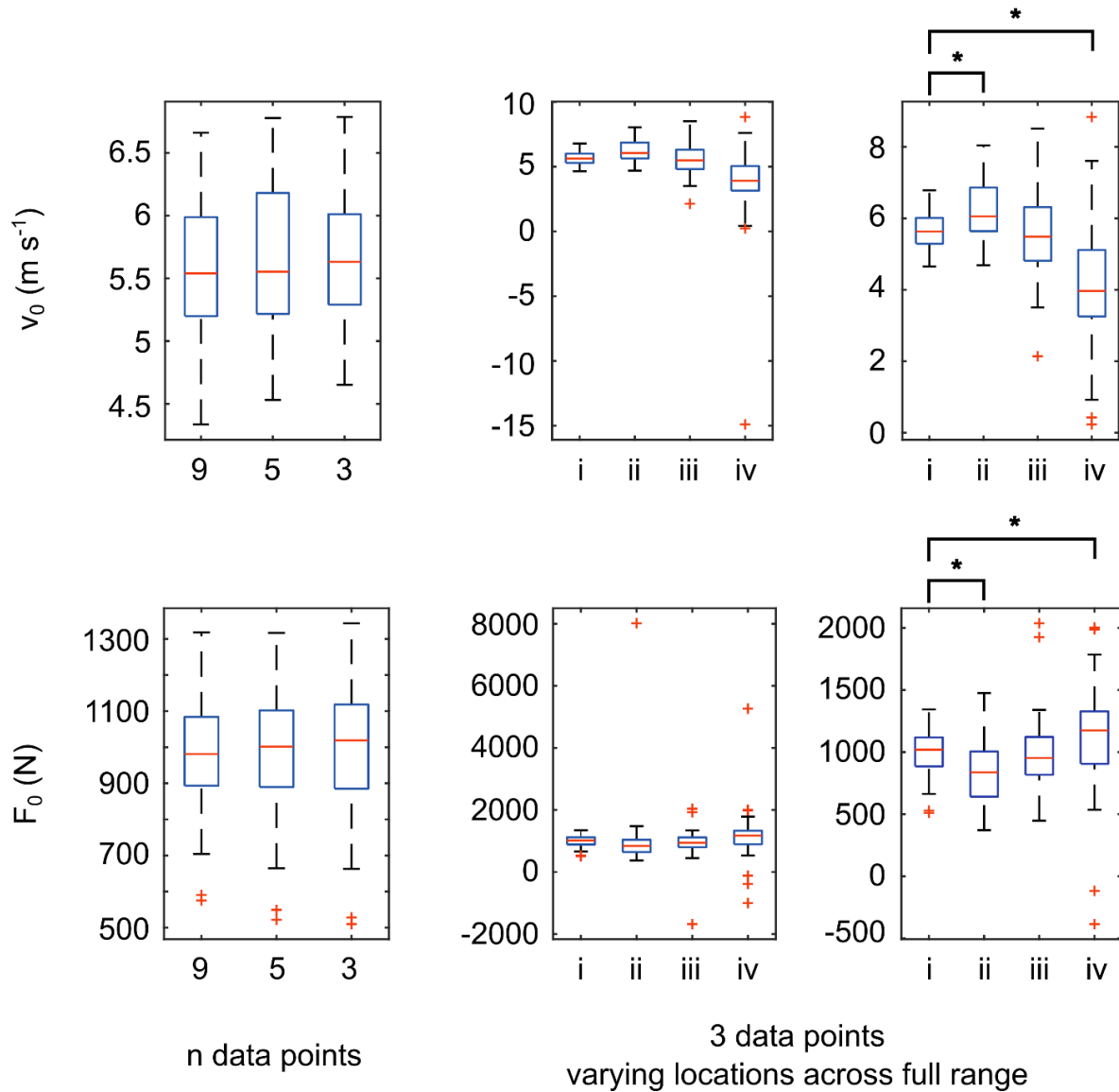


Figure 4-8: Varying constellations of load conditions were used to determine individual functional force-velocity (fFv) profiles. The effects of the varying constellations on the extreme values/axis intercepts of fFv profiles, v_0 (top row) and F_0 (bottom row) are shown. *Left column:* the number of data points included to fit the fFv profiles was varied (9 vs. 5 vs. 3, always including the lightest, heaviest, and middle load conditions). *Centre and Right columns:* the proximity of 3 data points to either one of the extreme ends of the relationship changed. i = 3 data points condition from left column, included load conditions that spanned the full range that was tested. ii = lightest load conditions. iii = central load conditions. iv = heaviest load conditions. Asterisks indicate significant differences with $p < .005$. Extreme outliers (greater than 5 times the interquartile range from the median) were excluded from statistical analyses (right column).

4.5 Discussion

Our primary aim for this study was to determine if the (dry-land) sled push test can be used to determine the functional push force-velocity capabilities of bobsled athletes. We assessed (i) the reliability of the measurements and (ii) the shape of the fFv profiles. Additionally, we tested how the number of data points i.e., load conditions, influences the individual fFv relationships.

Slopes of the linear regressions of 0.98 and 1.02, and r^2 values of 0.91 and 0.96 for sled speed and horizontal push force, respectively, indicate good test-retest reliability (with one week between test days), and we expect that changes in athletes' strength and/or speed capabilities greater than 32 N and $0.25 \frac{\text{m}}{\text{s}}$ (on average) due to training can be assessed. The variation that we see between test days for both push force sled velocity are reflected in the extrapolated axis intercepts, as well, with an average increase of $48 (\pm 63)$ N for F_0 , and an average decrease of $-0.20 (\pm 0.34) \frac{\text{m}}{\text{s}}$ for v_0 from test day to day two. The lack of an obvious relationship between F_0 and v_0 indicates to us that, if both are important, it really is useful to try and assess an athletes abilities close to both ends of the fFv profile. Inferring an athlete's strength qualities based on sprint running alone may be insufficient to predict performance.

Best fitting linear approximations of the data points provided good representation of the individual fFv relationships, with $r^2 > 0.85$ for all but one of the profiles.

The observation of linear functions being good fits of individuals' fFv data is in accordance with previous literature of functional force-velocity profiles (Bobbert, 2012; Challis et al., 2015; Jimenez-Reyes et al., 2014; McMaster et al., 2016; Rahmani et al., 2001; Samozino et al., 2010, 2016; Vandewalle et al., 1987). However, why do we care about the shape of the fFv function, or

what might be an advantage of a linear relationship? If the fFv relationship of sled pushing is indeed linear or can at least be represented well by a linear approximation, then it can be derived by testing just two or three resistances and any other data point can be calculated. This has practical implications. For example, performing fewer trials saves time which, especially with an elite athlete population, can be a precious resource, and reduces the risk of biased results due to fatigue. Furthermore, testing fFv relationships near the maximum force or maximum speed extremes is difficult, for some functional tasks maybe even impossible. For example, a push sled can never have zero resistance, thus the maximal speed/zero resistance condition cannot be tested practically. Similarly, it would be hard to test for maximum (isometric) force in many functional tasks and particularly in the push sled exercise, because movement pattern and body alignment would be completely different from the push sled exercise (Lockie et al., 2003; Markovic & Jaric, 2007; Onasch, personal observations).

With these concerns in mind, we tested how choosing a subset of trials affects the resulting fFv profiles, specifically the extrapolated maximum force and maximum velocity values, F_0 and v_0 . Reducing the number of data points from 9 to 5 or 3, while still including the lightest and heaviest load conditions, did not have a significant impact on F_0 and v_0 . This finding is consistent with previous reports (Janicijevic et al., 2020; Jaric, 2016). Calculating the best fitting linear regression based on the three lightest load conditions on average significantly reduced F_0 while increasing v_0 , relative to when the three loads spanned the entire test range. Conversely, choosing the three heaviest load conditions led to a significant decrease in v_0 – compared to when the three loads spanned the whole range, as well as a significant increase in F_0 .

This finding of systematic changes in F_0 and v_0 when varying the load conditions that were included in fitting the linear regressions prompted us to reconsider which type of function might

be best suited to fit our fFv data. The linear approximations were good fits, both visually and mathematically. Moreover, linear fFv profiles were in accordance with previous literature in the field, as demonstrated earlier in this discussion. By choosing a subset of data points, we decide that the selected data matter more than the rest – similar to forcing a regression through zero, where we essentially decide that the point (0,0) is weighted more than all the others. This decision may be a valid one to make if, for some reason, the respective data points are particularly important or interesting from a practical perspective. However, we would then probably accept that the resulting function will not necessarily represent the true range of data points (or in our case push forces that could be produced). At the same time, the observation of systematic changes in the axis intercepts when deriving the fFv profiles from subsets of data points can be interpreted as indication of sections with variable slope within the profiles or, in other words, that a straight line may not be the best representation of these data.

An alternative candidate in this context could be a hyperbolic fit, as famously used to describe the Fv relationship of individual muscles (Hill, 1938). However, while Hill's observations on heat production during concentric single muscle action provide the basis for the hyperbolic shape, no such explanation is readily available in a functional force-velocity setting. On the contrary, mechanisms have been proposed that could explain linear fFv relationships, even with underlying hyperbolic muscle force-velocity relationships. In a simulation study, Bobbert (2012) showed that when one muscle extended the knee in a leg press exercise the fFv relationship was 'quasi-linear', even though muscle action was modeled with a hyperbolic Fv curve. The author attributed this observation to segment dynamics canceling i.e., effectively straightening out the muscle force curve. After modeling isokinetic cycling, Bobbert et al. (2016) concluded that even at high cadence the shortening velocities of the muscles involved might be relatively slow, meaning that the

muscles would be operating on the more linear low-velocity portions of their individual Fv relationships. Secondly, the authors suggested that the muscles being activated for shorter periods of time at higher cadence led to a greater reduction in force and power compared to what was expected based on the modeled muscle properties, resulting in power and force-velocity curves resembling quadratic and linear functions, respectively. Additionally, Riviere et al. (2023) compared linear and hyperbolic representations of fFv profiles for ballistic lower limb extension and concluded that linear approximations were the appropriate choice to describe their fFv relationships. The authors stated that while, mathematically, hyperbolic functions were better fits than their linear counterparts, the improvement in coefficient of determination was not large enough to support the choice of hyperbolic approximations over linear ones. Moreover, the axis intercepts (F_0 and v_0) were overestimated with hyperbolic functions compared to the linear fits and, particularly, the results for v_0 were considered physiologically not realistic and therefore not relevant. It was further pointed out that when only a small range of movement velocities is tested, the observed overestimations could be even more dramatic when opting for a hyperbolic, rather than a linear fit.

I fit the individual fFv profiles from our study with hyperbolic functions, using Matlab's "fit" function (see Appendix for the code), and this is what I found: Wilcoxon paired samples test revealed (1) significantly greater F_0 ($p < .01$) and v_0 ($p < .001$) for the hyperbolic compared to the linear fits (**Figure A- 1**). r^2 values, too, were significantly greater ($p < .01$) for the hyperbolic compared to the linear fits (**Figure A- 1**), however, the data for which a linear regression resulted in a comparatively lower r^2 were still associated with the worst goodness of fit measures when approximated by hyperbolic functions. These observations (greater F_0 , v_0 , and r^2) are consistent with previous findings (Riviere et al., 2023). Moreover, for fourteen out of the thirty-five fFv

profiles, the automated fit produced essentially straight lines as the best fit option (even though the algorithm was prompted to fit a hyperbola; see **Figure A- 2** for examples). It can further be noticed that, although hyperbolas were very good fits for most of the fFv profiles, in many cases the data points were spread out along the straighter sections of the resulting hyperbolic functions, rather than the parts with the greater curvature. Therefore, it is not obvious that the fFv profiles in our study, albeit represented well by linear regressions, *are* in fact hyperbolic instead. It seems acceptable to proceed with linear fits and test how the results transfer and might be useful in an athlete population and to predict on-ice push ability.

The findings of our study suggest that sled push force-velocity profiling can identify an athlete's maximal strength and speed abilities for this task and could be a useful tool for the screening of bobsled athletes for performance capacity. However, the fFv testing can only be a first step. To make predictions about an individual's ability to perform in a different task the relationship between the two exercises needs to be established. Therefore, a next step would be to repeat the sled push fFv profiling with a group of athletes – and then relate the results to their on-ice performance. We designed the instrumentation for a 4-man bobsled that allows for measurements of the individual push contributions from each athlete in a real on-ice team push (Chapter 3.1; Onasch et al., 2023). The goal is to establish the relationship that may exist between the push sled and the bobsled conditions and to use these tests to inform provincial and national team selection, as well as athlete positioning within a team.

While linear fits proved to be good representations of the individual fFv profiles, it is crucial to be mindful of proper execution of the test. Moreover, when the goal is to compare fFv between athletes or within an athlete longitudinally, for example in the assessment of a training intervention

or when recovering from an injury/disease, it is important to be consistent with the test protocol (e.g., number of trials, measurement system/sensor set-up, equipment used, etc.).

There are limitations to this study. Our participants, albeit athletic individuals, were not elite level bobsled athletes. We found large differences in fFv profiles i.e., in extrapolated maximum speed and push force potential (see **Figure 4-7**), which is what we were hoping for, aiming to detect those differences and identify the strongest individuals in this task. Among elite bobsled athletes, the differences in fFv profiles would likely be much smaller than what is reported here. At the same time, highly trained athletes, who are used to performing maximum effort tasks, might perform the push sled test with greater reliability than our participants, thereby possibly increasing the test's sensitivity to inter-athlete differences. A second limitation may be that we deliberately chose the sled push test because we wanted athletes to perform a movement that is similar to the bobsled start. However, in a real bobsled push start, the sled will be on ice where friction is very low (approx. 0.004) for speeds between 1-10 $\frac{\text{m}}{\text{s}}$; (Poirier, Lozowski, Maw, et al., 2011). Estimates of the coefficient of friction in our experiment were $\mu = 0.35 - 0.65$, and the velocities that can be reached with the test sled are far from the speeds observed during an on-ice push start. In addition, a bobsled track has a considerable downhill slope that helps accelerate the sled and allows athletes to run faster than they would be able to run on a flat surface. Therefore, our testing might be more predictive of the performance capacity of bobsled athletes at the beginning of the start phase, where sled speeds are lower, and less predictive of the later part of the start phase, when force application on the sled becomes small, and speed of the sled and the running athletes is high.

We are also exploring a variation of the application of the sled push test, which is deriving entire fFv profiles from a single push trial. Challis and colleagues (2015) suggested that it might be useful

in a performance test to mimic the load conditions of the actual task. They had bobsled athletes perform a three-point fFv jump test and then extrapolated the resulting fFv profiles to a load equivalent to the mass of the sled used in an on-ice single push test. The corresponding estimated velocity and the time to complete the push test were highly correlated. A similar strategy could be adopted with our sled set-up by choosing one load that best resembles the situation that an athlete encounters when pushing a bobsled.

Finally, the sled push test might also be beneficial for evaluating athletes' performance potential in other power sports. For example, in football or rugby, athletes occupy different positions with varying physical requirements, and pushing opposing athletes for gaining an advantage is a big part of the game, with push sled exercises already as part of the regular training regime in these sports. Moreover, as the sled push system allows us to monitor push force and velocity development throughout an entire trial, it may provide metrics beyond the fFv information. Variables that might be interesting for performance evaluation include the initial impact force, rate of force development, time to peak speed for a given loading condition, or the duration for which peak speed can be maintained.

4.6 Conclusion

We conclude from the results of this study that the fFv relationship for the push sled exercise is well represented by a linear approximation and thus can be obtained with few test trials. However, since the choice of load conditions can affect the outcome, they should be consistent across tests. We further conclude that the push sled test is reliable in a group of athletic participants and thus might be used to compare performance capacity between or assess changes in performance within athletes.

4.7 Acknowledgements

We would like to thank Andrzej Stano for his invaluable technical support, Own the Podium for financial support, as well as all the volunteers for participating in this study.

Chapter 5

Force application during the 4-man bobsled push start

Individual contributions: Matt Jordan initiated the project. Franziska Onasch, Matt Jordan, Louis Poirier, and Walter Herzog developed the set of questions and parameters investigated as described below. FO performed the data collection, processing, and analysis – with help from Louis Poirier, developed the visualization, and wrote the chapter below (with input from MJ, LP, and WH). WH supervised the project and provided critical feedback. WH and FO acquired funding for the project.

5.1 Introduction

Bobsleigh is one of the fastest Winter sports with recorded top speeds of up to 150 km/h. The sole performance measure is the time it takes a team to complete their run, with fractions of a second separating teams at the finish line. In the 2-man competition at the 2018 Olympic Games, two teams tied for the gold medal with run times identical to the hundredths of a second, and at the most recent Games (Beijing 2022) the top 5 teams in the 4-man event all finished within just 1 second, with bronze medal and 4th place separated by only 6/100ths of a second.

The characteristic push start makes up about 10% of the total run time, and previous studies suggest a strong relationship between the time it takes a team to complete the start and their time clocked at the finish line (Brüggemann et al., 1997; Harrison, 2017; Morlock & Zatsiorsky, 1989; Smith et al., 2006). Moreover, it is widely accepted in the bobsled community that proper execution of the start phase is crucial for the outcome of a race. As a rule of thumb, teams expect that 1/10th of a second lost at the start can turn into 3/10ths by the time the sled crosses the finish line. This may seem like a very small amount of time to be concerned about but, considering that a team may be

separated from a medal by only a few hundredths of a second, even one tenth of a second certainly matters.

Teams start from a resting position, and then try to accelerate the bobsled as much as possible before loading i.e., jumping into the sled. The start block is located 15 m before the official start line, which means that there is a flying start into a run. The loading should be completed at 50m from the start line, at the latest. At the 50 m mark, the official start time is taken and the grooves that help keep the sled going straight for most of the start section end near this point. The track has a downward slope throughout the start stretch, with three distinct sections. First, there is a constant slope section from the block until the start line, then, there is a transition zone in which the slope increases (becomes steeper) and, finally, another constant slope section until the end of the start phase. The exact tilt angles depend on the track but on new tracks, we would expect about 1.1° for the first section, and 6.8° for the third (IBSF, 2019).

Even though bobsleigh has been part of the program of the Winter Olympics since the first ever Games held in 1924, most of the related scientific literature has only been published within the last decade. In previous publications, scientists discussed three broad topics. (1) External conditions, such as bobsled design and aerodynamics (Braghin et al., 2011; Dabnichki & Avital, 2006) and ice properties (Poirier, Lozowski, Maw, et al., 2011; Poirier, Lozowski, & Thompson, 2011). (2) The human contribution to race performance, with research groups investigating athletes' kinematics during the push start (Legwold, 1984; Lopes & Alouche, 2016; Park et al., 2017a, 2017b; Smith et al., 2006), their muscle activity (Park et al., 2018), or the effects of footwear (Park et al., 2017b). (3) Recruitment tests and athletic characterization of the typical bobsled athlete (Challis et al., 2015; DeWeese, 2012; Harrison, 2017; Osbeck et al., 1996; Tomasevicz et al., 2020).

What is still missing almost entirely, is information about the kinetics of the push start; how much athletes contribute to sled acceleration, and how they load i.e., jump into the sled. In a conference abstract, Leonardi et al. (1985) emphasized the necessity to measure individual athletes' contributions during the push start to enhance performance, but since then only two articles were published in which push force and/or sled speed data from bobsled athletes were quantified. Lee et al. (2015) instrumented a 2-man sled on wheels and recorded push forces from both the brakeman and the pilot, as well as sled speed. Dabnichki (2016) discussed the instrumentation of a 2-man bobsled that was pushed on ice. However, the author only reports sled acceleration and velocity, and uses computer simulations to show that adjusting the timing of loading the sled may increase sled exit speed at the end of the start phase. Collectively, these studies provide little information regarding the forces produced by athletes during the push start on a bobsled track and no such data currently exist for the 4-man bobsled event.

A 4-man crew consists of 4 athletes. The pilot (**P**), who pushes in front on the left side of the sled, one athlete who pushes behind the pilot on the left (**L**), and one who pushes across the sled from L on the right side (**R**). Number four is the brakeman (**B**)⁴, who pushes at the back of the sled. The pilot and the athletes on the left and right side of the sled push on bars. The brakeman holds on to handles that are an extension of the cowling, the shell/casing of the bobsled (**Figure 5-1**). As a result of this setup, there are four points of force application around the sled.

⁴ It is common practice in the bobsleigh community to refer to any athlete who is not a pilot as brakeman (or brakewoman), even when they are pushing on the side in a 4-man and are not actually in the position to pull the brakes at the end of the run. However, since the positions matter for the work presented here, and to make it clear which is being discussed, the term 'brakeman' will be used specifically for the athlete who pushes at the back of the bobsled.

We believe that to fully understand and possibly improve team performance during the 4-man push start, it is necessary to understand the contribution of each athlete. Therefore, we instrumented a 4-man bobsled to measure individual push forces and sled acceleration, and in cooperation with Bobsleigh Canada Skeleton, recorded data for 13 starts with elite level athletes.

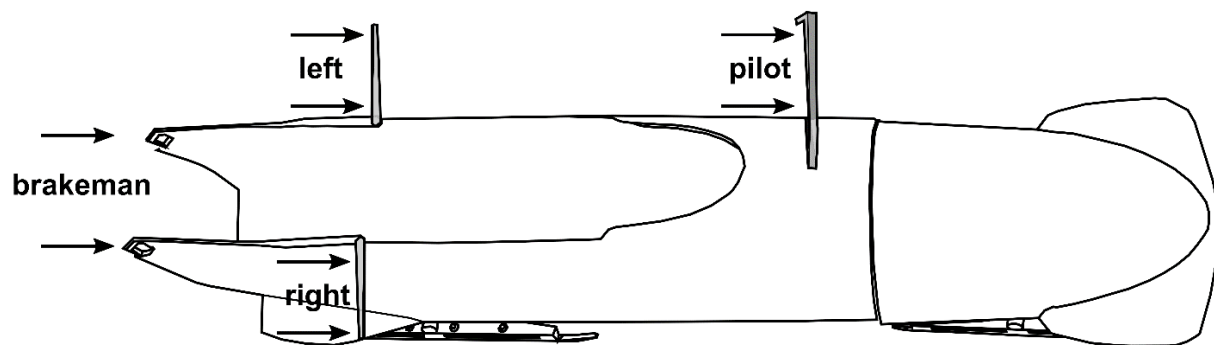


Figure 5-1: A 4-man bobsled with the arrows (one for each hand) indicating where the four athletes are in contact with the sled and push it.

In this chapter, the athletes' actions, and contributions during 4-man push are discussed. While the analysis is descriptive and of an exploratory nature, there were two aspects for which we had clear expectations. First, we hypothesized that push forces decrease over the course of the push start as sled speed increases. We view the push start as a force-velocity problem, where the athletes attempt to apply maximum propulsive force to the bobsled, as the speed of the sled continuously increases. (e.g., Bobbert, 2012; Challis et al., 2015; Jaric, 2016; Rahmani et al., 2001; Vandewalle et al., 1987). Second, with the ever-increasing sled velocity, there will be a point where the bobsled is moving too fast for even the fastest athlete to keep up with, let alone push. Since our participants were highly trained elite athletes with great experience in international competition, we hypothesized that they would load the sled before reaching the point where their push force reached zero or goes below zero (signifying pulling back on the bobsled).

5.2 Methods

This research project was approved by the Human Ethics Review Board at the University of Calgary (#REB19-1232). Participants were recruited from the Canadian National Bobsleigh team and gave written free and informed consent prior to the start of data collection.

A 4-man bobsled was instrumented such that it allowed for the measurement of individual 2D push forces, as well as 3D sled acceleration (Chapter 3.1; Onasch et al., 2023). The push bars were instrumented with strain gauges, and force sensors were used for the brakeman handles. 3D linear acceleration and 3D angular velocity of the bobsled were recorded with an inertial measurement unit (IMU; Opal, APDM Wearable Technologies Inc., Portland, OR), which was attached to the cowling near the tip of the bobsled, and both data streams were combined to determine sled speed. For a more detailed description of the instrumentation, please, refer to Chapter 3.1 in this thesis. Processing of the data was done in Matlab R2020b (Mathworks, Natic, MA) and Microsoft Excel (Office365, Microsoft, Redmond, WA). Linear acceleration and angular velocity data (recorded at 400 Hz) were used to calculate sled velocity (Rebula et al., 2013). Push force data were recorded at 400 Hz with an on-board data acquisition (DAQ) box (NI USB-621x, National Instruments, Austin, TX, USA), and processed using custom written Matlab scripts. To increase the signal to noise ratio in the signal, a physical low-pass filter (cut-off frequency 50 Hz) was integrated into the cables leading from the strain sensors on bars to the DAQ-box. 50 Hz was chosen as the cut-off frequency with the intention to not be too rigorous but eliminate higher frequency noise, including the 60 Hz electrical environmental noise. Data were then filtered a second time using a digital low-pass (cut-off frequency 20 Hz) recursive second order Butterworth filter. The 20 Hz cut-off frequency was subjectively chosen as the result of experimenting with different frequencies

(5, 10, 15, and 20 Hz) and observation of how they affected the data. Even with 20 Hz, filtered and original trace were not the same, but the shape and magnitudes of the traces filtered with cut-off frequencies of 5, 10, and 15 Hz were visibly different from the originals. To avoid removing real information from the data, I decided to proceed with a 20 Hz cut-off, which seemed to clean up the traces, make them smoother, but not change their appearance too much compared to the unfiltered data. Force and IMU data were synchronized using an additional 3D accelerometer that was mounted to the sled, next to the IMU. The accelerometer and force data were collected synchronously through the same DAQ box. Accelerometer and IMU were synchronized through a series of taps on the cowling of the bobsled. Video of the push trials was recorded as well, but the data were not synchronized with either the accelerometer and force or the IMU data.

The start of a push was determined from the acceleration data as the time point when sled acceleration in the forward direction was greater than 15 times the standard deviation of the baseline recording (**Figure 5-2A**). The end of a run was based on the angular velocity data that, by integration to angular displacement ($^{\circ}$), allowed for tracking the orientation of the IMU. After the last timing light (“start time”, as shown in **Figure 5-3**), the track starts to flatten out and then slopes upward. The end of each run was chosen as the point where the pitch angle of the bobsled started to decrease again, indicating that the sled had left the push start area and entered deceleration section of track. The end of a start was detected automatically using the Matlab function “findchangepts” (**Figure 5-2B**).

The data presented in this thesis were collected at the *Ice House*, in Calgary, during the team’s last training camp before the start of the 2021/2022 competition season. The Ice House features an indoor ice track with the exact profile of the start phase of the actual racing track, and the estimated slope profile is depicted in **Figure 5-3**.

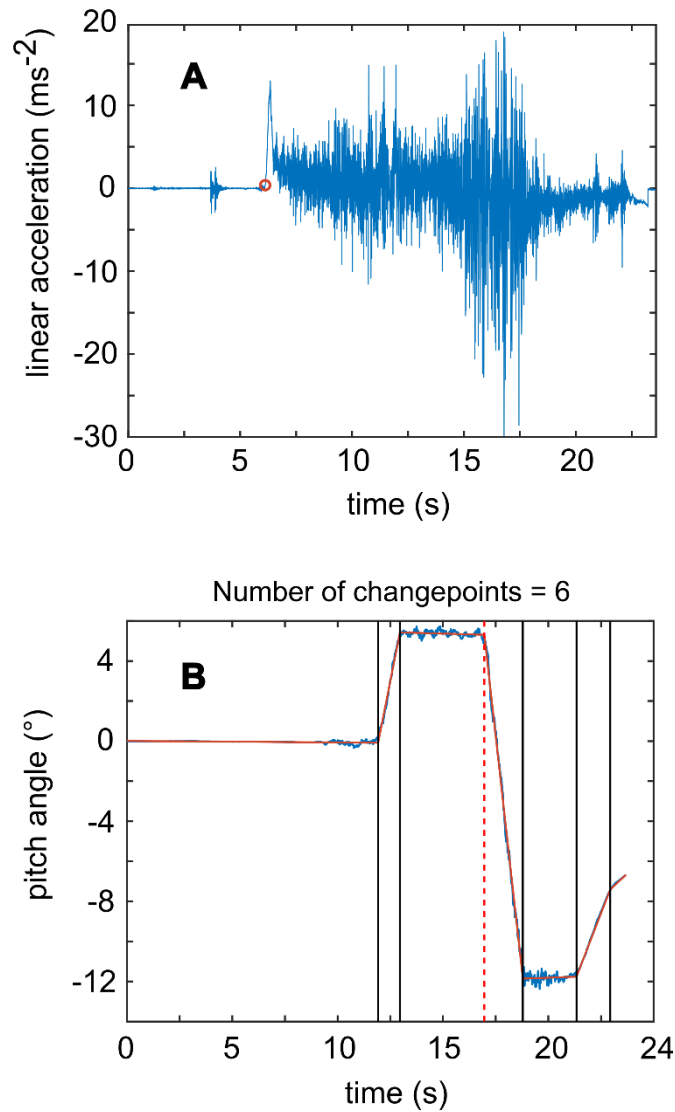


Figure 5-2: Examples of how start of movement (red circle, A) and end of a push start trial (dashed vertical line, B) were determined.

On two days, a total of 13 push starts were recorded with the instrumented 4-man sled, with complete crews for all but one of the trials where the pilot did not push. Two starts were performed by the same group of athletes, and for the remaining starts, athletes rotated between teams. Lastly, a note on the effort level of the push starts that were recorded for this project. We had planned for

full-effort execution of the task. However, data collection ended up taking place during the last team training camp before the beginning of the 2022 Olympic Season and the teams performed hard-level but not full-effort starts when pushing our instrumented bobsled.

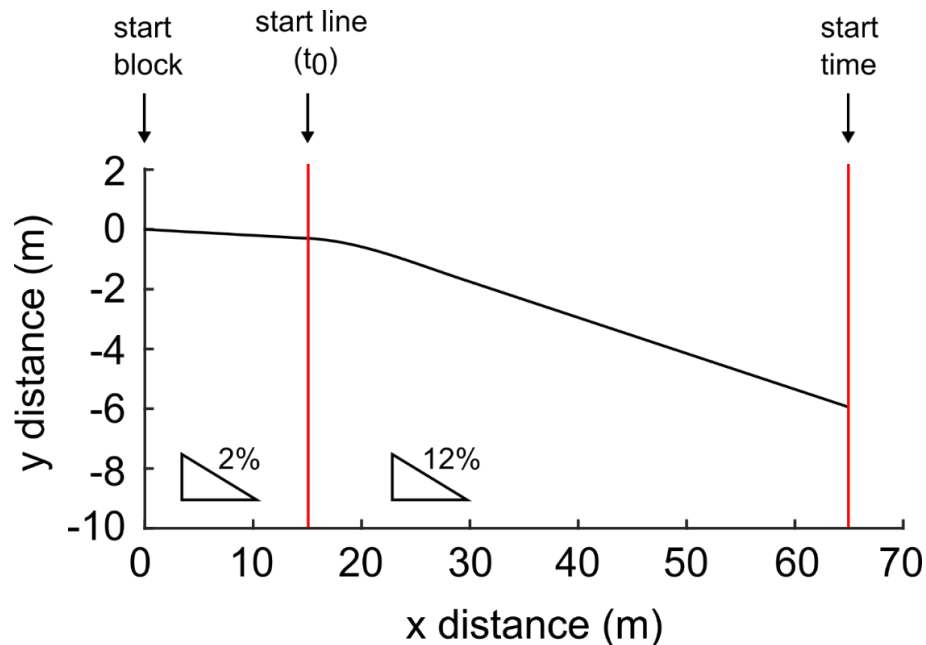


Figure 5-3: Schematic of the start section of the bobsled track at the Calgary Ice House. The track profile was derived from building plans and previous measurement (Poirier, 2011). This profile is consistent with the regulations published by the International Bobsled and Skeleton Federation (IBSF, 2019).

In the following, we will present the parameters deemed meaningful for the analysis and future improvement of push start performance for a team. When detailed timing is discussed, the results are based on 6 out of the 13 trials. These 6 trials were collected on the second experimental day when a better video setup was available that allowed for a more detailed analysis of the timing.

For statistical analysis, rank order correlations providing Spearman's rho (Spearman, 1904) were used.

In the following, the terms *propulsive force*, *normal force*, and *(sled) speed* will be used repeatedly. Propulsive force is the push force measured in the direction of movement of the sled, that is parallel to the ice surface and parallel to the track. Normal force is the force perpendicular to the propulsive force and perpendicular to the ice surface (**Figure 5-4**). Bobsled speed is the magnitude of the xyz-velocity vector, as derived from the xyz-acceleration that was recorded with the on-board IMU.

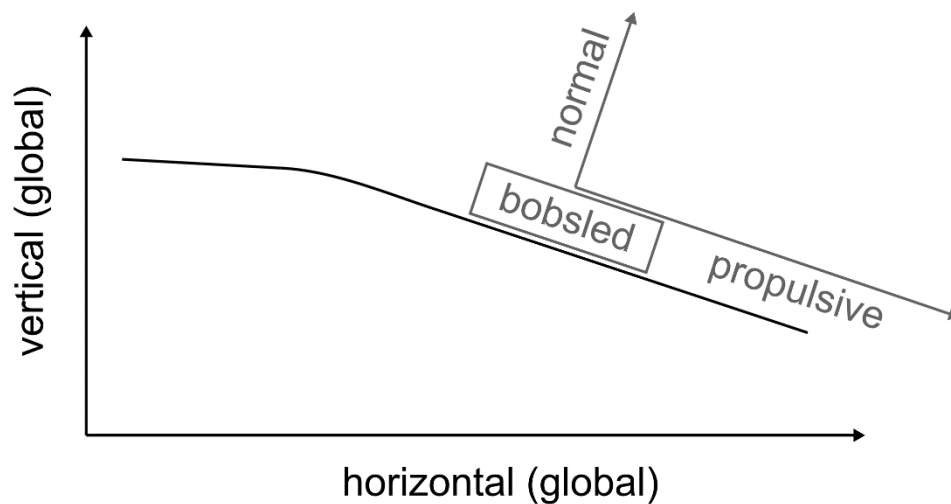


Figure 5-4: Schematic to define the directions ‘propulsive’ and ‘normal’ in the context of a bobsled on the ice track.

As discussed in Chapter 3.1, the force sensors for the brakeman handles did not work as intended. Based on discrepancies between measured sled velocity and estimated velocity derived from impulse calculations (utilizing the force data), it appears that the brakeman’s forces measured in the very first push in a push start are underestimated and their contributions during the remainder of push start are overestimated. However, some of the brakeman data are still included in the methods and results, to show what we measured, as that may guide future versions of the measurement system.

Specific Methods

This section is organized in four sub-sections: (1) The first push at the beginning of the start phase i.e., the hit, (2) the entire start phase, (3) a detailed analysis of two selected runs, and (4) the loading phase.

5.2.1 The hit

The very first push, when the athletes first exert a force against the stationary bobsled, is referred to as the hit. The hit is a skill that bobsled teams practice frequently to make sure that all athletes are coordinated and synchronized for this crucial part of the start phase. We explored the following questions:

(i) *is the importance of the hit reflected in the data.* For this purpose, the propulsive force impulses of all athletes across the duration of a push start were summed. Then, the impulses for the following three time points were determined: the instant immediately after the end of the hit, and when 50% and 90% of the peak impulse were achieved (**Figure 5-5**).

(ii) *Peak force vs. impulse.* Peak force was defined as the maximum force during the hit. The impulse for the hit was calculated from the start of the movement to the first local minimum of the summed propulsive force trace.

(iii) *team timing.* Team synchronization was assessed by calculating the time of peak force occurrence of all athletes relative to that of the pilot.

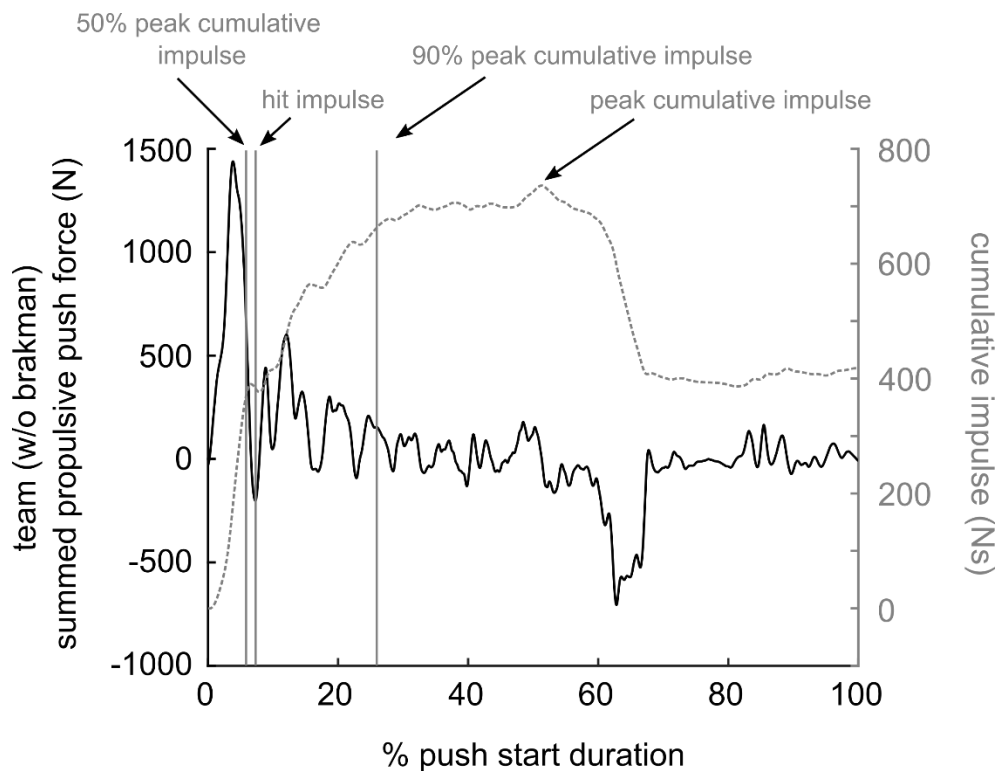


Figure 5-5: Visualization of how the instants of hit impulse, 50 %, and 90 % of peak impulse across a trial were determined.

5.2.2 Across the push start, from hit to load

The period between hit and loading phase can be considered a steady state where the team's focus lies on running and accelerating the bobsled. During this phase, the sled is in motion, and any reduction in force or pulling back is not related to the athletes' preparation and execution of the load. After careful consideration of the force and video data, I defined this steady state phase as 10 % - 45 % of total push start duration. Our analysis encompassed two parameters that are of significance during the push start and will be explained in more detail below: The development of the push force and push force effectiveness.

Development of push force. To examine how the push force changed over the course of the push start, each run was broken down into 5 % intervals (of total push start time). Mean propulsive and normal (to the track) force components were calculated for each interval for the individual athletes.

Force effectiveness. To quantify force effectiveness over the course of the start phase, each run was divided into 5 % intervals of total push start time. Mean propulsive and resultant push force were calculated for each interval, and force effectiveness was calculated as the ratio of the two mean values:

$$\text{push force effectiveness} = \frac{\overline{\text{propulsive force}}}{\overline{\text{resultant force}}} \quad [5.1]$$

Force effectiveness ranges from 0 to 1, with complete effectiveness (ratio equal to 1) occurs when the resultant force is equivalent to the propulsive force. Note, that the brakemen's data were left out of this analysis as, due to the design of their push handles and our sensor setup (Chapter 3.1), the brakemen were expected to have little to no control over the direction of their measured push forces. The force sensors on the brakeman handles are placed on the surface of the handles and they record force that is applied normal to their surface. Therefore, the propulsive and normal components of this normal force are dictated by the orientation of the handles relative to the surface of the track.

5.2.3 A closer look at two sample starts

Beyond providing overall observations from the recorded push starts, we would like to illustrate the insights gained from aligning video footage with force and speed data. Specifically, *(i) an observation to add to the discussion about a synchronized hit, and (ii) how some of the events that we can see in the video around the time of loading are reflected in the force and/or speed data.*

Two of the push starts (ExS_A and ExS_B) from day two were selected for this discussion. We chose these starts because a) we had better video coverage of the starts on that test day, b) a full crew of four athletes pushed in both starts and, c) based on the data from the other push starts that day, we were not entirely sure, that all the pilots had put full focus on the first hit. The pilot was the same in the two selected example starts, but the other three crew members were different between ExS_A to ExS_B. To synchronize the different data streams, we chose the hit as the reference point. In the force data, the hit was defined as the instant of peak propulsive force summed across the athletes. In the video, due to a lack of digital synchronization between the two modalities, the hit was determined through visual inspection as the time point when the athletes were all leaning into the sled just before it started moving.

5.2.4 The load

We had several questions about the load. *(1) What are the sled speeds at the instants of loading for the different athletes? (2) How far into the push start do the athletes load? (3) Do the athletes load before they stop contributing to propulsion? (4) Were the team loads positive? (A positive load would be one where sled speed is greater at the end of the load than in the beginning or, in other words, where the net change in speed across the load was positive.) And if they were positive, how efficient were the team loads i.e., how much time did they lose due to their execution of the load?*

For questions (1) through (3), the instant of loading for an athlete was defined based on the video recordings as the last frame with their toe on the ice.

For question (4), based on the observation that, in competition, it takes about three seconds for an elite bobsled team to complete the loading phase, the duration of a team load was defined as the 3

second period from the pilot's last foot-ground contact before jumping into the sled. The last step was chosen as the starting point here because if the athlete were to pull on the sled, it would be more likely to happen in the last ground contact phase, rather than in the moment they leave the ice. The net change in sled speed was calculated as the change in speed during the 3 seconds loading phase, and a rank order correlation was performed for change in speed vs. speed at the beginning of the loading phase.

Furthermore, we aimed to derive a meaningful metric that provides athletes and coaches with objective feedback about how well a loading phase was executed. Therefore, we propose the following approach: by integrating the speed-time curve across the duration of the load, we can calculate a distance that the bobsled would have travelled during the 3 second loading period. Similarly, we can calculate the distance that the sled would have covered if the athletes had achieved a constant acceleration during the load, instead of a variable acceleration pattern. The constant acceleration for a given trial was determined based on the recorded speeds in the beginning and at the end of the load. Subsequently, the difference in distance for the two conditions can be calculated and then divided by the speed that a team reached at the end of the load, and the resulting time could be interpreted as time that was lost during the loading (**Figure 5-6**). [6 out of the 13 runs were included in this analysis.]

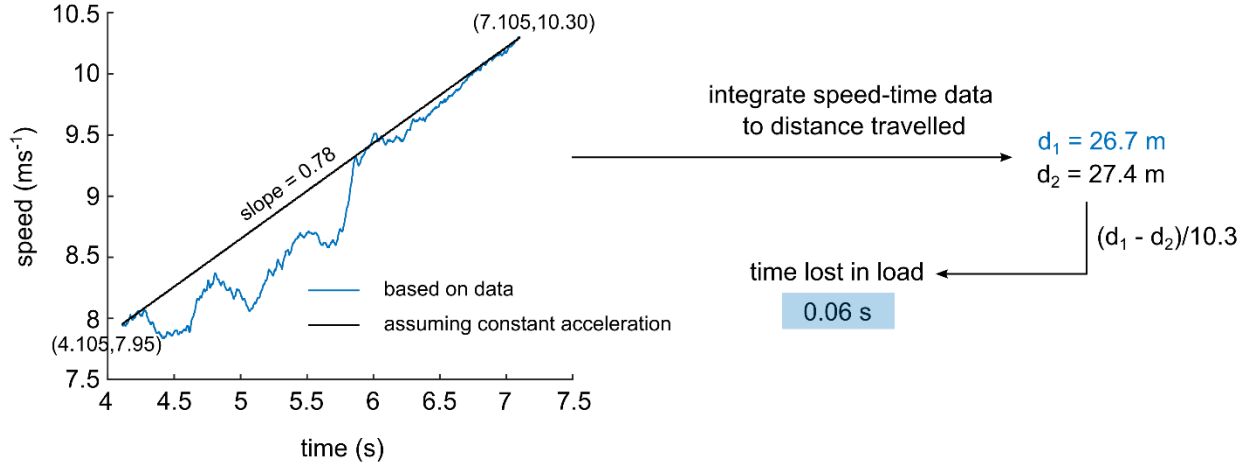


Figure 5-6: Exemplar calculation the proposed approach to determine team performance during the load. The data used for this figure are from example push start A (ExS_A).

Question (3) requires more of a discussion up front to properly introduce the problem. In an ideal scenario, the athletes load the bobsled shortly before their push contribution becomes detrimental to the acceleration of the sled or, in other words, when they contribute more to the increase of sled speed by sitting in the sled compared to applying an external push force. When the loading takes place, the bobsled is already on the steeper section of the track, with a slope of $\sim 6.8^\circ$. Here, the sled would keep moving and accelerating, even without any additional work done by the athletes. The forces acting on a bobsled are (1) gravity (G_{slope}), (2) friction (F_F), (3) air resistance or drag (F_D), and (4) if someone is pushing, push force (F_{Push}). The instantaneous acceleration of the sled can be calculated as:

$$a(\text{sled}) = \frac{G_{\text{slope}} - F_F}{m(\text{sled})} - \frac{F_D}{m(\text{sled})} + \frac{F_{\text{Push}}}{m(\text{sled})} \quad [5.2]$$

If the athlete loads the sled, the last term on the right side of Equation 5.4 vanishes, leading to

$$a(\text{sled} + \text{athlete}) = \frac{G_{\text{slope}} - F_F}{m(\text{sled} + \text{athlete})} - \frac{F_D}{m(\text{sled} + \text{athlete})} \quad [5.3]$$

However, G_{slope} and F_F are also functions of sled mass.

$$\vec{G}_{slope} = m_{sled} * \vec{g} * \sin(6.8^\circ) \quad [5.4]$$

$$F_F = m_{sled} * g * \cos(6.8^\circ) * \mu \quad [5.5]$$

(with μ as the coefficient of friction for a bobsled on ice), rendering the first term on the right side of **Equations [5.2] and [5.3]** independent of the sled mass and, therefore, independent of whether the athlete is inside the sled or not. The second term (acceleration due to drag) on the other hand becomes smaller with increasing sled mass. Consequently, increased sled acceleration through added mass is achieved by a decrease of the decelerating effect of air resistance. This is true, if the added mass does not also increase the surface area of the bobsled, or at least not so much that drag force is increased in equal proportion compared to the mass.

We can define a ‘critical push force’ at which (for a given athlete mass) the acceleration of the sled plus athlete will be equal to the acceleration of the sled with the athlete pushing. This point might be a reasonable instant for loading the sled, as beyond this instant, the athlete pushing the sled would contribute less to sled acceleration than the athlete adding their mass to the bobsled. The critical push force can be determined as

$$a(sled) = a(sled + athlete) \quad [5.6]$$

$$\frac{G_{slope}-F_F}{m(sled)} - \frac{F_D}{m(sled)} + \frac{F_{crit}}{m(sled)} = \frac{G_{slope}-F_F}{m(sled+athlete)} - \frac{F_D}{m(sled+athlete)} \quad [5.7]$$

Assuming a constant coefficient of friction, $\frac{G_{slope}-F_F}{m(sled)}$ and $\frac{G_{slope}-F_F}{m(sled+athlete)}$ are equal, which leads to:

$$- \frac{F_D}{m(sled)} + \frac{F_{crit}}{m(sled)} = - \frac{F_D}{m(sled+athlete)} \quad [5.8]$$

$$F_{crit} = - \frac{F_D}{m(sled+athlete)} * m(sled) + F_D \quad [5.9]$$

$$F_{crit} = F_D * (1 - \frac{m(sled)}{m(sled+athlete)}) \quad [5.10]$$

Therefore, an athlete should load the sled shortly before or at the time when the acceleration due to the push force becomes less than the decrease in air resistance that is achieved with loading ('critical push force'). To explore this relationship in more detail, **Equations [5.2] and [5.3]** were used to calculate sled acceleration for varying push force magnitudes (0 to 100 N) and to compare the results to the acceleration with load (i.e., added mass). Sled mass was set to 218 kg, athlete mass = 100 kg. For an estimate of friction and drag, the following coefficients from the literature were used (Poirier, 2011): coefficient of friction $\mu = 0.004$, air density = $1.18 \frac{\text{kg}}{\text{m}^3}$, cross sectional area of a bobsled = 0.342 m^2 and drag coefficient $C_d = 0.55$. Drag was calculated for three different velocities: 8, 10, and $12 \frac{\text{m}}{\text{s}}$ as

$$F_D = 0.5 * \text{air density} * CSA_{bobsled} * C_d * v^2 \quad [5.11]$$

The original question was whether the athletes load before they stop contributing positive propulsive push force and we determined the differences between critical push force and recorded push force at the time of loading the bobsled (**Figure 5-7**). For this analysis, push force and sled speed at the time of loading were calculated as the median values across the one second prior to athlete loading. Assumptions were made regarding body mass, as exact body mass data were not available for all athletes. Body mass for the athletes ranged between 90 and 110 kg. To account for the uncertainty in my body mass estimates, I also calculated the propulsive weight force component for my estimates of body mass ± 10 kg.

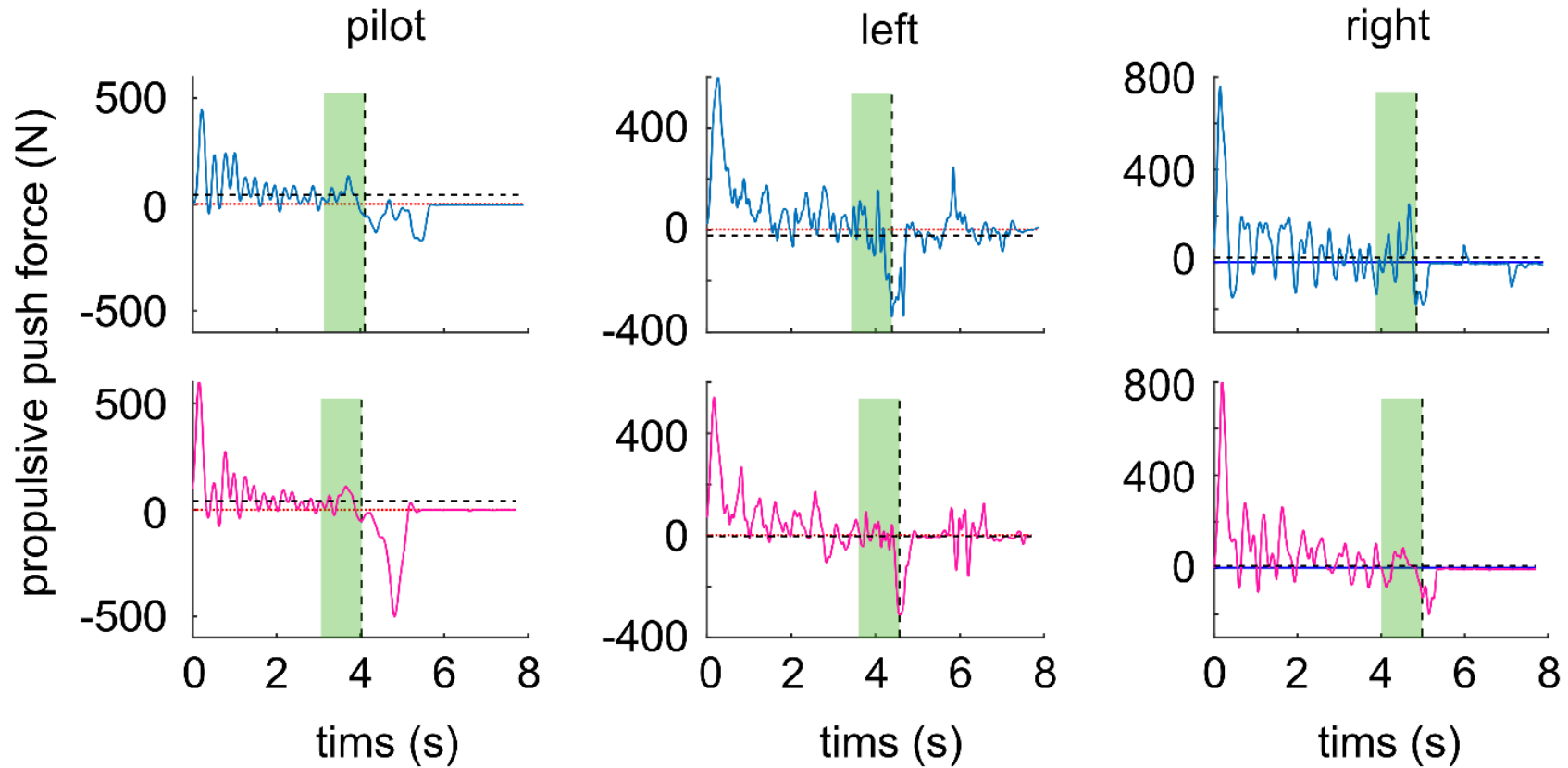


Figure 5-7: Comparing push force at loading to the theoretical critical push force, below which an athlete would contribute more to sled acceleration by sitting inside the bobsled than when pushing. The vertical and horizontal black dashed lines indicate time of last ground contact before loading and average push force for the last second (shaded green bar) prior to this point respectively. The red dotted lines represent the critical forces as calculated for the conditions at the time of loading. To account for potential error in the estimates of the athletes' body masses, critical force was calculated three times (for estimated body mass and estimated body mass $\pm 10\text{kg}$). Consequently, there are three red dotted lines in each graph but the effect of variation in mass on critical force was so small, that the three lines lie on top of each other. The graphs in the top row show data from example trial A (ExS_A), the bottom row from example trial B (ExS_B). A dashed black line above the red dotted lines means that an athlete loaded before they reached critical force – and may have loaded the sled too early. A dashed black line below the red lines means that an athlete loaded the sled when they already contributed less than the critical force.

5.3 Results

This section is structured into the same four groups as the methods section: (1) The first push i.e., the hit, (2) parameters determined across the duration of the start phase, (3) a detailed study of two selected starts, and (4) the loading phase.

5.3.1 The hit

The hit, on average, accounts for 41% of the peak impulse produced by the teams throughout their push starts (median = 41 %; 25th percentile = 25 %, 75th percentile = 38 %).

50 % of the peak impulse were realized at 10 % of push start duration (with 10 % and 11 % for 25th and 75th percentile of the distribution, respectively). 90 % of the peak impulse were realized at 35 % of push start duration (with 33 % and 36 % for 25th and 75th percentile of the distribution, respectively; **Figure 5-8**).

Peak force vs. impulse

The greatest peak propulsive push forces were produced by the two athletes pushing on the left (**L**, behind the pilot) and right (**R**) side of the bobsled, across all trials (median peak force = 740 N and 719 N for **L** and **R**, respectively, compared to 445 N for **P** and 418 N for **B**). The total impulse of the hit was smallest for the pilots (~37 % of **L**), but comparable between **L**, **R**, and brakeman (**B**), across pushes (**Figure 5-9**).

Team timing

The biggest time difference for instants of peak force between the pilot and any one of the remaining three athletes was 0.30 s (**Figure 5-10**), with an average of 0.17 ± 0.09 s between first and last athlete on a team to reach peak push force on the hit. Correlating the standard deviations of time delays within runs with the associated peak accelerations recorded for the teams resulted in a not-significant ($p = .161$) Spearman's rho of -0.41.

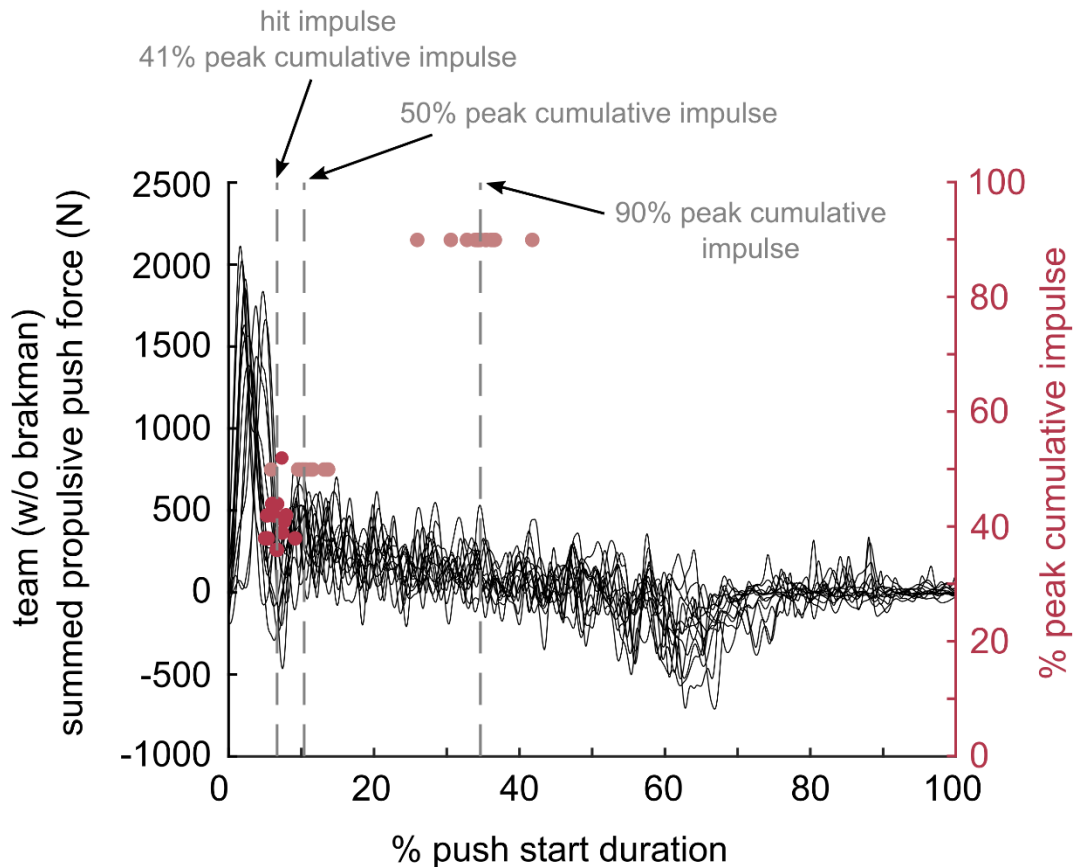


Figure 5-8: Push force data of all push starts, normalized to total push start duration. The dashed vertical lines correspond to the median time of the occurrence of (1) the end of the hit, (2) the point where 50 % of peak cumulative impulse were achieved, and (3), the point where 90 % of peak cumulative impulse were achieved. The horizontal spread of the dots around each lines indicates the variation in time associated with an event. The horizontal spread in the distribution of the darker red dots indicates the variation in what percentage of peak impulse the hit accounted for in each push start (right y-axis, median = 41 %).

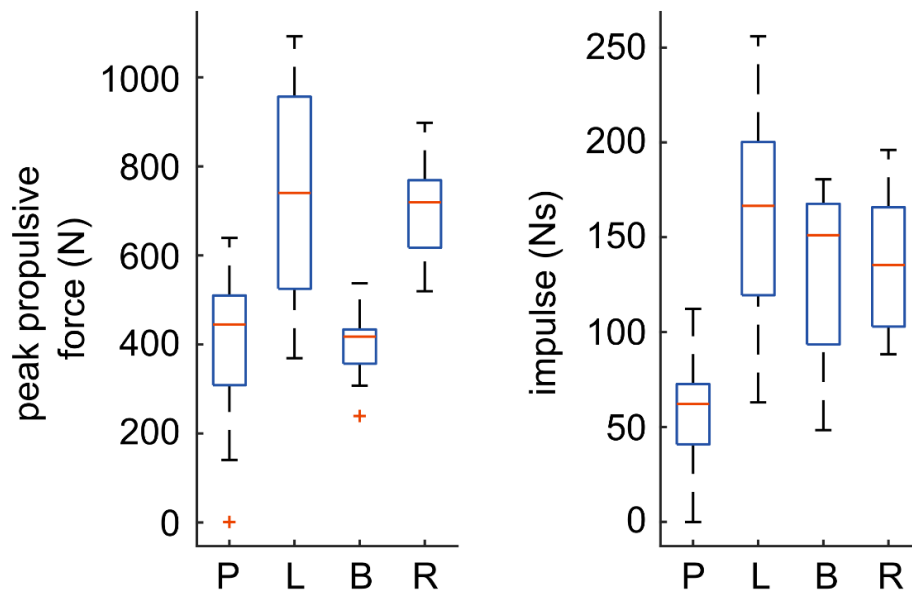


Figure 5-9: Box-and-whiskers plots presenting the distributions of peak force (left panel) and impulse (right panel), as produced by the individual athletes during the first hit on the sled across the 13 recorded runs. A red line represents the median. Upper and lower bounds of a box represent 75th and 25th percentile, respectively. Outliers are defined as values that are more than 1.5 times the interquartile distance away from the median; the whiskers extend to the most extreme data points that are not considered outliers. The x axis shows the four positions of athletes. P = Pilot, L = athlete on the left, R = athlete on the right, and B = the brakeman.

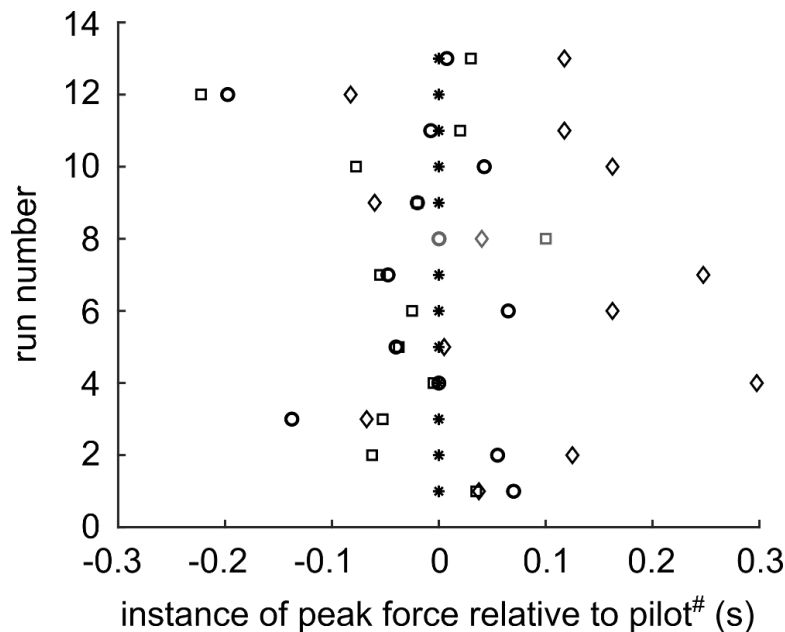


Figure 5-10: Times of peak propulsive push force on the first hit, relative to the pilot (#relative to the athlete on the left, run 8, as the pilot was not pushing). Time differences are presented for each run, with the athletes represented by different markers. Asterisk = pilot, circle = athlete on the left, square = athlete on the right, diamond = brakeman in the back. Negative values indicate that the associated athlete reached peak force before the pilot did, a positive value means that they reached it later.

5.3.2 Across the push start, from hit to load

Development of push force

For the three athletes pushing on bars (**P**, **L**, and **R**), we see steady decreases in mean propulsive push force throughout the push start, while the force component normal to the track surface appears almost constant, until loading. The brakemen's push forces are more constant and remain high (or even increase) throughout the push. However, as mentioned earlier, due to technical difficulties with the sensor setup, the brakemen's push forces should be considered with caution. For the athletes pushing on bars, means of the normal push force component increase from the first 5 % of push start duration to the second 5 % interval and then remain about constant, and negative (towards the track) until the athletes start to load the sled (**Figure 5-11**).

Force effectiveness

Push force effectiveness was greatest, ranging between 0.5 and 1, for approximately the first 10 %, and then again for roughly the last 40 % percent of the push start (**Figure 5-12**). In the very beginning (the first 5 %), median force effectiveness was 0.65 (with 25th and 75th percentile = 0.51 and 0.85, respectively) for the pilots, 0.75 (25th = 0.59, 75th = 0.90) for the athletes pushing on the left, and 0.69 (25th = 0.36, 75th = 0.88) for the athletes pushing on the right side of the bobsled.

Across the 'steady state sprinting' phase, from about 10 % to 45 % (roughly between hit and the time when the pilots would start loading), median force effectiveness was 0.22 (with 25th and 75th percentile = 0.14 and 0.33, respectively) for the pilots, 0.34 (25th = 0.20, 75th = 0.44) for the athletes on the left, and 0.23 (25th = 0.07, 75th = 0.43) for the athletes on the right (**Figure 5-13**).

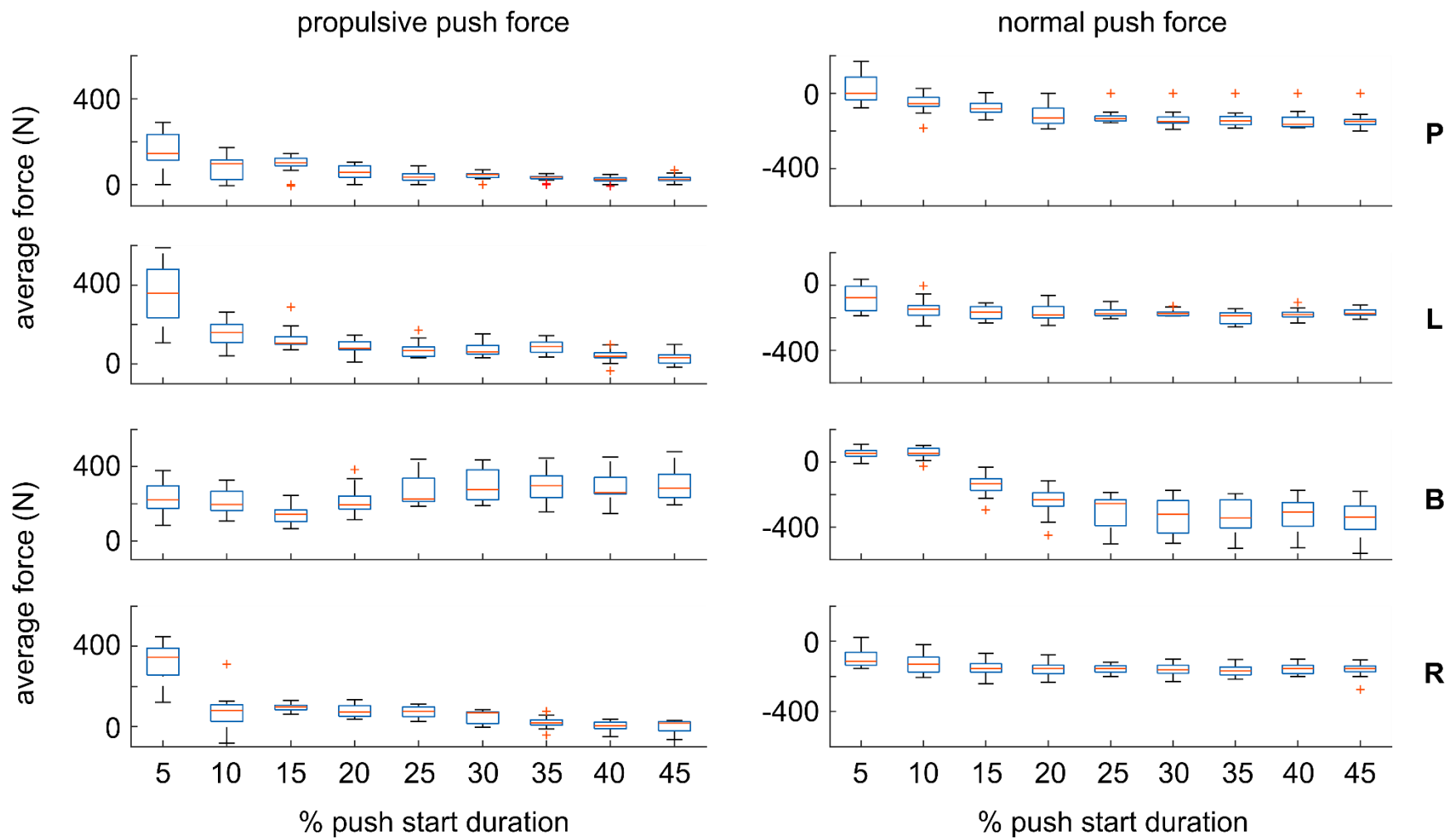


Figure 5-11: Boxplots of the mean propulsive (left column) and normal (right column) push force for the first 45 % of the start phase. The rows represent from top to bottom: the Pilot (**P**), Left (**L**), Brakeman (**B**), Right (**R**) athlete.

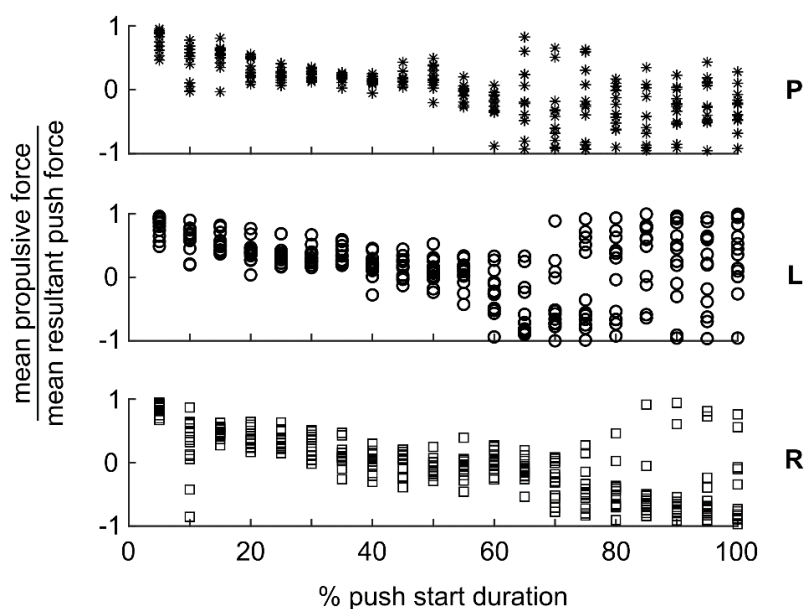


Figure 5-12: Mean force effectiveness for each 5 % interval across the push starts. The top panel contains data for all the pilots (**P**), middle for the athletes who pushed on the left (**L**), and bottom for the athletes who pushed on the right (**R**). Each circle corresponds to the value of force effectiveness for a given interval in a push start trial.

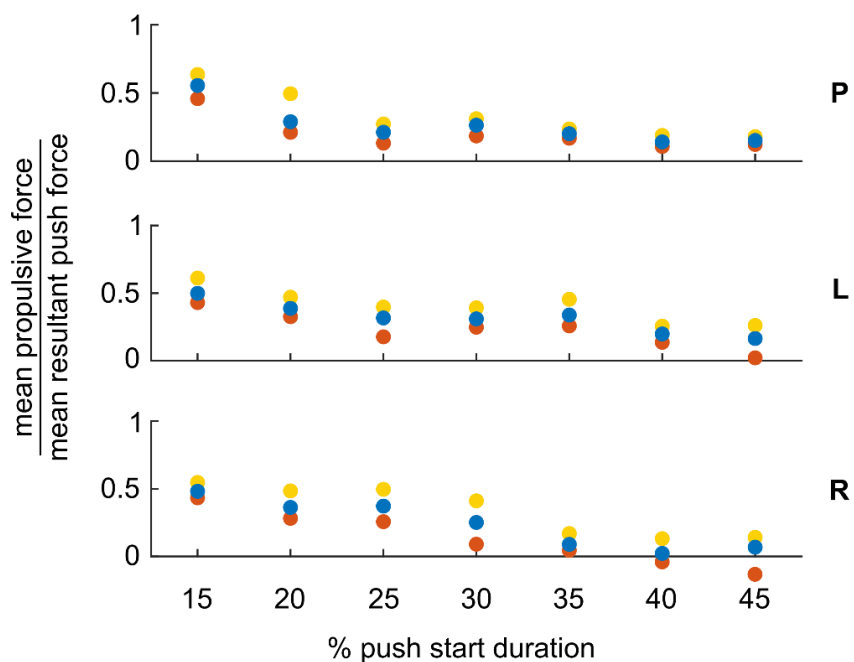


Figure 5-13: Push force effectiveness from the time after the first hit to before the start of loading. The top panel contains data for all the pilots (**P**), middle for the athletes pushing on the left (**L**), bottom for the athletes pushing on the right (**R**). Each vertical chain of dots indicates the spread of values for push force effectiveness for a given push position across all trials. The centre dot (blue) indicates the median, bottom (red) the 25th percentile of the distribution, and top (yellow) the 75th percentile. Push force effectiveness was calculated as the mean absolute propulsive force during the 5 % of the push intervals, divided by the mean absolute normal force measured during that same period.

5.3.3 A closer look at two sample starts

In example trial B (ExS_B), there was a small plateau in the bobsled speed in the first second of the push start, but such a loss of speed was not observed in example trial A (ExS_A). Examining the corresponding push forces revealed that the total propulsive push force generated by the athletes was near zero when the sled speed plateaued in ExS_B. In contrast, the total propulsive force in ExS_A remained high and bobsled speed kept increasing (**Figure 5-14**).

Around the time of loading load, the one event that can be clearly identified in the force traces is the moment when an athlete takes their hands (or the last one) off the push bar or handle. From the video records, the instant of last ground contact, defined as the onset of the loading phase, can be identified. Some pilots load the sled by jumping in and fully leaning on their push bar, others move one hand onto the cowling when they are still running and then might lean on both bar and sled when jumping in. The athletes on the left and right side of the bobsled do not jump when loading but rather step on a bunk (like a little step) on the side of the sled, and then into the sled from there. The brakemen can swing into the sled in one move, but they can also briefly rest on the back of the sled and then slide in. We cannot see these smaller details in the push force or speed traces. What we can confirm, is that clearly visible drops in sled speed occur at loading (as determined in video recordings) and can be associated with preceding reductions in and/or negative propulsive push forces for a given athlete. At the same time, (negative) push forces can still be recorded when the athletes are already in or on the bobsled and still holding on to their bars or handles (**Figure 5-15 & Figure 5-16**).

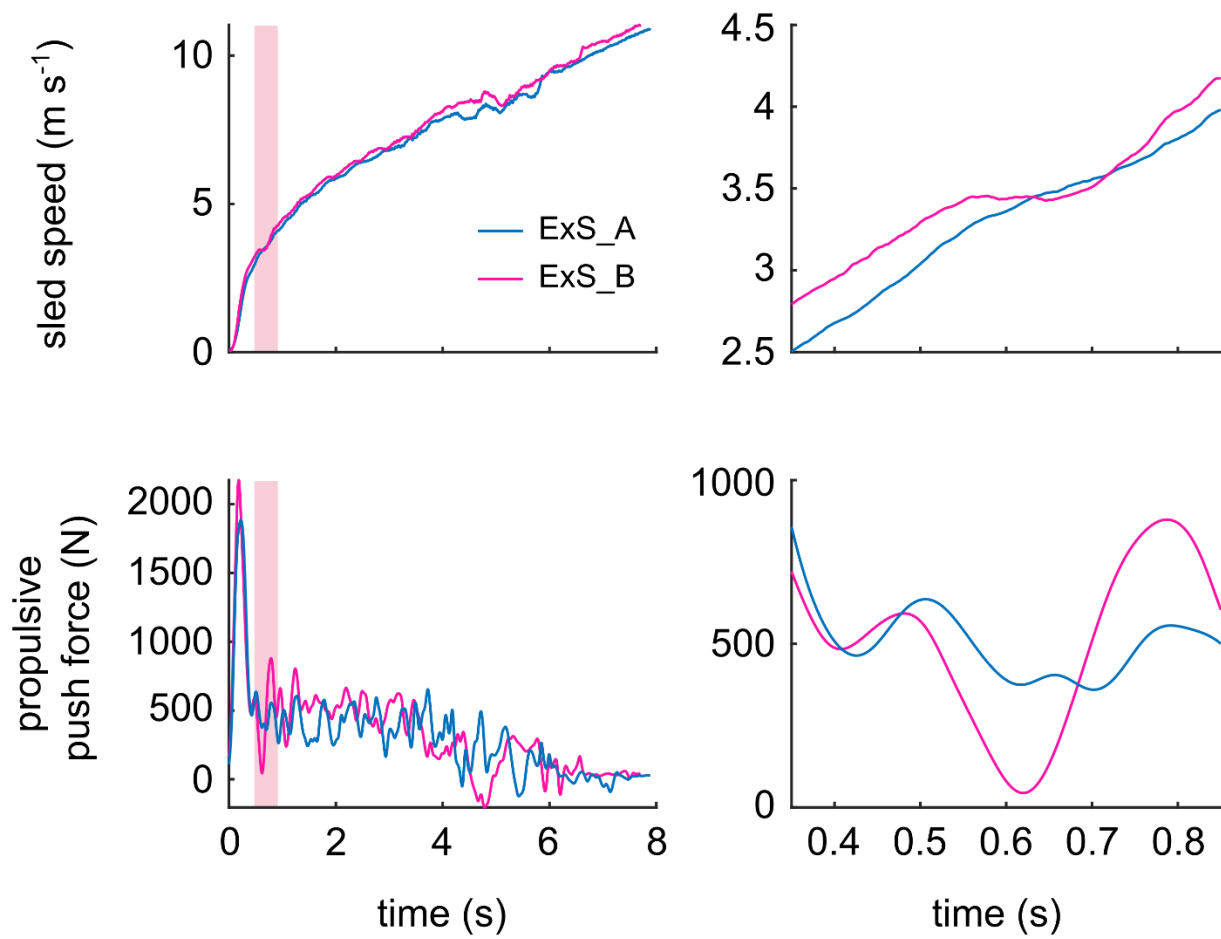


Figure 5-14: Time series data of sled speed and propulsive push force for two exemplary trials (ExS_A and ExS_B). Complete time series data are presented in the left column for speed (top) and total propulsive push force (sum of all four athletes; bottom) and zoomed in views of the region of interest (red shaded area) are presented in the right column. A plateau in the speed trace of trial ExS_B corresponds with push a force magnitude near zero.

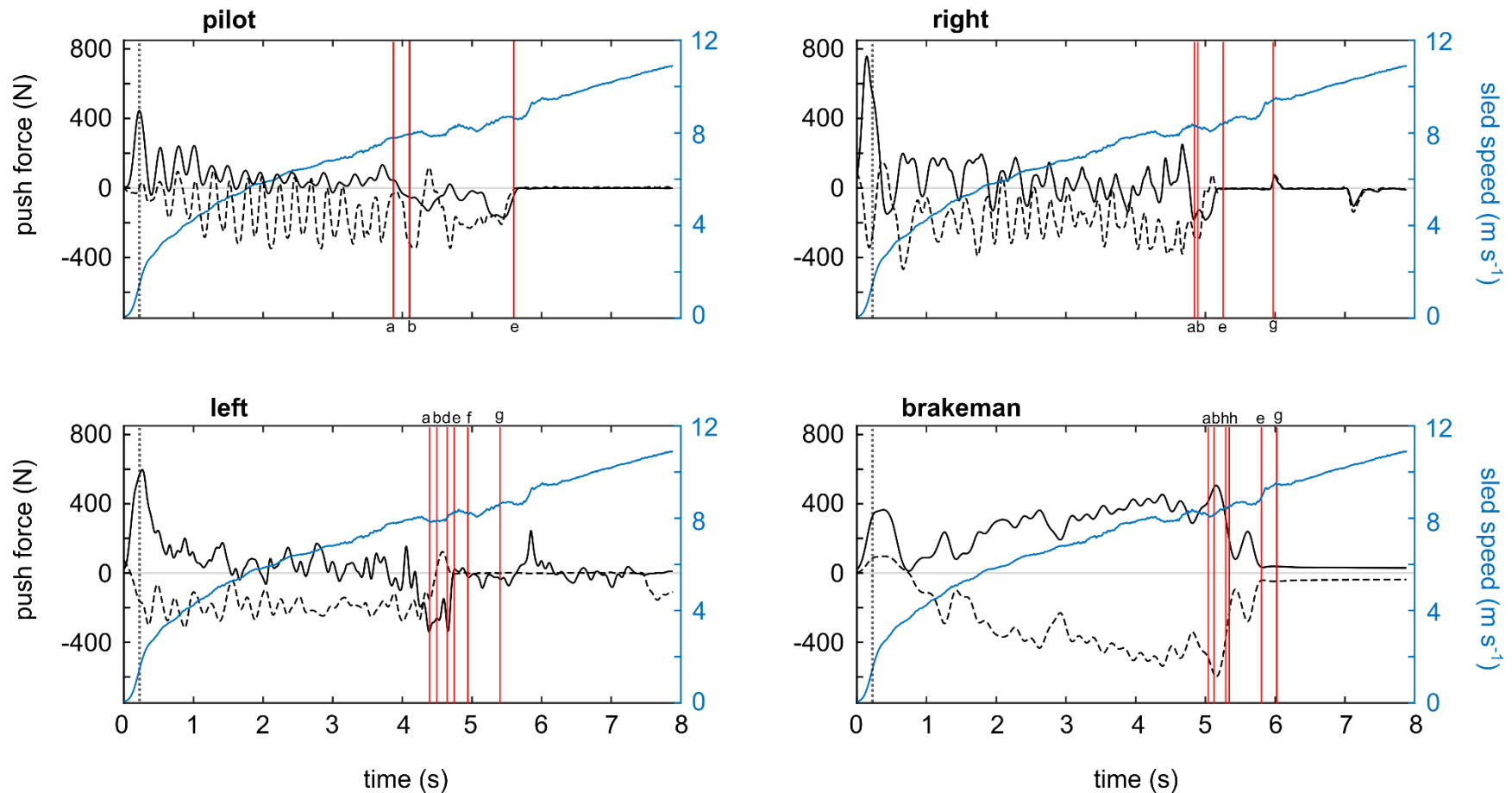


Figure 5-15: Example trial A (ExS_A). The top left panel shows the pilot data, bottom left the ones for the athlete who pushed on the left side of the bobsled behind the pilot. The top right panel shows the data for the athlete who pushed on the right side of the bobsled, bottom right the ones for the brakeman. Solid black traces represent the propulsive push force component, dashed black traces represent the normal push force component. The steadily increasing blue line associated with the right y-axis represents sled speed across the push start. The dashed vertical line near time zero indicates the instant of peak force as determined from the sum of propulsive push force from all four athletes. The solid vertical lines mark certain events in the loading process that can be observed in the video data. The labels (small caps letters) indicate what happened in the specified instant. With **a** = ground contact last step, **b** = toe off to load, **d** = foot on bunk (left or right athlete), **e** = last hand off the push bar or handle(s), **f** = move off bunk into the sled (left or right athlete), **g** = sitting or standing inside the sled, and **h** = brakeman rests on sled before moving inside.

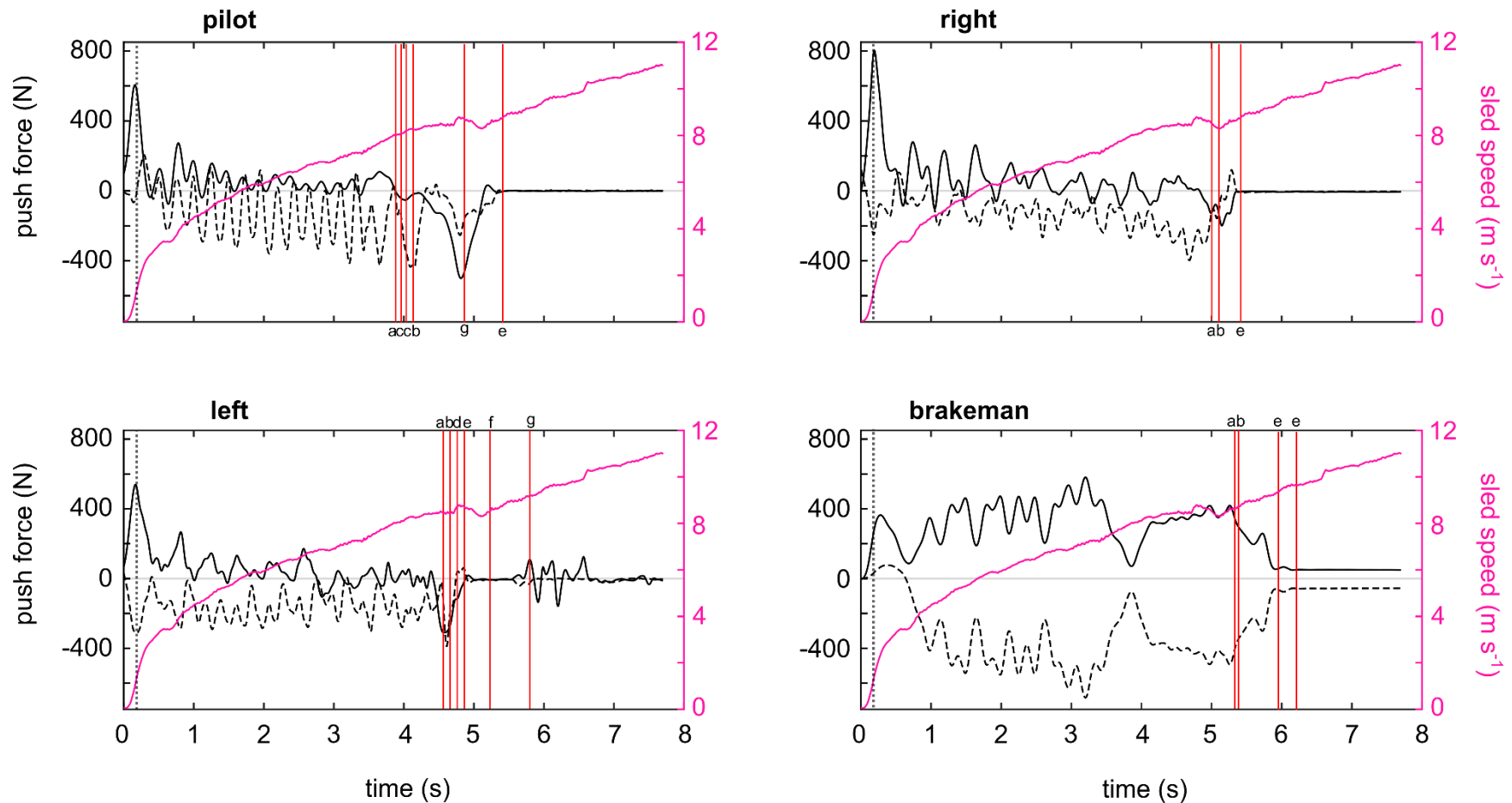


Figure 5-16: Example trial B (ExS_B). The top left panel shows the pilot data, bottom left the ones for the athlete who pushed on the left side of the bobsled behind the pilot. The top right panel shows the data for the athlete who pushed on the right side of the bobsled, bottom right the ones for the brakeman. Solid black traces represent the propulsive push force component, dashed black traces represent the normal push force component. The steadily increasing pink line associated with the right y-axis represents sled speed across the push start. The dashed vertical line near time zero indicates the instant of peak force as determined from the sum of propulsive push force from all four athletes. The solid vertical lines mark certain events in the loading process that can be observed in the video data. The labels (small caps letters) indicate what happened in the specified instant. With **a** = ground contact last step, **b** = toe off to load, **c** = pilot moves one hand across the push bar and over onto the cowling – before starting the load, **d** = foot on bunk (left or right athlete), **e** = last hand off the push bar or handle(s), **f** = move off bunk into the sled (left or right athlete), **g** = sitting or standing inside the sled, and **h** = brakeman rests on sled before moving inside.

5.3.4 The load

Sled speed at loading ranged from 7.65 to 8.91 $\frac{\text{m}}{\text{s}}$ (**Figure 5-17**). Pilots never initiated the loading before the team had pushed the sled across the start line and over the crest, and all four athletes in a crew were off the ice within the first half of the steeper-slope section (**Figure 5-18** for a qualitative presentation).

The difference in time between instant of load and the crossover point of push force contribution and (theoretical) weight force contribution was variable across all trials and athletes, ranging from 0.15 s to 1.59 s. The differences between and critical push force and propulsive push force at load ranged from 5.60 to -93.10 N, with a median value of -11.3 N (with -20.9 N and 14.3 N for 25th and 75th percentile, respectively), which means that on average athletes' push force at load was 11.3 N greater than the calculated critical force. Separated by athlete, median calculated drag at the time of load was 5.90 N (5.70 N; 6.10 N) for the pilots (**P**), 7.30 N (6.70 N; 7.50 N) for the athletes pushing on the left side (**L**), and 7.80 N (7.60 N; 7.90 N) for the athletes pushing on the right side (**R**) (**Figure 5-19A**). Median critical force across all trials was 1.80 N (1.80 N; 1.80 N) for **P**, 1.80 N (1.70 N; 1.90 N) for **L**, and 1.4 N (1.4 N; 1.6 N) for **R** (**Figure 5-19B**). Lastly, median push force at the time of loading was 23.40 N (20.10 N; 42.70 N) for **P**, -11.5-N (-21.60 N; 14.10 N) for **L**, and -0.70 N (-11.50 N; 13.40 N) for **R** (**Figure 5-19C**).

An increase in drag would result in the reduction of the accelerating effect of a given amount of push force, as well as in the increase of the critical force (**Figure 5-20**).

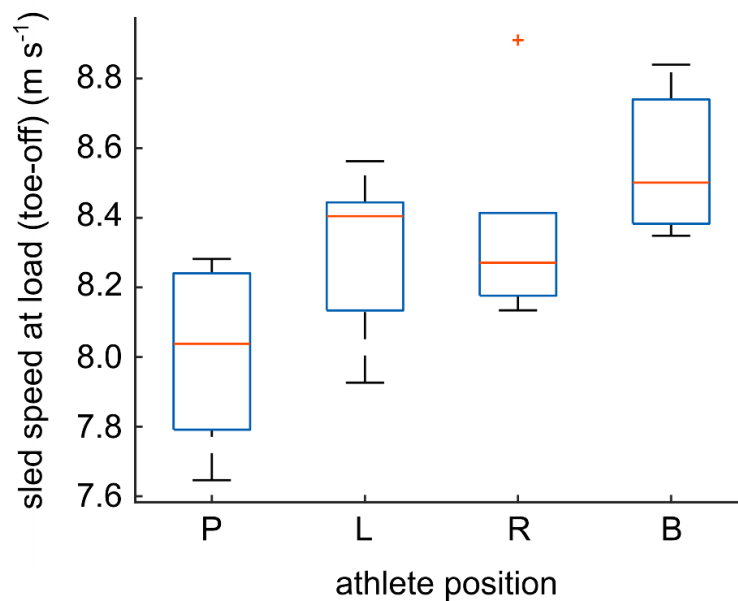


Figure 5-17: Box-and-whiskers plots presenting the estimated sled speed at the instant of loading (toe off the ice), grouped by position. P = Pilot, L = athlete on the left, R = athlete on the right, B = brakeman in the back.

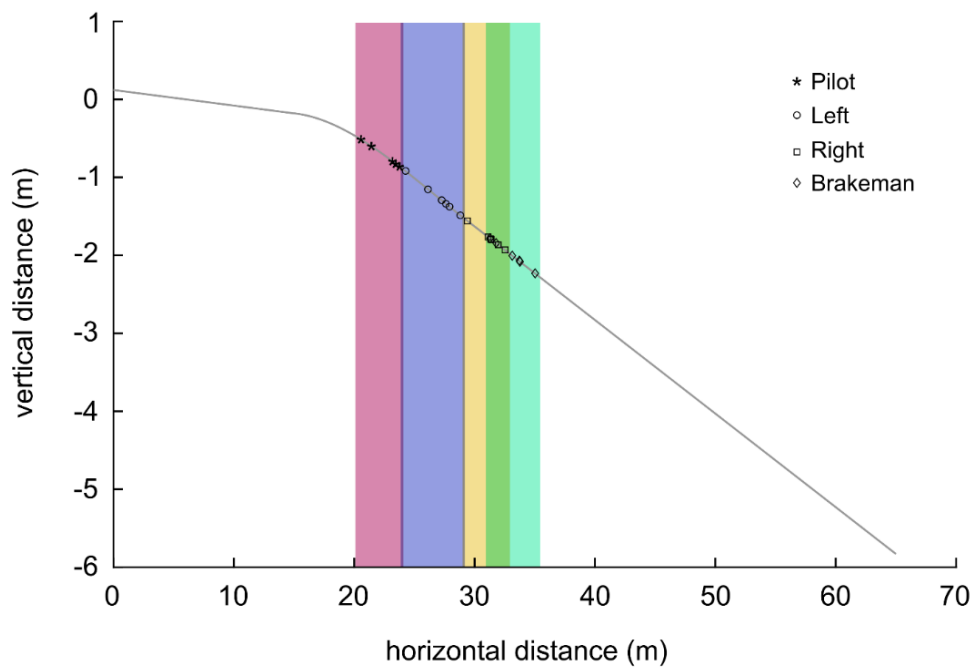


Figure 5-18: Estimated sled positions along the track at the instant of loading (toe off the ice), grouped by position: Asterisks and magenta shaded bar (first from the left) = pilots, circles and blue bar (second) = athletes on the left, squares and yellow bar (third) = athletes on the right, diamonds and green bar (rightmost) = brakemen in the back. Note, that the different 'loading regions' are not completely separated. The loading order (pilot, left, right, brakeman) was consistent across starts. However, overall loading timing was earlier in some trials than in others, causing the markers for a given team to shift left relative to others and the bars to overlap.

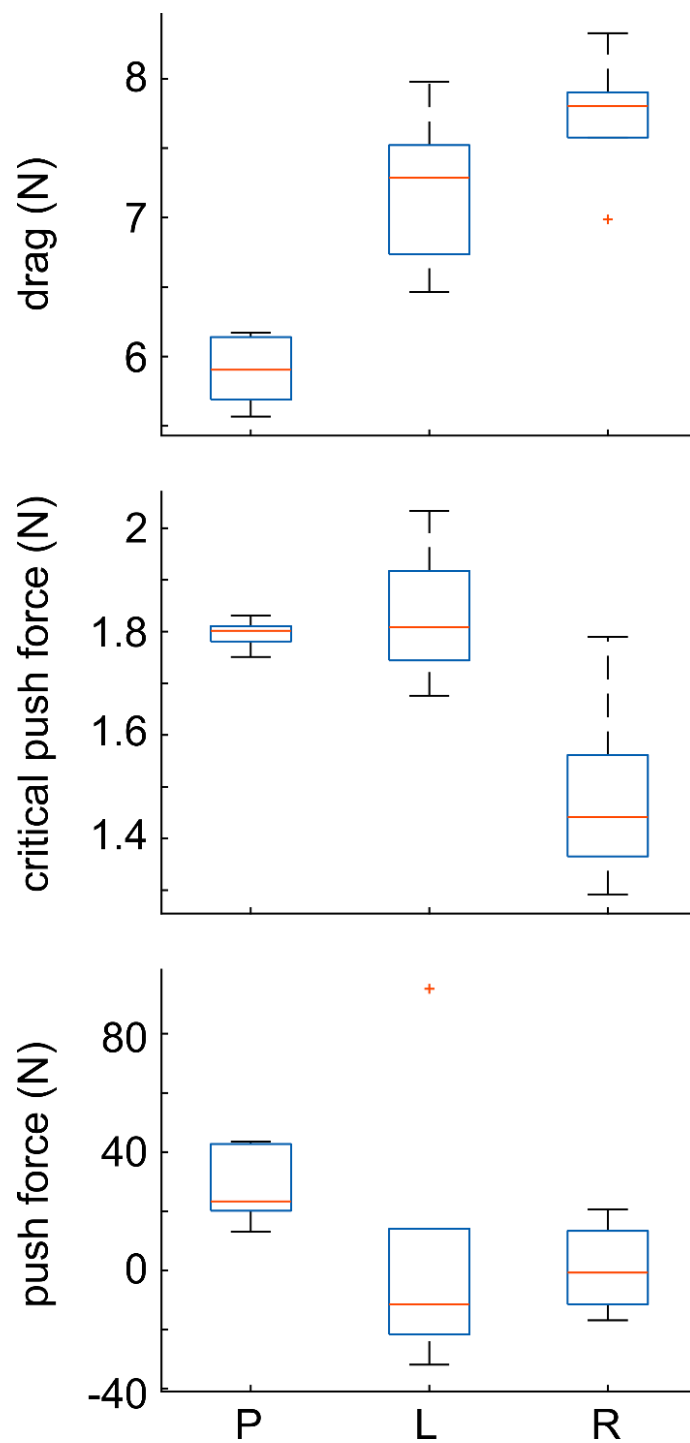


Figure 5-19: Box-and-whiskers plots representing - separated by athlete (**P** = pilot, **L** = left side, **R** = right side) **A:** the force of air drag based velocity of the bobsled measured at the instant of load, **B:** the critical push force at which an athlete would contribute more to sled acceleration by sitting inside the bobsled than by pushing it – calculated for the associated drag conditions, and **C:** the average propulsive push force recorded in the last second prior to the instant of loading.

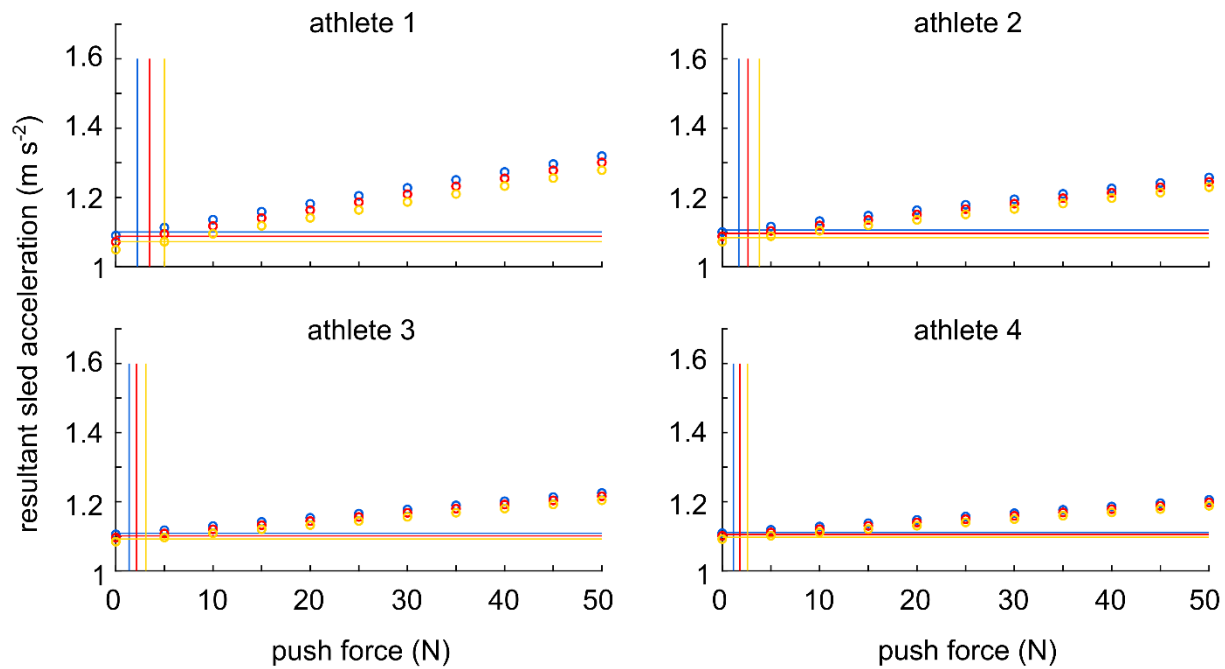


Figure 5-20: Sled acceleration as simulated for push forces ranging from 0 to 100N (circles) The different colours represent different drag magnitudes based on varying sled velocities: blue = $8 \frac{\text{m}}{\text{s}}$, red = $10 \frac{\text{m}}{\text{s}}$, and yellow = $12 \frac{\text{m}}{\text{s}}$. The horizontal lines indicate the acceleration of the sled if the athlete ceased pushing and jumped in the sled instead. The vertical lines indicate the critical forces for the different drag conditions.

All loads were positive, with speed increases ranging from 2.22 to $2.66 \frac{\text{m}}{\text{s}}$ (Table 5-1). Spearman correlation of sled speed at the beginning of the load with increase in speed during the load resulted in a not significant $r = -0.40$ ($p = 0.43$). Differences in distance (travelled based on data vs. simulated at constant acceleration) ranged from 0 to 0.7 m, which resulted in time lost during the load (based on this approach) ranging from 0 to 0.06 s (Table 5-1).

Table 5-1: Overview of the parameters that were used to determine the efficiency of a team load: (1 & 2) The measured sled speed at the onset and at the end of the load (Start speed and End speed, respectively), (3) the difference between the two speeds (delta s), (4) the distance traveled during the loading process as calculated based on the recorded sled speed (d data), (5) the theoretical distance traveled during the loading process as calculated based the assumption of a constant acceleration from start speed to end speed (d constant acceleration), (6) the difference between the two distances (delta d), and (7), delta d, the distance that theoretically could have been travelled expressed as a time (Time lost).

Trial#	Start speed ($\frac{m}{s}$)	End speed ($\frac{m}{s}$)	Δs ($\frac{m}{s}$)	d data (m)	d constant acceleration (m)	Δd (m)	Time lost (s)
1	8.03	10.53	2.51	27.50	27.90	-0.30	-0.03
2	7.78	10.00	2.22	26.50	26.70	-0.20	-0.02
ExS_A	7.95	10.30	2.35	26.70	27.40	-0.70	-0.06
4	7.71	10.37	2.66	27.20	27.10	0.00	0.00
5	7.60	10.12	2.52	26.30	26.60	-0.30	-0.03
Ex_S_B	8.17	10.49	2.32	27.30	28.00	-0.70	-0.06

5.4 Discussion

The purpose of this research project was to gain insights into the athlete contribution during the 4-man bobsled push start. We investigated the kinetics during the hit (i.e., the very first push in a trial) and across the push start from hit to loading; the effects of force application as they can be observed in a sled speed graph, as well the timing and efficiency of the load. Following the structure of the methods and results sections, the following is organized as (1) The hit, (2) from hit to load, (3) a closer look at two runs, (4) the load. However, at this point in the chapter, the lines between the groups are a bit blurred and some items shifted between groups.

5.4.1 The hit

Our results indicate that the hit is an important part of the push start, as it allows the athletes to produce the greatest propulsive push force, and a large impulse, resulting in a large increase in sled velocity in the first second of the start. The data suggest that the hit accounts for about 41 %

of the peak impulse but we need to keep in mind that this number is based on push force data exclusive of the brakeman. We did run the same analysis including the brakeman forces, which lowered the value to about 20 %. We believe that the brakemen might be able to produce a more constant push force than their crew member (because of their position behind the sled) just not as much more as we measured. Therefore, I would expect that for four athletes the hit impulse relative to peak impulse would lie somewhere between 20 and 41 %.

Peak propulsive push force was larger for the athletes pushing on the left (**L**) and right side (**R**) of the sled, compared to pilot and brakeman. On the first hit, **L** and **R** might be in the best position for propulsive force application. While the brakeman almost throws himself into the bobsled at first and then needs to transition into the first step, both **L** and **R** take a step right away. Like the brakeman, both athletes also get to place their feet on the start block, which might give them an advantage over the pilot as well. who starts with both feet on the ice. Push force rose quickly for **L** and **R**, meaning that they applied their high forces quickly, while the brakemen seemed to apply force for a longer period of time. The latter is said with caution since we are wary of the recordings from the brakeman handles. However, having observed athletes on the track as well as in videos, it is conceivable that, due to different hit technique, a brakeman might apply force for slightly longer than the others. Such differing patterns could result in similar impulse magnitude between the three of them, compared to the pilot.

As for the timing between athletes on the hit, the differences that we measured were small, less than a third of a second across all runs. Whether this difference is large and meaningful is hard to tell at this point. It seems small, however, considering that we are talking about bobsleigh, small differences can still be meaningful. But why might perfect synchronization on the hit matter for a team? Considering the functional force-velocity profiles for the push start, we would expect the

greatest push force capacity at zero velocity, and a decrease in force with increasing velocity. If an athlete were to hit the sled later than everyone else, it could be problematic for two reasons. First, the sled might move away from them, and they would have to catch up (possibly by pulling it back) before being able to contribute to propulsion. Second, by missing the instant of zero velocity and greatest resistance of the sled, the athlete might miss out on the chance to contribute maximum push force, which might affect the outcome of the push start and, thereby, the outcome of a run. It is also possible that the timing of peak force is not the parameter that really matters, but that the timing of onset (and potentially the end) of the hit impulse are more important. In this context, I want to pull in what can be observed in the comparison of the two sample starts. The total push force of the team dropping to near zero, which aligned with a brief plateau in sled speed (ExS_B), can only be achieved when all athletes stop pushing forward at about the same time i.e., in a synchronized manner (or if one of them pulls back very strongly to counteract the others, but that seems unlikely). Conversely, with offset push timing, moments of (near) zero acceleration will not occur. Perhaps both are just different but valid strategies for the push start, or particularly the hit. It does look like in ExS_B the team goes into the plateau with a higher speed than team ExS_A, which might be the result of a better coordinated hit, after all. However, more data, more examples would be required to be certain about this.

5.4.2 Across the push start, from hit to load

Propulsive push force was largest on the hit and then decreased over the duration of the push start, as we had expected (**Figure 5-11**). This finding is true for pilot, athlete on the left, and athlete on the right side of the sled. As mentioned earlier in this chapter, we have reason to believe that the force sensor set-up for the brakeman handles did not work as intended, and that we need to be

careful when it comes to drawing conclusions about the recorded forces. Therefore, the continuously high (or even further increasing) force output that we see for the brakemen across all pushes, is likely not correct and the brakeman force will not be discussed further in this paragraph. This result of decreasing propulsive push force over time – and with increasing sled speed – is exciting. It supports the idea that the push start is a functional force-velocity problem and that, therefore, functional force-velocity testing might be a useful tool in the recruitment and training process. Somewhat unexpected was how quickly force magnitude dropped after the hit. Two potential explanations might be (1) that for this specific task, we are looking at a non-linear functional force-velocity relationship, as has been reported a couple of times previously in other sports (Herzog et al., 2015; Rudsits et al., 2018) or (2) that the conditions (specifically sled speed and resistance) and as result the athletes movements are different on the hit compared to the following steps that the two parts could be considered two different tasks. Such an observation has been made previously (Kawamori et al., 2014; Lockie et al., 2003; Markovic & Jaric, 2007) and it would mean that a meaningful functional force-velocity profiling might have to be exclusive of the hit – or specifically account for the two different phases. The relatively constant magnitude in normal push force was surprising to me. This detail may suggest that the normal push force is mainly an artifact of the athletes' movements, a result of the vertical displacement of their centre of mass during sprinting, and that their conscious push force application really is mainly directed forward, in the main direction of movement – which is a neat segue to force effectiveness.

Force effectiveness seems to be particularly important in the world of cycling and has been studied for decades (e.g. Bini et al., 2013; Faria & Cavanagh, 1978; Kistemaker et al., 2023) But it has also been considered in other sports – and is worth at least discussing in the context of the bobsled push start as well. Push force effectiveness was expressed as the ratio of the propulsive force

component relative to the resultant push force component (**Figure 5-12 & Figure 5-13**). Our results suggest that for the hit, most of the athletes' push force was directed such that it resulted in acceleration of the bobsled, with median force effectiveness of 0.65, 0.75, and 0.69 for pilot, athlete on the left, and athlete on the right, respectively. After that, the pattern was reversed, and the normal push force became the dominating component of the resultant force, with reductions in median force effectiveness of 66, 55, and 67 % for pilot, athlete on the left, and athlete on the right, respectively. An important question in this context is whether force effectiveness is important enough to be emphasized, monitored, and practiced. To answer this question, one needs to consider both the data discussed earlier in this section as well as the setup of the push bars. Bobsled athletes are typically tall individuals. The side push bars (left and right) are only about thigh high for them, and the pilot's bar approximately at hip height, which means that the athletes need to bend down to hold on to and push against their bars. Based on this constraint in posture, it can be speculated that it is easier for them to apply force directed towards the ground than directed forward. Moreover, the task is to sprint and push at the same time, and with every step they move forwards, but also accelerate their centre of mass upwards to achieve a flight phase. It seems plausible that the resulting vertical fluctuation would carry through to their arms and into their interactions with the sled. As a result, we would expect to measure not only propulsive forces, but normal forces, as well. When counting the number of steps an athlete took from hit to loading based on both their normal force records and the video recordings, the numbers matched. Considering further that, unlike the propulsive push forces, the normal forces did not seem to follow the decreasing trend with increasing sled speed may suggest that they are a necessary part of the movement and therefore likely very hard to control, let alone prevent. Lastly, greatest force effectiveness coincided with the greatest propulsive force magnitude where it, arguably, matters most. Based on

these findings, it may be useful for a coach to remind the athletes of the importance of the hit, where the potential for high push force magnitudes is greatest, and good force effectiveness seems feasible. Beyond the hit, however, prioritizing or enforcing maximum push force effectiveness is likely counterproductive and detrimental to performance.

5.4.3A closer look at two sample starts

The force traces clearly show the moments when athletes let go of their push bars or handles. Loading is associated with reductions in sled speed as well as reduced or negative propulsive push force for a given athlete. These connections make sense, which is reassuring, but without video, we may only be able to roughly determine the period of loading but cannot point to a specific event (like the last step or toe-off). An important improvement for future testing would be to include video recording for all trials, and have it synchronized with the system on board of the bobsled. Another way to improve our understanding of how athletes' actions manifest in the force and speed data might be a series of experiments under comparatively controlled conditions. I believe that the athletes know quite well what they do and that they would be able to modify certain parameters between trials to see if and how those changes would be reflected in the data. For example, we could ask them to systematically load earlier or later, at specific points along the track, and to focus on their load and try to slide forward and into the sled versus just dropping down in it. We could ask a brakeman to push while squeezing the handles versus not squeezing, to see if that can account for some of the elevated baseline that we see in the data. The IMU could be mounted on a single push sled, where only one athlete pushes at the time and most of the acceleration of the sled can be attributed to them.

5.4.4 The load

Estimated sled speeds at loading ranged from 7.65 to $8.91 \frac{\text{m}}{\text{s}}$ (**Figure 5-17**), which is supposedly less than any of the athletes' maximum sprint speeds. However, since loading requires coordination, a new direction of movement (sideways instead of just further down), and that they are still moving at least as fast as the sled (to minimize pulling back), it is reasonable that the athletes would not go to their absolute maximum before attempting to load. For all teams, the loading order was pilot, athlete on the left, followed by the athlete on the right, and the brakeman last. Not one of the teams started loading before they had reached the steeper section of the track (**Figure 5-18**). A caveat with these findings is that they are approximate values. The instants of load were detected in videos and then had to be manually aligned with the force and speed data, as no automatic synchronization mechanism was in place. Secondly, sled speed is based on integrating acceleration data, and the distance travelled along the track comes from a second integration step of the same data. These issues are discussed a bit more in the limitations section below. Important to note here is that the values for the position on the track around the time of load align with what we can observe in the videos, which makes me confident in that our estimates here are reasonable approximations.

Loads were positive (i.e., sled speed was greater at the end than in the beginning) for all trials, which indicates that it is not the most useful metric and, since we were dealing with elite athletes, this result is not too surprising. What is interesting however, is that there was only a non-significant moderate negative correlation between the increase and speed during the load and the speed at the beginning of loading. The non-significant result is likely due to the very small sample size. At the same time, considering the data (**Table 5-1**), it becomes apparent that the relationship 'slower speed

in the beginning results in greater gain during the load' is also not straightforward. This finding at least suggests that higher speed at the beginning of loading does not make bigger gains (compared to other teams) impossible.

The comparison between push force at load and the theoretical critical force reveals a mixed picture. For some athletes the difference was near zero, for most, however, it was negative. A negative value indicates that push force was greater than the critical force. Calculated drag forces were very small, less than 10 N. For some athletes, the difference of the two values was positive, which indicates that around the time of load, their propulsive force contribution was negative. It is important to keep in mind that these findings are based on the assumption that drag does not change when the athletes load the sled. In reality, however, the athletes would likely increase drag, at least temporarily, by increasing the cross-sectional surface area of the bobsled which is part of the formula used to calculate drag force (**Equation [5.11]**). Even if they find the perfect positions once they are sitting in the sled, between jumping off the ice and sitting down, they must increase the surface area of the bobsled, which would result in increased air resistance. Increased drag would reduce the accelerating effects of a given amount of push force and increase the critical force (**Equations [5.2] and [5.10] ; Figure 5-20**). So theoretical, so good, but what do these findings mean for the real-life application? Ideally, we would be able to define an optimal time to load, calculate it, and return it to a team as an objective instruction to improve start performance. However, while the theory makes sense, it suggests that critical push forces would be very low, with values ranging between 1 and 2 N. If an athlete were to be at a point where they are only able to apply about 2 N of force to the bobsled, they most likely cannot keep up with the sled anymore (or at least not much longer). Therefore, it seems reasonable to assume that, if they cannot push anymore, loading will be challenging and may require them to pull back on the bobsled and slow it down. Consequently,

although we can calculate the point at which athletes' contribution to acceleration would be greater if they were inside the sled, it should not be used as a reference for when to load. Instead, the athletes should probably load when they can still contribute more than the critical force as that should increase the likelihood of their load being successful. Whether this point can be calculated is not clear/obvious based on our data, it might be something that only the athletes can feel and refine by trial and error. The instrumented sled could be utilized to assess if they were successful.

Finally, we developed an approach to quantify the efficiency of a team load, aiming to determine potential to improve the process and provide feedback to the athletes in a meaningful metric – which is time. It is possible for a team to achieve a zero-loss load as well as, technically, to make time with the loading. Teams that did not lose any or the least time during their load (**Table 5-1**) managed to keep accelerating the sled for about the first third of the total load duration, such that their sled speed trace lies on top of the theoretical constant acceleration speed graph – or even exceeds it. This makes sense as, mathematically, a greater speed at the end of the load could be achieved, for example, by (a) constant acceleration, (b) zero acceleration and then great acceleration later, (c), deceleration followed by acceleration, and (d) acceleration followed by zero acceleration or deceleration. Then there could also be multiple variations of these five examples, but the point is that while the result might be same in speed, it would not be in distance travelled. Therefore, increased acceleration in the beginning must be a good strategy, as it allows for a longer distance covered on the track. This conclusion suggests that the efficiency of the load mainly depends specifically on the pilot's load (and maybe the load of number two, depending on how close to each other they go) and whether he can add to the momentum of the sled when pushing off the ice, rather than slowing it down. This does not mean that the other three athletes do not matter. If they could all add to the velocity of the sled with their load, it would make their run

better. But, as discussed above, later acceleration of the sled would not have the same effect as early acceleration. Moreover, it is possible that with a later load at increased sled speed it becomes more difficult and thus less likely to add much more with loading.

5.4.5 Limitations

There are a few limitations to consider when reviewing the data and results from this project.

I) The force records from the brakeman handles. It is very unfortunate that we cannot rely on these measurements, which affects both force magnitudes and force-time parameters like instants of peak force or the duration of the hit. Based on comparisons with the video recordings, we can determine onset of push and the moment when an athlete took their hands off the handles from the force traces. Anything in between those two events, however, is uncertain. A first step towards a better understanding of what is going on with the force sensors might be to go back to the track and, if possible, have brakemen push the sled alone. Matching the resulting push force measurements with the acceleration of the sled, might show more clearly where the problems lie. Beyond that, a future version of this instrumentation will likely have to include a new solution for the brakeman handles. When we designed our set-up, we discussed trying to cut the brakeman handles off the sled, installing load cells in their stead, and then bolting the handles back on. At the time, we decided against that route, and here are the reasons why: (1) Moving the handles back relative to the rest of the sled could interfere with how the team is used to executing the start. Longer sled, further from the block, L and R cannot stand on the block anymore and touch their bars at the same time. (2) Load cells would be more expensive than force sensors, especially if they were smaller to keep the sled-load cell-handle sandwich as thin as possible. (3) Most importantly, While the steps to this alternative brakeman handle set-up sound simple, we are not

certain, that it would work. With limited time and only one sled to work with, such an invasive approach seemed too risky, especially since the force sensors seemed to work well during initial testing and calibration.

II) We were not able to record full effort starts, which would have been closer to a competition situation. We tested a new system in this study, which is meant to say that the athletes were not used to pushing our test sled. While we designed out instrumentation based official specifications for competition bobsleds, it was not feasible to provide an exact replica of the 4-man sled the teams would use regularly. As a result, some of the athletes were wary of the set-up, the bars and handles did not feel familiar, and there was no opportunity for a familiarization period. Furthermore, the bobsled that we got to use was an older model and narrower than the one the teams were mainly using in training and competitions that season. The lack of room inside the sled (comparatively) may have affected the way the athletes loaded it. Loading looks smooth from the outside but that does not negate the fact that it is a tight fit and, not to forget, the athletes are only able to sprint on the ice because they wear track spikes (with more spikes). Therefore, a serious load comes with the danger/great likelihood of bruises and wounds/scars, and it is at least conceivable that athletes might like to save that for race day.

An additional note on some athletes being, let's say, cautious with their enthusiasm about the instrumented sled. I believe that there was some worry about what exactly the data might be used for and that any findings might have serious implications for individual athletes. These concerns were likely amplified by the fact that all data collections happened in the final weeks before team selection for the following season, which is a tense time for everyone involved. I do not know if this circumstance had any influence on anyone's effort level but, either way, I think the fact is worth noting and keeping in mind for any future testing. Even if the intention is not to make anyone

look bad, we need to be aware that there is the potential for it to happen. At the same time, there is the potential to help athletes to further improve what they are doing well already. The important thing is to get them on board, not least because their input on instrumentation set-up and data output could still be valuable.

III) The synchronization of force and acceleration data with the video. Wherever timing information from video is combined with timing information from push force or sled velocity data, they are most likely not perfectly aligned. While force and acceleration data were collected at 400Hz, video recording frequency was 60Hz and the two modalities were not directly synchronized. A sanity check that we have for the matching of video and forces are the moment when the athletes take their hands off their respective bars or handles. These instants can be seen in the force traces, and they seem to align with the times determined in the video. However, now we know that, for future data collection with this sled, we need the video recording. Probably two cameras to cover what happens on both sides of the sled. They would likely need to be positioned somewhere halfway down the track, so that both hit and load can be captured, and synchronized with the system on the sled. A problem with that could be that the bigger the set-up the less likely the teams might be to make use of it, but such an extended set-up may not be necessary forever. With more data, video and force/speed combined, it should be possible to understand how important events manifest in the push force and/or sled speed traces (what is important could still be redefined, in collaboration with the team).

IV) Using IMU data to calculate speed and position. This process might seem relatively straightforward, basically a one-time or double integration of the original acceleration data, it bears a problem. With a certain error in any measurement, this error accumulates during integration, resulting in greater error with every integration step. We are, however, confident that our results

are reasonable approximations of the real numbers. We had validated peak IMU speed against video data before in a gym sled push task. Moreover, as mentioned earlier, the positions along the track that we calculated for the time of loading match what we can see in the video data that we have of the trials. That said, we are still working on combining the IMU data with timing information from timing gates that are installed along the track in the Ice House. The goal is to use the additional timing and position information to correct any error in the velocity (and subsequently the position) estimates.

5.5 Conclusion

There is a lot going on, in a 4-man bobsled push start, and a lot can be learned from our data. Pilot, Left, and Right produce the largest push forces on the hit (i.e., the very first push), with greatest force magnitudes recorded for the athletes pushing on the left (behind the pilot) and right. After the hit, the propulsive push force decreased quickly. We proposed a method to quantify the efficiency of a team load and made some suggestions for how to improve the measurement system. More systematic data collection with a larger number of trials would be required to substantiate our findings and potentially implement them in team practice in the future.

5.6 Acknowledgements

I would like to thank *Bobsleigh Canada Skeleton*, athletes and staff, for facilitating the data collection for this project, *Own The Podium* for financial support, the *Science Workshop* at the University of Calgary for technical support, *Andrzej Stano* and *Andrew Sawatsky* for their invaluable contribution to the design of the sled instrumentation, *Art Kuo*, *Rob Griffiths*, *Jeremy*

Wong, and especially Louis Poirier and Matt Jordan for their help with data analysis and interpretation.

Chapter 6

Active Control of Static Pedal Force Direction Results in Decreased Maximum Isometric Force Output

This chapter is based on: Onasch, F. & Herzog, W., “Active Control of Static Pedal Force Direction Results in Decreased Maximum Isometric Force Output”. *In revision*; resubmitted (R1) to the *Journal of Biomechanics* on May 12, 2023.

Individual contributions: Franziska Onasch and Walter Herzog conceived the experimental protocol. FO collected and analyzed the data and wrote the manuscript with input from WH. WH supervised the research, provided feedback, and helped shape the story.

6.1 Abstract

Complete mechanical force effectiveness in cycling is achieved when the forces applied to the pedal are perpendicular to the crank. However, empirical observations show that resultant pedal forces display substantial radial components in recreational and even highly trained elite cyclists. Therefore, we hypothesized that attempting to maximize mechanical effectiveness for the entire downstroke of the pedal cycle must be associated with a penalty that outweighs the benefits of perfect effectiveness. Twenty recreational cyclists performed maximum isometric voluntary contractions at five crank positions in the downstroke phase of cycling for two testing conditions: (i) a non-constrained (NC) condition, where athletes were asked to produce the maximum force possible on the pedal without consideration of the force direction. (ii) a constrained (C) condition, with the instruction to produce maximal pedal forces perpendicular to the crank. Resultant and effective force (force perpendicular to the crank in the NC conditions) were compared to the force

in the C condition that was, by definition, perpendicular to the crank. Maximum effective force in the NC condition was greater (mean = 50 %, range = 38 - 69 %) than for the C condition across all crank positions. Applying forces perpendicular to the crank in the downstroke of the pedal cycle resulted in severe reductions in force magnitude, suggesting that coaches and athletes should not attempt to change cycling technique to achieve perfect force effectiveness.

6.2 Introduction

Cycling is a common mode of transportation, a recreational activity, and a high-performance sport. One approach to improve performance is to increase pedal force effectiveness (Bini, Hume, Croft & Kilding, 2013; Cavanagh & Sanderson, 1986; Gregor, Broker & Ryan, 1991). When pedaling, only the force component perpendicular to the crank results in propulsion and is referred to as effective force. Forces along the crank do not contribute to propulsion and have been considered wasted (Bini et al., 2013; Bini, Hume & Croft, 2014; Cavanagh & Kram, 1985). Perfect force effectiveness in cycling occurs when the resultant pedal force is directed perpendicular to the crank. Athletes, coaches, and scientists have tried to implement this knowledge into training sessions, and it has been shown that cyclists can adapt their pedaling technique to improve their force effectiveness (Hasson, Caldwell & van Emmerik, 2008; Henke, 1998). However, whether improved cycling effectiveness is associated with improved racing performance has not been demonstrated. In fact, previous research suggests that increased force effectiveness may be associated with decreased muscular and metabolic efficiency and, thus, might not be beneficial for performance (Korff et al., 2007; Mornieux et al., 2008). Furthermore, neither recreational nor elite cyclists naturally produce forces purely perpendicular to the crank throughout the pedaling cycle and, for some sections, the resultant pedal force direction deviates substantially from perpendicular

(Cavanagh & Sanderson, 1986; Ettema et al., 2009; Hasson et al., 2008; Kautz & Hull, 1993; Mornieux et al., 2008; Rossato et al., 2008; Zameziati et al., 2006). This observation raises the question if cyclists really could and should make an effort to improve performance by increasing pedal force effectiveness or if, by exploration, trial and error, and practice, they already found the best solution, even though it seems mechanically ineffective.

The purpose of this study was to determine the effect of a task constraint, prescribing force application in a specific direction, on the magnitude of effective force output in the downstroke phase of cycling.

Applying force in a particular direction relative to the environment, such as ground reaction forces in walking and running, or pedal forces in cycling, requires the activation of multiple muscles and a specific force ratio among the activated muscles: a muscle synergy (Andrews, 1987; d'Avella, Saltiel & Bizzi, 2003; Kaya, Leonard & Herzog, 2006; Ting & Macpherson, 2005; van Ingen Schenau, Boots, de Groot, Snackers & van Woensel, 1992). Muscle synergies must change when the direction of an external force is changed (Hof, 2001; Kaya et al., 2006; Ting, Kautz, Brown & Zajac, 1999; van Ingen Schenau et al., 1992). Moreover, it has been suggested that there are two functional groups of muscles in the body, one group which is mainly associated with contributing to force magnitude, and another group that is primarily responsible for controlling the external force direction (Jacobs & Macpherson, 1996; van Ingen Schenau et al., 1992). Different muscle synergies may be associated with vastly different capabilities of the leg muscles to produce force, e.g., due to suboptimal configuration with regard to the muscle's force-length properties (Gordon, Huxley & Julian, 1966; Kulig, Andrews, Hay, 1984) or suboptimal utilisation of muscles with a great force capacity when a specific force direction is required (e.g., Housh et al., 1995; Kaya et al., 2006).

Pedal force application and force effectiveness in cycling have been studied before. For example, researchers have discussed the effects of cadence or seat height on the index of effectiveness (R. Bini et al., 2013; Ettema et al., 2009; Leirdal & Ettema, 2011); described pedal (or foot) force and its components (Cavanagh & Sanderson, 1986; Gruben et al., 2003b; Kautz & Hull, 1993; Lafortune & Cavanagh, 1983); or conducted intervention studies, attempting to improve force effectiveness (Hasson et al., 2008; Korff et al., 2007; Mornieux et al., 2008). While force magnitudes and effective force were reported in some of these studies, any changes in (effective) force magnitude were not the focus of the project and, therefore, not specifically discussed. To the best of our knowledge, the present study might be the first systematic investigation of maximal pedal force magnitude for constrained and unconstrained conditions, and the reduction in effective force associated with trying to exert force perpendicular to the crank.

We asked recreational cyclists to exert maximal isometric force to the pedal of a bicycle in different phases of the downstroke, while we recorded three-dimensional pedal forces and muscle activation patterns. Participants were asked to (i) exert forces just as they would normally do if they were cycling (non-constrained condition, NC) and (ii) exert forces only perpendicular to the crank direction (constrained condition, C).

We hypothesized that, when applying maximum pedal forces perpendicular to the crank at different crank angles of the downstroke phase of pedaling, the effective forces (F_{eff}) are smaller than the F_{eff} when participants are free to push on the pedal in what way they perceive as the most natural direction. Since redirecting pedal forces requires changes in muscle synergies, we further hypothesized that the decrease in effective force in the constrained compared to the unconstrained condition is caused, and therefore accompanied by, reduced activation of the primary leg extensor muscles acting at the hip and the knee.

6.3 Methods

This study was approved by the Conjoint Health Research Ethics Board of the University of Calgary and twenty healthy participants (28 ± 4 years, 1.77 ± 0.05 m, 74 ± 8 kg; 5 female) gave free informed written consent prior to testing. All participants were recreational cyclists and free from injuries to the lower extremities.

Protocol: After a five-minute warm up at submaximal intensity on a velo[®] ergoselect bicycle ergometer (Ergoline, Blitz, Germany), participants were prepared for testing. Surface electromyography (EMG) electrode pairs (Kendall[™] 100 Foam Electrodes, Covidien, Masnfield, USA) were placed on the skin above the muscle belly of the left tibialis anterior (TA), vastus lateralis (VL), rectus femoris (RF), gluteus maximus (GMAX), biceps femoris (BF), gastrocnemius medialis (MG), and soleus (SOL). Moving the leg through the downstroke in cycling mainly requires leg extension, and we chose the muscles accordingly. Gluteus maximus and vastus lateralis were chosen as the largest leg extensors (hip and knee, respectively) with the greatest capacities to produce force among the leg extensors. The bi-articular muscles rectus femoris, biceps femoris, and gastrocnemius medialis (acting as hip flexor & knee extensor, hip extensor & knee flexor, and knee flexor & ankle plantar flexor, respectively) were chosen because of their supposed ability to contribute sensitively to force direction control (van Ingen Schenau et al., 1992). Finally, soleus and tibialis anterior were chosen as two important antagonists at the ankle joint. As the latter two are mainly stabilizers of the ankle rather than contributing to propulsion, they were excluded from the EMG analysis. The inter-electrode distance for all muscles was 1.5 cm. A single ground electrode was placed on the left tibia. Skin preparation and electrode placement were done in accordance with the SENIAM guidelines (Hermens, Freriks,

Disselhorst-Klug & Rau, 2000). The respective sites were shaved, and the areas cleaned with isopropyl alcohol. Next, the participants were comfortably positioned on a VELOtron bicycle ergometer (RacerMate™, Seattle, USA) with strain gauge-instrumented clipless pedals (Sensix, Poitiers, France) and were instructed to perform isometric maximum voluntary contractions (IMVCs) in two different testing conditions:

(1) Non-constrained (NC): Participants performed a 5 second IMVC at five different crank angles (30°, 60°, 90°, 120°, and 150°, **Figure 6-1**), in a randomized order.

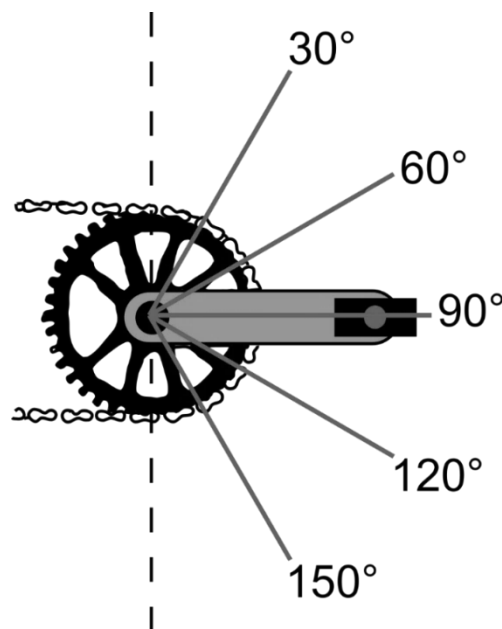


Figure 6-1: The crank positions that were tested in this study.

Participants were asked to keep both hands on the handlebars, to stay seated, and to keep the pedal approximately parallel to the ground, as they would during normal cycling. (2) Constrained testing condition (C): The five crank angles were tested in the same order as in the NC condition. The instructions were identical to the NC conditions, except that participants were also asked to direct the pedal force perpendicular to the crank. Real time visual feedback about the force direction

relative to the crank was provided. An index of effectiveness (IE), as defined previously (Bini et al., 2013; Cavanagh & Kram, 1985; Lafortune & Cavanagh, 1983), was calculated for all conditions:

$$IE = \frac{\text{Effective force}}{\text{Resultant Force}} \quad [6.1]$$

The IE for the constrained condition had to be > 0.95 for the C trial to be accepted for analysis.

Data acquisition and analysis: EMG signals were pre-amplified within 11 cm of the recording electrodes (Biovision, Wehrheim, Germany), and were recorded at a sampling rate of 2000 Hz, using WinDaq data acquisition software (DATAQ[®] Instruments, Akron, Ohio, USA). Pedal force data were collected at 250 Hz, using “I-Crank” software (Sensix, Poitiers, France). Data processing and analysis were conducted with Matlab (R2016a, The Mathworks, Natick, MA, USA) and R (R 4.1.3, <https://www.r-project.org/>).

The relevant force and EMG data were extracted as follows: For the *NC condition*, a uniformly weighted moving average with a window size of 500 ms was applied to the resultant force trace. The window with the largest average force was then used to calculate the associated effective force component and the index of effectiveness. For the *C condition*, the same moving average was applied to the recordings of the IE, with the aim to find the region where the effort was maximal but with the index closest to 1, indicating perfect effectiveness. As before, the window with the largest average IE value was used to calculate the corresponding pedal forces/ force components. *EMG data* were band pass filtered (second order recursive Butterworth, 10-500 Hz). Root Mean Square (RMS) values of the EMGs were calculated for the same 500 ms time windows identified for the maximal resultant force and IE values (in NC and C condition, respectively). To allow for

comparison of EMG results between the NC and C conditions, the EMG data were normalized to the maximum RMS value produced by each participant for a given muscle across all crank positions. VL and GMAX as the strongest leg extensors, and RF, BF and MG as the primary bi-articular muscles were selected for analysis.

Normal distribution of the data was assessed through Shapiro-Wilk tests (Shapiro & Wilk, 1965). A two-way repeated measures Friedman's test (Friedman, 1937; Zimmerman & Zumbo, 1993) (test condition x crank angle) was chosen to test for main effects and interactions. If the results showed statistically significant interactions (testing condition*crank angle) or main effects, we proceeded with Wilcoxon's paired tests for the individual comparisons. Since those individual comparisons were run outside of the Friedman design, Bonferroni corrections for multiple tests were applied ($\alpha = 0.0025$ for IE and 0.005 for effective force).

6.4 Results

Pedal Force

Significant main effects of test condition and crank angle were observed for the effective force ($F_{1,152} = 194.2847$, $p < .001$, $\eta^2 = .56$ and $F_{4,152} = 57.2896$, $p < .001$, $\eta^2 = .60$, respectively).

Pedal forces perpendicular to the crank (effective forces, F_{eff}) were smaller for the C condition (mean of 369 ± 69 N) than the NC condition (724 ± 264 N) across all crank angles (**Figure 6-2**).

Paired post-hoc comparisons between crank angles across both testing conditions (**Table 6-1**) showed that effective force was smaller at 150° compared to all other crank angles and was greater

at 60° (762 ± 296 N) and 90° (697 ± 257 N), compared to the other three crank positions (426 ± 275 , 450 ± 251 , and 228 ± 94 N for 30°, 120°, and 150°, respectively; **Figure 6-2**).

Force Effectiveness

We found significant test condition*crank angle interaction for the index of effectiveness ($F_{4, 152} = 11.971$, $p < .001$, $\eta^2 = .24$). Paired post-hoc comparisons showed that IE was a) greatest at 60°, as well as greater at 90° than at 30, 120, and 150° for the NC condition and b) statistically the same at all crank angles in the C condition, as required by experimental design (**Figure 6-2**).

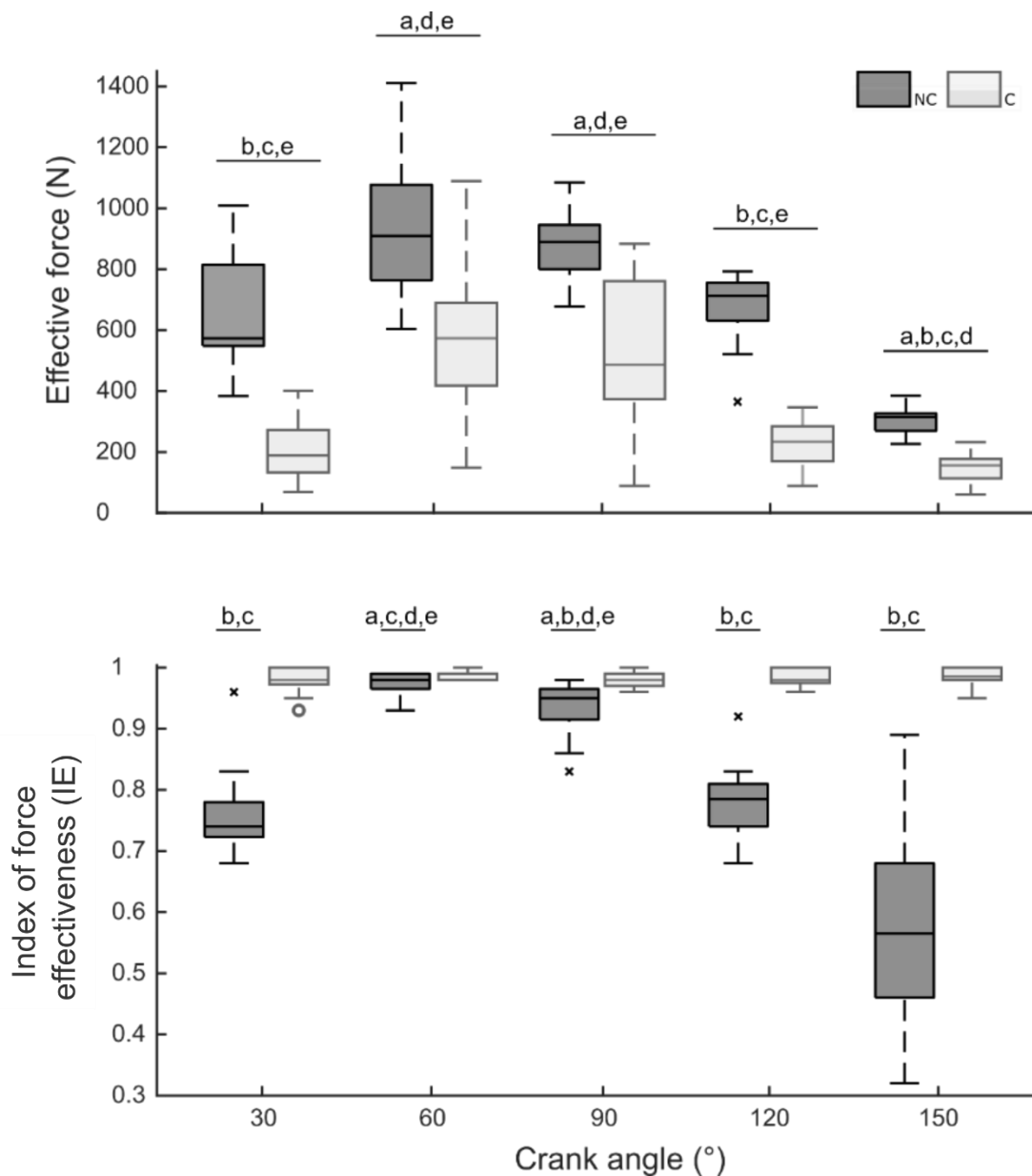


Figure 6-2: Effective force (F_{Eff} , top panel) and index of effectiveness (IE, bottom panel), separated by test condition (NC = dark grey boxes, C = light grey) and crank position. An individual box represents the distribution of a batch of data as follows: The horizontal line inside the box indicates the median, top and bottom end of the box stand for 75th and 25th percentile, respectively. The whiskers extend to the most extreme values not considered outliers. An outlier is any value more than 1.5 times the difference between 75th and 25th percentile away from the median. Paired comparisons were made across testing conditions for F_{Eff} , and separately within each testing condition for IE. Letters above the horizontal lines indicate significantly different from: a = 30°, b = 60°, c = 90°, d = 120°, e = 150°, with $p \leq .001$.

Table 6-1: Overview of the Post-hoc comparisons for effective force (F_{Eff}) and index of effectiveness (IE). This table contains the differences of the means for each group comparison ($\bar{a} - \bar{b}$), as well as the corresponding test statistics (t). The top row illustrates the different combinations of crank positions. For F_{Eff} (white background) between angle comparisons were run on data combining both testing conditions. For IE (shaded background) between angle comparisons were performed within testing condition. All the differences shown here were statistically significant with $p \leq .001$.

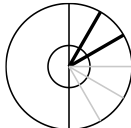
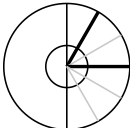
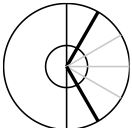
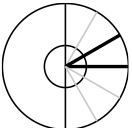
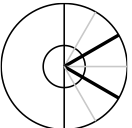
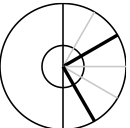
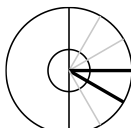
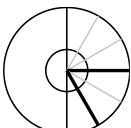
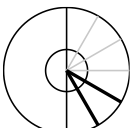
							
		30° _a :60° _b	30° _a :90° _b	30° _a :150° _b	60° _a :90° _b	60° _a :120° _b	60° _a :150° _b
F _{Eff}	Mean difference (N)	-330	-220	214		301	531
	t	-7.398	-6.620	4.218		7.549	12.846
IE NC	Mean difference	-.215	-.150		.040	.198	.402
	t	-7.192	-3.386		4.519	7.852	9.531

Table 6-1: continued.

				
	90° _a :120° _b	90° _a :150° _b	120° _a :150° _b	
F_{Eff}	Mean difference (N)	216	442	222
	t	6.679	12.008	5.313
IE NC	Mean difference	.148	.346	
	t	3.592	5.430	

Muscle Activation

Muscle activation (relative to maximum activation) was greater in the NC than in the C condition (**Figure 6-3**) for VL (0.55 ± 0.3 vs. 0.32 ± 0.29), RF (0.37 ± 0.31 vs. 0.3 ± 0.33), GMAX (0.63 ± 0.27 vs. 0.29 ± 0.26), BF (0.52 ± 0.31 vs. 0.39 ± 0.31), and MG (0.50 ± 0.30 vs. 0.28 ± 0.25).

The corresponding statistical analysis revealed significant main effects of test condition ($F_{1, 134} = 47.0232$, $p < .001$, $\eta^2 = 0.26$; $F_{1, 134} = 10.8861$, $p = .001$, $\eta^2 = 0.08$; $F_{1, 134} = 70.7009$, $p < .001$, $\eta^2 = 0.35$; $F_{1, 134} = 10.5717$, $p = .001$, $\eta^2 = 0.07$; $F_{1, 134} = 40.5357$, $p < .001$, $\eta^2 = 0.23$, for VL, RF, GMAX, BF, and MG, respectively.)

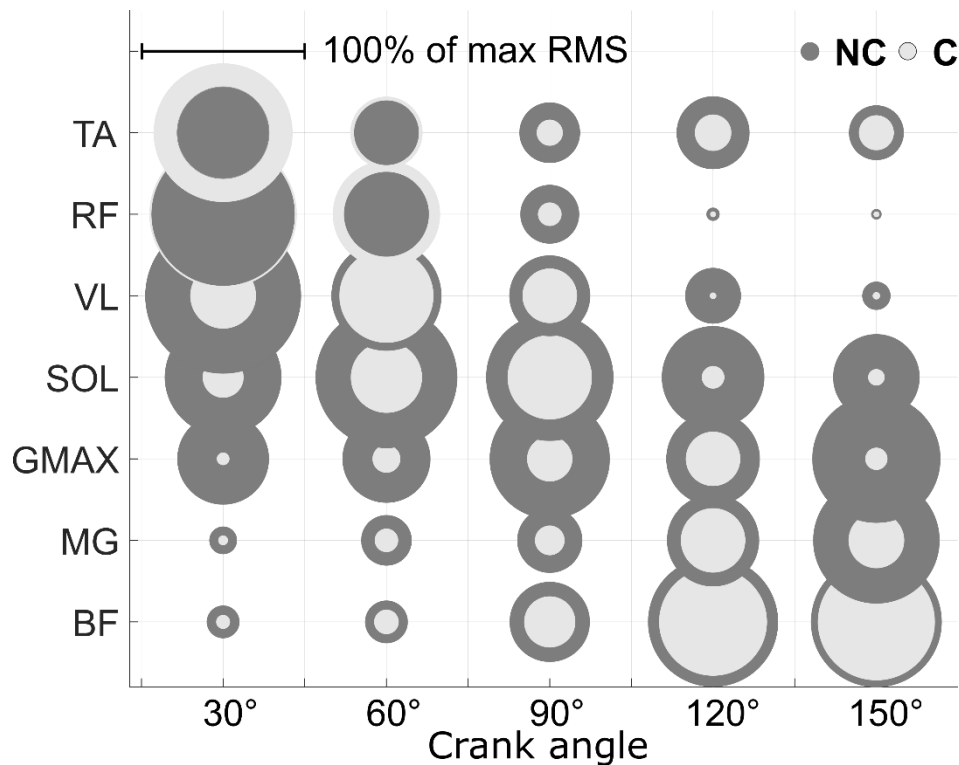


Figure 6-3: Median muscle activation (as % of maximum activation measured in this test) separated by crank angle and test condition (dark grey = NC, light grey = C). TA = tibialis anterior, RF = rectus femoris, VL = vastus lateralis, SOL = soleus, GMAX = gluteus maximus, MG = medial gastrocnemius, BF = biceps femoris.

6.5 Discussion

The purpose of this study was to determine maximal effective (i.e., perpendicular to the crank) pedal forces in the downstroke of the crank cycle in two different testing conditions, non-constrained (NC) and constrained (C). In the NC condition, participants were asked to push as hard as they could. In the C condition, they were asked to push as hard as they could while directing the pedal force perpendicular to the crank.

The findings of this study support our first hypothesis. Increased force effectiveness in the constrained condition was realized at the cost of considerable decreases in effective pedal force (69 %, 38 %, 41 %, 67 %, and 52 % at 30°, 60°, 90°, 120°, and 150°, respectively).

It appears, that the concept of perfect force effectiveness being desirable is based on the idea that we are easily able to redirect an external force in any direction while conserving its magnitude. There is, however, reason to assume that directional constraints would compromise force production of a synergistic muscle system. The magnitude of the force that a muscle can produce depends on its contraction velocity (Hill, 1938) and length (Gordon et al., 1966; Kulig et al., 1984). In addition, the direction of force from a specific muscle depends on the muscle's line of action, as well as the orientation of the bones to which the muscle is attached (Kaya et al., 2006). In other words, for a given lower limb configuration, activation of a muscle produces a force on the pedal in a specific direction. By changing the muscle's level of activation, only the magnitude of the force but not its direction is changed (Kaya et al., 2006; van Ingen Schenau et al., 1995). The direction of a resultant pedal force can only be changed by activating other muscles that naturally produce force vectors in different directions. Therefore, when prescribing a specific force direction (i.e., perpendicular to the crank in cycling), the ability of each muscle to contribute to the

corresponding pedal force will be limited by the directional constraint. The feasible muscle coordination solution space will be reduced (Kaya et al., 2006; Kuo & Zajac, 1993; McKay & Ting, 2008; Valero-Cuevas, Zajac & Burgar, 1998), thereby potentially reducing the force potential of a system of synergistic muscles (Crowninshield & Brand, 1981; Hasson et al., 2008; van Ingen Schenau et al., 1992).

Indeed, our results show significant decreases in muscle activations of VL, GMAX, BF, MG and, for the most part RF, in the C compared to the NC condition (Figure 3). This finding supports our second hypothesis and the assumption that directional constraints require altered patterns of muscle activation, i.e., different synergies. We propose that this observation explains the large reductions in effective force that were observed in this study for the C compared to the NC condition.

Aside from the fact that some muscles might be strong but not useful when it comes to creating force in a certain direction, it has been demonstrated in an animal model that force sharing among synergistic muscles as controlled by the nervous system is task-specific (Kaya et al., 2008). Trying to control individual muscle groups and to potentially override the natural solution of the system to execute a task can be challenging. While some participants did not have any problems with the requirement of applying forces perpendicular to the crank, others struggled. Even though they understood the task and what they needed to do, translating that into the appropriate muscle synergies seemed difficult and, in some cases, required extensive trial and error contractions before the constrained tasks could be successfully completed. Especially at the beginning (30°) and end of the downstroke (150°) ‘reprogramming’ muscle activity to satisfy the directional constraints often required extra time and practice, and the increased effectiveness was still accompanied by a significant reduction in effective force magnitude. Therefore, even though intermuscular control

is something that can be improved with practice, we believe that having to alter muscle synergies may limit force capacity to an extent that negates potential training effects in active muscle control.

The effective forces were greatest at the 60° and 90° crank positions, across the C and NC testing conditions. This observation might not seem particularly interesting until we consider the effect of crank angle on force effectiveness in this context. Participants displayed far from perfect effectiveness at the different crank angles in the non-constrained testing conditions, except for the 60° and 90° crank angles. The average IE values were 0.77, 0.78, and 0.58 at the 30°, 120° and 150° crank angles, respectively, while the average IE values at the 60° and 90° crank positions were 0.97 and 0.94, respectively. The general finding of less than perfect force effectiveness is in line with previous studies reporting that cyclists naturally produced pedal forces with considerable radial, i.e., parallel to the crank, components (Cavanagh & Sanderson, 1986; Hasson et al., 2008; S. A. Kautz & Hull, 1993; Mornieux et al., 2008; Rossato et al., 2008; Zameziati et al., 2006). Importantly, the index of effectiveness in the NC condition was maximized, and close to perfect effectiveness (i.e., 1.0) at the crank positions at which participants produced the largest effective pedal forces. The effective forces were drastically reduced when participants tried to increase force effectiveness, and effectiveness was naturally already close to perfect at the crank positions where participants were strongest.

At the 60 and 90° crank angle, the IE was almost the same for the non-constrained and constrained conditions, i.e., the direction of force application for the two conditions was similar. At the same time, the effective force differed substantially between testing conditions. This result may seem non-intuitive, but there are at least three possible explanations. First, small differences in force direction might make a great difference in the capacity to produce force; second, the shift in focus required to push in a constrained direction may affect muscle activation; third, independent of

focus considerations, targeting a specific force direction that deviates from an individual's preferred one might significantly interfere with their acquired neuromuscular control strategy.

The first possibility seems rather unlikely from a mechanical and a muscle mechanics perspective. The second possibility is supported by studies indicating that a dual task paradigm, or shifting focus to different aspects of a task, may be detrimental to performance of the primary task (Dai et al., 2018; Wulf et al., 2010). As for the third possibility, Gruben and colleagues discovered that pedaling in the downstroke is accomplished with a stereotypical pattern of pedal force direction, which is not perfectly perpendicular to the crank and seemed to be consistent across participants, as well as across test settings (static versus dynamic). This can be interpreted as an inherent control strategy that is present in different individuals (Gruben et al., 2003c; Gruben et al., 2003a; Gruben et al., 2003b). Deviating from such a pattern might be difficult and associated with a loss of force due to an inability to activate muscles effectively in newly acquired and unusual synergies. This evidence suggests that the reductions in maximal force production that we observed when prescribing a specific pedal force direction might not only be the result of anatomical constraints but also a control problem due to interference with preferred neuromuscular control strategies, or due to the dual nature of the task.

Cycling is a dynamic sport, and the static nature of our tests might be a limitation of this study. During actual pedaling, inertial forces will also contribute to the pedal forces (Kautz & Hull, 1993; Sanderson, 1991), and muscle forces will differ from isometric, as measured here, due to activation/deactivation dynamics, as well as force-velocity and history-dependent effects (Abbott & Aubert, 1952; Edman, Elzinga & Noble, 1982; Lakie, Walsh & Wright, 1984; Lakie & Campbell, 2019; McGowan, Neptune & Herzog, 2010; Noble, 1992). Inertial forces were neglected here, but inertial forces contribute to the total pedal forces in cycling, and they seem to

primarily contribute to the ineffective force patterns that are observed in cyclists (Kautz & Hull, 1993; Leirdal & Ettema, 2011; Lorås et al., 2009). It is reasonable to assume that inertial forces change the task requirements i.e., the extent to which muscle forces need to be adjusted to achieve better force effectiveness. However, inertial pedal forces do not affect the muscle force capacity (at a given cadence) or muscle force direction (at a given lower limb position), which were the topics of interest in this study. Moreover, in our static testing, participants could realize the different muscle synergies that were required at the different positions of the downstroke for the constrained conditions. As mentioned above, accommodating these different muscle synergies for the time constrained imposed by actual cycling is probably impossible. While movement and contraction velocity may affect muscle force capacity, the structural conditions (joint angle and attachment sites) are the same for both scenarios. In other words, a given muscle produces force in the same direction for static and dynamic conditions for corresponding limb/pedal configurations. Therefore, the reduction in effective pedal forces in the constrained task for the static conditions can be expected to translate directly to dynamic conditions. Furthermore, having performed the data collection, we are not sure how the directional target in the constrained condition could have been achieved to a satisfying degree of accuracy in a dynamic pedalling situation. As mentioned before, many participants struggled with the force control in the static situation, particularly at crank angles of 30° and 150°. Some participants were never able to learn the constrained task and their data were excluded from analysis. This variation in ease of accomplishing the task indicates that not only are the NC and the C condition two different tasks, but so are the different crank positions within the C condition. Our interpretation is that constrained cycling (when aiming for perfect force effectiveness) requires many different muscle synergies during the downstroke of pedaling. At competitive pedalling rates of around 80-90 revolutions per

minute, the downstroke lasts between 333 to 375 ms. Changing muscle synergies multiple times within such a short period of time appears impossible due to the slow activation/deactivation dynamics of human skeletal muscles. Therefore, we believe that even with extensive training, it is impossible to produce pedal forces that are purely perpendicular to the crank throughout the downstroke phase of cycling at competitive pedaling rates.

Finally, we tested maximal effort contractions while most of cycling is performed sub-maximally. It is possible that force constraints in submaximal cycling are not as important as they seem to be for maximal contractions, while energetic cost might dominate muscle coordination strategies. There is evidence that, with a pedalling technique that deviates from cyclists' preferred pedalling pattern, increased force effectiveness comes at the cost of reduced metabolic efficiency (Korff et al., 2007; Mornieux et al., 2008). Therefore, it appears that (experienced) cyclists through practice arrive at what is (for them) the most efficient way of pedaling. The notion that freely chosen movement strategies are most efficient is in agreement with other activities where, when unconstrained in their movements, individuals seem to choose techniques or gait patterns that minimize their metabolic cost, for example in running or cross-country skiing (Herzog et al., 2015; Snyder & Farley, 2011).

The findings of this study suggest that even though participants were able to redirect their pedal force for the C condition, doing so required a change in muscle activation patterns compared to those naturally used in the NC conditions and resulted in a severe loss in force capability. Aiming for perfect force effectiveness makes sense from a theoretical and mechanical point of view, assuming the available forces are constant and independent of direction. Adapting training processes and techniques accordingly, however, does not seem to be beneficial. Our participants naturally displayed close to maximum effectiveness at the crank positions at which they were also

strongest (i.e., produced the greatest effective forces). Even if they were able to improve effectiveness even further, that gain would be small compared to the associated loss in force output. Elite cyclists produce effective and radial crank forces (perpendicular and parallel to the crank, respectively), despite years of training and development of their cycling technique (Faria & Cavanagh, 1978; Jamar, Vries & Hesselink, 2015; Kautz, Feltner, Coyle & Baylor, 1991). Even if cyclists never thought of the mechanics of cycling, they presumably arrived at an optimal technique for their body type and individual muscular strengths by trial and error. As a result, we assume that the technique naturally employed by elite cyclists is near optimal, possibly utilizing a single muscle synergy for the entire downstroke phase of the pedal cycle. Cycling with an index of effectiveness of 1.0 during the entire crank cycle is probably sub-optimal, likely impossible, and should not be enforced by coaches or scientists.

6.6 Conclusion

While applying forces perpendicular to the crank in the downstroke of cycling is mechanically effective, it appears to be biomechanically ineffective because pushing perpendicular to the crank was associated with severe reductions in force. These findings suggest that, when it comes to enhancing performance, training aimed at increasing an athlete's general pedal force production capabilities would be more useful than attempts to change their cycling technique with the goal of achieving perfect force effectiveness throughout the downstroke of cycling.

6.7 Acknowledgements

We would like to thank Rafael Fortuna for help with the data collection, as well as Andrzej Stano for technical support.

Chapter 7

Discussion and Conclusions

7.1 Summary

The overarching objective of this thesis was to quantify different aspects of force application in bobsleigh and cycling, as they relate to performance in both sports. More specifically, in the context of bobsleigh, the aims were to explore the potential of functional sled push force-velocity testing to enhance team performance and to investigate individual athlete push force contributions, timing and coordination within the team during the 4-man push start. The cycling project examined the effects of constrained pedal force direction on effective pedal force magnitude throughout the downstroke phase of the cycle, as well as on the activation of the primary hip and knee extensor muscles.

An important component of the bobsleigh project was the development of an instrumentation setup for two test sleds: a prowler gym sled and a 4-man bobsled. Chapter 3 provides a description of the design process and the final setup for both sleds. While the prowler is pushed by one person at a time, in the 4-man bobsled, each of the four athletes has their own point(s) of contact with the sled on which they push during the start. Three athletes are positioned left and right of the sled and push on push bars, while the fourth pushes on handles (extensions of the body of the sled) in the back. The developed measurement systems allow for recording 3D linear sled acceleration and angular velocity, as well as individual 2D push forces (for each bar and handle) during push tests at the gym or on ice, providing data that were not previously available in the literature.

In the first study (Chapter 4) recreationally active participants performed a functional sled push force-velocity test on two different days, with sled loads ranging from 25 to 200 % body mass. Push force and peak sled speed were repeatable between test days, with $r^2 = 0.96$ and 0.91 , and mean differences of $32 (\pm 26)$ N and $0.25 (\pm 0.22) \frac{\text{m}}{\text{s}}$, respectively. Linear regressions were good representations of the resulting fFv profiles, with $r^2 > 0.85$ for all but one of the participants on one day of testing. Reducing the number of load conditions in the test did not significantly affect the fFv profiles as long as the two most extreme load conditions (lightest and heaviest) were still included. Choosing only the three lightest load conditions for a profile significantly increased the extrapolated maximum speed (v_0), while decreasing the extrapolated maximum push Force (F_0). Conversely, determining the fFv profile based only on the three heaviest load conditions significantly decreased v_0 while increasing F_0 . The observation that linear functions provide a good approximations for fFv profiles is consistent with previous literature for whole-body human movement (Bobbert, 2012; Challis et al., 2015; Jimenez-Reyes et al., 2014; Rahmani et al., 2001; Samozino et al., 2012, 2016; Vandewalle et al., 1987) and the ability to derive consistent fFv profiles using a limited number of testing conditions, provides the opportunity for expedited fFv testing to be performed. At the same time, our findings regarding the effects of the choice of load conditions on the fFv profiles suggest that consistency in the testing is essential and that an individual's results may vary depending on the exact protocol. This interpretation aligns with the observations made in a previous study, where the authors compared fFv testing results for different tasks (Lindberg et al., 2021).

The second study was one of the first to investigate the kinetics of the 4-man bobsled push start and, to the best of our knowledge, the first to provide any 4-man push force data. Chapter 5 provides a description and analysis of various events during the 4-man bobsled push start, with a

focus on the hit (i.e., the very first push on the sled) and the loading phase. Absolute peak push forces, recorded from the push bars, were recorded during the hit, with the athletes pushing on the left (**L**, behind the pilot) and right side of the sled (**R**) contributing about 1.6 times as much as the pilot (**P**) each (with median values of 740.0 N and 719.0 N vs. 445.0 N for **L** and **R**, respectively). Following the hit, propulsive push forces decreased rapidly. Average propulsive push force was calculated for 5 % intervals of total push start duration to describe the force development across a trial, and we observed reductions of 56 % to 77 % within the first 1.5 seconds of the push start. At 25 % of the total push start time, median propulsive push force was 35.0 N for the pilots (25th percentile = 20.0 N, and 75th percentile = 51.0 N), 67.0 N for the athletes on the left side (25th = 38.0 N and 75th = 86.0 N), and 75.0 N for the athletes on the right side (25th = 49.0 N and 75th = 98.0 N). By the time the athletes started loading (after roughly 45 % of the total push start time, equivalent to 10 to 12 steps), the average propulsive push forces had dropped below 50 N for **P**, **L**, and **R** (median = 25.0 N, 25th percentile = 18.0 N and 75th percentile = 33.0 N for **P**; median = 32.0 N, 25th = 4.0 N, and 75th = 46.0 N for **L**; median = 17.0 N, 25th = -21.0 N, and 75th = 24.0 N for **R**). An average push force of approximately 30 N or less prior to loading is small relative to the weight of the sled. More research is required to determine whether this strategy is suited to maximize the acceleration of the bobsled. The loading phase is another crucial part of the push start, and we proposed a method to quantify the efficiency of a team load which may be used as feedback for athletes. Our data suggest that a positive, i.e., bobsled accelerating, beginning of the load phase is particularly beneficial. Since the pilots and, in our case, the athletes pushing on the left side of the sled behind the pilot were the ones to load first and second, our findings can be interpreted such that the way these two athletes execute their load is especially important. Our data show no team that managed the load without any reduction in sled speed along the way. However,

if at least the beginning of a load could be positive (i.e., increasing sled speed) or, in other words, if the first athlete (or the first two) could accelerate the sled with their load rather than slow it down, the team could reduce their start time, even if the speed at the end was the same.

The study presented in Chapter 6 was focused on force effectiveness in cycling. Only the pedal force component that is directed perpendicular to the crank can produce torque and move the crank, and subsequently the bike, forward. Therefore, more specifically, participants in this study applied maximum pedal force at different crank positions during the downstroke of the cycle in two testing conditions. First, in an unconstrained manner, then in a constrained condition with the instructions to direct pedal force purely perpendicular to the crank (i.e., in a maximally effective manner). Pedal force effectiveness was increased in the constrained compared to the unconstrained condition. However, the increase in effectiveness came at the cost of significant reductions in effective force magnitude (ranging from -38 to -69 % across the different crank positions, relative to the unconstrained testing condition), and was further accompanied by reduced activation of the primary leg extensor muscles. The observation of reduced force output aligns with recently published results from a modeling project, where the authors estimated a ~50 % reduction in mechanical power output when no ineffective (i.e., not perpendicular to the crank) forces were accepted (Kistemaker et al., 2023). Moreover, previous work on cycling and wheelchair propulsion provides evidence that constraining external force direction is associated with increased energetic cost (Bregman et al., 2009; Korff et al., 2007; Mornieux et al., 2008). The results of our study suggest that, to enhance performance, training aimed at increasing an athlete's general pedal force production capabilities would be more beneficial than focusing on increasing force effectiveness.

With the projects presented in this thesis, we provide novel data on the 4-man bobsled push start, propose a new approach to training and recruitment in the sport of bobsleigh, and contribute

empirical evidence to the discourse about the utility of aiming for increased force effectiveness in cycling or other sports (e.g., bobsleigh).

7.2 The Utility of force measurements in a sports context

The research projects discussed in this thesis highlight the importance of force measurements in a sports context. Even with the two very different applications that were studied for this thesis, bobsleigh and cycling, the common denominator is that greater force production will enhance performance. Cyclists need to exert force on the pedal to create torque about the centre of the crank to move the bike forward, but probably the most important performance metric in the sport is mechanical power output (Coyle et al., 1991; Ettema et al., 2009; Martin & Spirduso, 2001; Vandewalle et al., 1987). To produce greater power, greater force needs to be produced at a certain speed, or within a given time. Therefore, to measure mechanical power one must also measure the force applied by an athlete. One aspect that is discussed in the context of improving cycling performance is pedal force effectiveness or, how much of the force applied to the pedal produces the desired torque to move the crank (Bini et al., 2013; Coyle et al., 1991; Dorel et al., 2010; Ericson & Nisell, 1988; Lafortune & Cavanagh, 1983). To evaluate this parameter, at least 2D pedal force measurement is a necessity (Bini et al., 2014; Coyle et al., 1991; Dorel et al., 2010).

And what about bobsleigh? A team's goal during the start phase is to achieve maximal sled velocity in the shortest possible time (Brüggemann et al., 1997; Morlock & Zatsiorsky, 1989). This means that the athletes need to perform work on the bobsled to change the velocity and thereby the momentum of the sled. Moreover, they need to do it quickly which, again, means maximizing power production. The more force a team can apply to the bobsled in a short period of time, the faster the sled will move in the end. Analyzing the velocity of the sled may reveal where speed

was lost or gained but, without directly measuring push forces, individual contributions cannot be determined. This problem extends further into the preparation and recruitment stage. Without quantifying the athletes' impact on the bobsled, any predictions that are made based on individual performance assessments cannot be tested, which means that there are parts of the task that can only be improved by chance. A potential problem with novel measurement systems like ours is that the implementation process can be slow. It may take time until the data are understood, important parameters identified, and the testing and its results can be confidently implemented in the training or recruitment process. These obstacles may make it seem like suboptimal return on investment when there is a very simple metric for performance that decides the outcome of a competition – run time. On the other hand, and especially in a more complex task or a team performance situation, information about the individuals seems crucial for improvement (Dabnichki, 2016; Lee et al., 2015; Leonardi et al., 1985). Considering that in the 4-man bobsled push start very small improvements can make a meaningful difference, any additional information and objective measurements can enhance our understanding of the task. This, in turn, can provide coaches and athletes with valuable insights into how to modify their training and perform better.

7.3 Functional Force velocity profiling – a useful tool in bobsleigh?

As alluded to earlier, performance in many sports is determined by an athlete's or a team's ability to produce power (Adams et al., 1992; Baker, 2001; Coyle et al., 1991; Cronin & Hansen, 2005; Hawley et al., 1992). Mathematically, power is defined as the dot product of force and velocity, which in practice means that an individual's ability to generate power can be described as the force they can exert in a task as a function of velocity, or the velocities they can realize when producing varying amounts of force. The relationship between force and velocity, and thereby an individual's

power capacity, is not obvious by mere observation. However, functional force-velocity testing has proven to be effective in assessing these characteristics and predicting performance in various sports; for example, in sprinting (Cross et al., 2017) cycling (Dunst et al., 2022; Vandewalle et al., 1987), marathon running (Nikolaidis & Knechtle, 2020), ice hockey (Stenroth et al., 2020), and single push bobsled testing (Challis et al., 2015). Functional force-velocity relationships may also be referred to as just force-velocity or load-velocity relationships. However, throughout this thesis, the term functional force-velocity (fFv) was used for all such relationships that describe velocity as a function of load or force measured as a function of velocity for muscle groups, multi-joint or full-body movement tasks. The term force-velocity was reserved for the property of single muscle or muscle fibres. We proposed that functional sled push force-velocity profiling could serve as a valuable off-ice testing tool for bobsled athletes. The observation of decreasing propulsive push forces with increasing sled velocity over the course of the push start is reminiscent of a typical functional force-velocity relationship, where increasing speed is associated with decreasing force and, vice versa, decreasing speed with increasing force production (Bobbert, 2012; Bobbert et al., 2016; Jaric, 2016; Jimenez-Reyes et al., 2014; Samozino et al., 2012, 2016; Vandewalle et al., 1987). Consequently, fFv profiles may help predict an individual athlete's push force capacity during the push start and could potentially facilitate force-matching between athletes on opposite sides of a bobsled. Moreover, the sled test setup could also be used as a training tool, focusing athletes' attention on enhancing their force at specific points along the velocity curve to increase power output.

How well on-ice performance can be predicted by fFv metrics requires further testing. It may not be feasible to recreate the same conditions that the athletes would find on ice, such as low friction and an inclined track, in an off-ice setting. The peak sled speeds achieved in our study with the

prowler sled were approximately $3\text{--}5 \frac{\text{m}}{\text{s}}$ slower than the speeds at which the athletes loaded the bobsled in their on-ice pushes. Nevertheless, fFv testing might still be predictive of performance, particularly for the first part of the push start where sled speed is slower and the most force is applied to the bobsled. It is also plausible that elite athletes would reach significantly higher sled speeds in the off-ice testing than our active but non-elite participants did. Considering previous work describing the importance of specificity in training (and therefore, presumably, in testing as well) (Hicks et al., 2020; Kristensen et al., 2006; Stone et al., 2022), we speculate that greater similarity in speed demands between the two tasks (on and off ice) may improve the fFv push test's transferability to the on-ice task performance.

7.4 Should maximal force effectiveness in sports tasks be enforced?

The results from our bike setup (Chapter 6) clearly show that constraining oneself to generating maximal force effectiveness is highly suboptimal for producing maximal pedal force magnitudes. It seems unlikely that experienced athletes, after hours and years of practice and exploration, gravitate towards a technique that would be suboptimal, especially since the discussion of force effectiveness has been going on for decades (Cavanagh & Sanderson, 1986; Ericson & Nisell, 1988). This hunch is supported by the fact that we see similar patterns of imperfect force effectiveness in two very different sports; in our own data from the bobsled push starts (Chapter 5) and in previous publications for cycling (e.g., Cavanagh & Sanderson, 1986; Hasson et al., 2008; Kautz et al., 1991). The findings from our bike experiment suggest that trying to apply a force direction perpendicular to the crank drastically reduces maximum pedal force magnitude. This negative relationship between task constraint and force production capacity is supported by the outcomes of a recent study by Kistemaker and colleagues (2023). The authors used a

musculoskeletal model to show that reducing the radial (i.e., ineffective) pedal force component would result in a considerable reduction (about 50 %) in power output (Kistemaker et al., 2023). As discussed earlier in this thesis in the context of the bobsled data, I believe that some ineffective force application may be necessary as part of the movement, particularly in situations of maximum effort and maximum force production. Kistemaker et al. (2023) made the same argument in the discussion of their modeling results, describing pedal forces radial to the crank as a by-product of maximum effective pedal force production. In sprinting, ground reaction force measurements have revealed both negative and positive horizontal components, as well as a substantial positive vertical component (Morin et al., 2011; Samozino et al., 2016). This makes sense as, based on physics, we know that the horizontal component of a ground reaction force is the one that moves a person forward. However, applying exclusively (or predominantly) horizontal force to the ground will result in a zero- (or near zero) movement velocity. Force application in both the vertical and horizontal directions are required to lift the centre of mass (COM) and achieve a flight phase, and to travel forward. The same is true when pushing a bobsled and, therefore, we would also expect to see the athletes producing force in both the vertical and horizontal directions. Since the athletes hold on to the push bars while running, it seems conceivable that not only the horizontal acceleration of the COM but also some of the vertical oscillations would be transferred to the bobsled and therefore manifest in the push force records. Previous work on force effectiveness in cycling indicates that reducing movement velocity can help to achieve greater force effectiveness (Dorel et al., 2010; Ettema et al., 2009; Kautz & Hull, 1993; Leirdal & Ettema, 2011). This finding may apply to bobsleigh as well i.e., slower running velocities would likely enable the athletes to better control the direction of their push forces. That said, moving at a slower speed would, of course, be counterproductive to the goal of maximizing sled velocity by the end of the start phase.

Finally, increased force effectiveness has been associated with increased metabolic cost in both wheelchair propulsion (Bregman et al., 2009) and cycling (Korff et al., 2007; Mornieux et al., 2008). Whether this pattern would hold in bobsleigh is not known. However, given that the push start is a comparatively short maximum effort exercise, a potential reduction in force magnitude and/or sled speed due to modified technique is likely the dominating concern. All evidence considered, prioritizing force effectiveness cannot be recommended for cycling or bobsleigh.

7.5 Limitations and Future Directions

A few limitations to this work as well as ideas for potential next steps and experiments, which could be performed to explore new questions and ideas that emerged from completing the projects discussed in this thesis, are discussed below.

I) Sled velocity was determined by integrating linear acceleration (recorded with an IMU) to linear velocity, which comes with the problem of measurement error accumulation (Rebula et al., 2013; Smyth & Wu, 2007). To improve the accuracy of the velocity estimates in the future, we are working on combining IMU data with data from timing lights that are installed along the track in the Ice House, aiming to use the additional timing and position information to correct any errors in the velocity estimates.

II) Functional force-velocity profiling has been proven to be valid in assessing individuals' capacity to produce power and even to predict performance (Challis et al., 2015; Samozino et al., 2011, 2012; Vandewalle et al., 1987). At the same time, previous research, as well as the findings presented in this thesis (Chapter 4) suggest that variations in the testing protocol can significantly affect the outcomes of the test (Janicijevic et al., 2020; Jimenez-Reyes et al., 2014). This finding

indicates that the interpretation of the results of such a functional force-velocity test is not straightforward and the relationship between the test results and the task to be predicted needs to be tested carefully. Therefore, logical next steps would be to repeat the off-ice sled push test with elite bobsled athletes and to combine the results from on- and off-ice testing to establish the relationship between metrics derived from each task.

III) To fully understand the significance of the data collected from the instrumented bobsled and the specific parameters that were discussed, more data are required, both (1) from team pushes with the bobsled, in a systematic manner, where specific instructions can be given to the athletes, and (2) from off-ice recruitment and assessment tests. The latter can then be correlated with the measurements obtained from the instrumented bobsled to illuminate the relationship between individual off-ice test metrics and on-ice in-team performance, the former explore the relationship between on-ice metrics and on-ice performance as measured in start time and exit velocity.

7.6 Conclusions

Performance in many sports is governed by an athlete's or a team's ability to produce power. Greater power generation requires greater force production over a given distance and within a given time frame. The overarching theme of the work for this thesis was force application in two different sports. More specifically, we developed the instrumentation for a 4-man bobsled and a prowler/gym sled to describe and analyze individual athletes' push force contributions during the push start. Furthermore, we investigated the impact of constraining pedal force on force output during the downstroke in cycling. The data and results presented in this thesis highlight the complexity of the 4-man bobsled push start, even without considering potential environmental influences. We gained a better understanding of the important steps involved in the push start and

were able to describe individual athletes' actions and contributions to sled acceleration. With the off-ice prowler sled push force-velocity profiling, we proposed a promising new test set-up that could be used as an assessment tool in bobsleigh. Bobsleigh is a sport with a long tradition and coaches and athletes with a lot of experience and intuition about many of its aspects but, on the other hand, there is a scarcity of objective measurements beyond split and run times. We believe that the findings of this thesis have practical implications for coaches and athletes in that they can provide new ways to evaluate and, subsequently improve, performance. Finally, we add empirical evidence to the discussion about the importance of force effectiveness, providing support for the notion that maximal pedal force effectiveness should not be prioritized, as constraining force direction would be detrimental to an athletes' capacity to produce power.

Bibliography

Abbott, B. C., & Aubert, X. M. (1952). The force exerted by active striated muscle during and after change of length. *The Journal of Physiology*, 117(1), 77–86.

<https://doi.org/10.1113/jphysiol.1952.sp004733>

Adams, K., O'Shea, J. P., O'Shea, K. L., & Climstein, M. (1992). The Effect of Six Weeks of Squat, Plyometric and Squat-Plyometric Training on Power Production. *The Journal of Strength & Conditioning Research*, 6(1), 36.

Altman, D. G., & Bland, J. M. (1983). Measurement in Medicine: The Analysis of Method Comparison Studies. *Journal of the Royal Statistical Society: Series D (The Statistician)*, 32(3), 307–317. <https://doi.org/10.2307/2987937>

Andersen, L. L., Andersen, J. L., Magnusson, S. P., Suetta, C., Madsen, J. L., Christensen, L. R., & Aagaard, P. (2005). Changes in the human muscle force-velocity relationship in response to resistance training and subsequent detraining. *Journal of Applied Physiology*, 99(1), 87–94.

<https://doi.org/10.1152/japplphysiol.00091.2005>

Baker, D. (2001). A Series of Studies on the Training of High-Intensity Muscle Power in Rugby League Football Players. *The Journal of Strength & Conditioning Research*, 15(2), 198.

Bini, R., Hume, P., Croft, J., & Kilding, A. (2013). Pedal force effectiveness in cycling: A review of constraints and training effects. *Research Outputs 2013*.

<https://ro.ecu.edu.au/ecuworks2013/891>

Bini, R. R., Hume, P. A., & Croft, J. L. (2014). Pedaling Technique Changes with Force Feedback Training in Competitive Cyclists: Preliminary Study. In R. R. Bini & F. P. Carpes (Eds.), *Biomechanics of Cycling* (pp. 85–95). Springer International Publishing.

https://doi.org/10.1007/978-3-319-05539-8_9

Bini, R. R., Hume, P. A., & Croft, J. L. (2011). Effects of saddle height on pedal force effectiveness. *Procedia Engineering*, 13, 51–55. <https://doi.org/10.1016/j.proeng.2011.05.050>

Bobbert, M. F. (2012). Why is the force-velocity relationship in leg press tasks quasi-linear rather than hyperbolic? *Journal of Applied Physiology (Bethesda, Md.: 1985)*, 112(12), 1975–1983. <https://doi.org/10.1152/japplphysiol.00787.2011>

Bobbert, M. F., Casius, L. J. R., & Van Soest, A. J. (2016). The Relationship between Pedal Force and Crank Angular Velocity in Sprint Cycling. *Medicine & Science in Sports & Exercise*, 48(5), 869. <https://doi.org/10.1249/MSS.0000000000000845>

Bobsleigh Canada Skeleton. (2022). *Bobsleigh Canada Skeleton*.

<https://www.bobsleighcanadaskeleton.ca/en/team/recruitment/>

- Braghin, F., Cheli, F., Donzelli, M., Melzi, S., & Sabbioni, E. (2011). Multi-body model of a bobsleigh: Comparison with experimental data. *Multibody System Dynamics*, 25(2), 185–201. <https://doi.org/10.1007/s11044-010-9218-7>
- Bregman, D. J. J., Drongelen, S. van, & Veeger, H. E. J. (2009). Is effective force application in handrim wheelchair propulsion also efficient? *Clinical Biomechanics*, 24(1), 13–19. <https://doi.org/10.1016/j.clinbiomech.2008.09.003>
- Brüggemann, G.-P., Morlock, M., & Zatsiorsky, V. (1997). Analysis of the Bobsled and Men's Luge Events at the XVII Olympic Winter Games in Lillehammer. *Journal of Applied Biomechanics*, 13, 98–108. <https://doi.org/10.1123/jab.13.1.98>
- Cahill, M. J., Cronin, J. B., Oliver, J. L., P. Clark, K., Lloyd, R. S., & Cross, M. R. (2019). Sled Pushing and Pulling to Enhance Speed Capability. *Strength & Conditioning Journal*, 41(4), 94. <https://doi.org/10.1519/SSC.0000000000000460>
- Cavanagh, P. R., & Kram, R. (1985). Mechanical and muscular factors affecting the efficiency of human movement. *Medicine and Science in Sports and Exercise*, 17(3), 326–331.
- Cavanagh, P. R., & Sanderson, D. J. (1986). The biomechanics of cycling: Studies of the pedaling mechanics of elite pursuit riders. Science of Cycling. Edited by Burke ER. Champaign, IL: Human Kinetics, 104–106.
- Challis, G. G., Sekulich, Q., Groves, E. M., & Jordan, M. J. (2015). *Profiling Take-off-Velocity in Loaded Squat Jumps Discriminates On-Ice Push Performance in Elite Male Bobsledders*. SPIN, Toronto, ON.
- Coyle, E. F., Feltner, M. E., Kautz, S. A., Hamilton, M. T., Montain, S. J., Baylor, A. M., Abraham, L. D., & Petrek, G. W. (1991). Physiological and biomechanical factors associated with elite endurance cycling performance. *Medicine & Science in Sports & Exercise*, 23(1), 93.
- Cronin, J. B., & Hansen, K. T. (2005). STRENGTH AND POWER PREDICTORS OF SPORTS SPEED. *The Journal of Strength & Conditioning Research*, 19(2), 349.
- Cross, M. R., Brughelli, M., Samozino, P., & Morin, J.-B. (2017). Methods of Power-Force-Velocity Profiling During Sprint Running: A Narrative Review. *Sports Medicine*, 47(7), 1255–1269. <https://doi.org/10.1007/s40279-016-0653-3>
- Crowninshield, R. D., & Brand, R. A. (1981). THE PREDICTION OF FORCES IN JOINT STRUCTURES: DISTRIBUTION OF INTERSEGMENTAL RESULTANTS. *Exercise and Sport Sciences Reviews*, 9(1), 159–182.
- Dabnichki, P. (2016). Computer analysis of bobsleigh team push. In P. Chung, A. Soltoggio, C. W. Dawson, Q. Meng, & M. Pain (Eds.), *Proceedings of the 10th International Symposium on Computer Science in Sports (ISCSS)* (pp. 193–200). Springer International Publishing. https://doi.org/10.1007/978-3-319-24560-7_25

- Dabnichki, P., & Avital, E. (2006). Influence of the position of crew members on aerodynamics performance of two-man bobsleigh. *Journal of Biomechanics*, 39(15), 2733–2742. <https://doi.org/10.1016/j.jbiomech.2005.10.011>
- Dai, B., Cook, R. F., Meyer, E. A., Sciascia, Y., Hinshaw, T. J., Wang, C., & Zhu, Q. (2018). The effect of a secondary cognitive task on landing mechanics and jump performance. *Sports Biomechanics*, 17(2), 192–205. <https://doi.org/10.1080/14763141.2016.1265579>
- De Groot, S., Veeger, D. (H. E. J.), Hollander, A. P., & V. Van Der Woude, L. H. (2002). Wheelchair propulsion technique and mechanical efficiency after 3 wk of practice. *Medicine & Science in Sports & Exercise*, 34(5), 756.
- DeWeese, B. (2012, December 1). *UNDERSTANDING THE PHYSICAL CHARACTERISTICS OF BOBSLEIGH ATHLETES IN THE UNITED STATES: AN ATTEMPT TO BEGIN A MEANINGFUL TALENT IDENTIFICATION PROGRAM*.
- Dorel, S., Couturier, A., Lacour, J.-R., Vandewalle, H., Hautier, C., & Hug, F. (2010). Force-Velocity Relationship in Cycling Revisited: Benefit of Two-Dimensional Pedal Forces Analysis. *Medicine & Science in Sports & Exercise*, 42(6), 1174–1183. <https://doi.org/10.1249/MSS.0b013e3181c91f35>
- Dunst, A. K., Hesse, C., Ueberschär, O., & Holmberg, H.-C. (2022). Fatigue-Free Force-Velocity and Power-Velocity Profiles for Elite Track Sprint Cyclists: The Influence of Duration, Gear Ratio and Pedalling Rates. *Sports*, 10(9), Article 9. <https://doi.org/10.3390/sports10090130>
- Dwyer, D. B., Molaro, C., & Rouffet, D. M. (2022). Force–velocity profiles of track cyclists differ between seated and non-seated positions. *Sports Biomechanics*, 1–12. <https://doi.org/10.1080/14763141.2022.2092029>
- Edman, K. A. (1988). Double-hyperbolic force-velocity relation in frog muscle fibres. *The Journal of Physiology*, 404(1), 301–321. <https://doi.org/10.1113/jphysiol.1988.sp017291>
- Edman, K. A., Elzinga, G., & Noble, M. I. (1982). Residual force enhancement after stretch of contracting frog single muscle fibers. *Journal of General Physiology*, 80(5), 769–784. <https://doi.org/10.1085/jgp.80.5.769>
- Edman, K. A. P., Mulieri, L. A., & Scubon-Mulieri, B. (1976). Non-Hyperbolic Force-Velocity Relationship in Single Muscle Fibres1. *Acta Physiologica Scandinavica*, 98(2), 143–156. <https://doi.org/10.1111/j.1748-1716.1976.tb00234.x>
- Ericson, M. O., & Nisell, R. (1988). Efficiency of Pedal Forces During Ergometer Cycling. *International Journal of Sports Medicine*, 09(2), 118–122. <https://doi.org/10.1055/s-2007-1024991>
- Ettema, G., Lorås, H., & Leirdal, S. (2009). The effects of cycling cadence on the phases of joint power, crank power, force and force effectiveness. *Journal of Electromyography and Kinesiology*, 19(2), e94–e101. <https://doi.org/10.1016/j.jelekin.2007.11.009>

- Faria, I., & Cavanagh, P. R. (1978). *The physiology and biomechanics of cycling*. John Wiley & Sons.
- Fenn, W. O. (1938). The Mechanics of Muscular Contraction in Man. *Journal of Applied Physics*, 9(3), 165–177. <https://doi.org/10.1063/1.1710406>
- Fenn, W. O., & Marsh, B. S. (1935). Muscular force at different speeds of shortening. *The Journal of Physiology*, 85(3), 277–297. <https://doi.org/10.1113/jphysiol.1935.sp003318>
- Friedman, M. (1937). The Use of Ranks to Avoid the Assumption of Normality Implicit in the Analysis of Variance. *Journal of the American Statistical Association*, 32(200), 675–701. <https://doi.org/10.1080/01621459.1937.10503522>
- Gordon, A. M., Huxley, A. F., & Julian, F. J. (1966). The variation in isometric tension with sarcomere length in vertebrate muscle fibres. *The Journal of Physiology*, 184(1), 170–192. <https://doi.org/10.1113/jphysiol.1966.sp007909>
- Gregor, R. J., Broker, J. P., & Ryan, M. M. (1991). 4 The Biomechanics of Cycling. *Exercise and Sport Sciences Reviews*, 19(1), 127–170.
- Gruben, K. G., Rogers, L. M., & Schmidt, M. W. (2003a). Direction of Foot Force for Pushes Against a Fixed Pedal: Role of Effort Level. *Motor Control*, 7(3), 229.
- Gruben, K. G., Rogers, L. M., Schmidt, M. W., & Tan, L. (2003b). Direction of Foot Force for Pushes Against a Fixed Pedal: Variation With Pedal Position. *Motor Control*, 7(4), 362.
- Gruben, K., López-Ortiz, C., & Schmidt, M. (2003c). The control of foot force during pushing efforts against a moving pedal. *Experimental Brain Research*, 148(1), 50–61. <https://doi.org/10.1007/s00221-002-1276-5>
- Harrison, A. (2017). The Bobsled Push Start: Influence on Race Outcome and Push Athlete Talent Identification and Monitoring. *Electronic Theses and Dissertations*. <https://dc.etsu.edu/etd/3313>
- Hasson, C. J., Caldwell, G. E., & van Emmerik, R. E. A. (2008). Changes in muscle and joint coordination in learning to direct forces. *Human Movement Science*, 27(4), 590–609. <https://doi.org/10.1016/j.humov.2008.02.015>
- Hawley, J. A., Williams, M. M., Vickovic, M. M., & Handcock, P. J. (1992). Muscle power predicts freestyle swimming performance. *British Journal of Sports Medicine*, 26(3), 151–155. <https://doi.org/10.1136/bjism.26.3.151>
- Henke, T. (1998). REAL-TIME FEEDBACK OF PEDAL FORCES FOR THE OPTIMIZATION OF PEDALING TECHNIQUE IN COMPETITIVE CYCLING. *ISBS - Conference Proceedings Archive*. <https://ojs.ub.uni-konstanz.de/cpa/article/view/966>
- Herzog, W. (1994). Biomaterials—Muscle. In B. M. Nigg & W. Herzog (Eds.), *Biomechanics of the musculo-skeletal system* (pp. 154–190). Wiley.

- Herzog, W., Killick, A., & Boldt, K. R. (2015). Energetic Considerations in Cross-Country Skiing. In K. Kanosue, T. Nagami, & J. Tsuchiya (Eds.), *Sports Performance* (pp. 247–260). Springer Japan. https://doi.org/10.1007/978-4-431-55315-1_20
- Herzog, W., & Loitz, B. (1994). Biomaterials—Tendon. In B. M. Nigg & W. Herzog (Eds.), *Biomechanics of the musculo-skeletal system* (pp. 133–153). Wiley.
- Hettinga, F., Valent, L., Groen, W., Drongelen, S., Groot, S., & Woude, L. (2010). Hand-Cycling: An Active Form of Wheeled Mobility, Recreation, and Sports. *Physical Medicine and Rehabilitation Clinics of North America*, 21, 127–140. <https://doi.org/10.1016/j.pmr.2009.07.010>
- Hicks, D. S., Schuster, J. G., Samozino, P., & Morin, J.-B. (2020). Improving Mechanical Effectiveness During Sprint Acceleration: Practical Recommendations and Guidelines. *Strength & Conditioning Journal*, 42(2), 45. <https://doi.org/10.1519/SSC.0000000000000519>
- Hill, A. V. (1922). The maximum work and mechanical efficiency of human muscles, and their most economical speed. *The Journal of Physiology*, 56(1–2), 19–41. <https://doi.org/10.1113/jphysiol.1922.sp001989>
- Hill, A. V. (1938). The heat of shortening and the dynamic constants of muscle. *Proceedings of the Royal Society of London. Series B - Biological Sciences*, 126(843), 136–195. <https://doi.org/10.1098/rspb.1938.0050>
- Hill, A. V., Long, C. N. H., & Lupton, H. (1924). The effect of fatigue on the relation between work and speed, in contraction of human arm muscles. *The Journal of Physiology*, 58(4–5), 334–337. <https://doi.org/10.1113/jphysiol.1924.sp002136>
- Huxley, A. F. (1957). Muscle structure and theories of contraction. *Progress in Biophysics and Biophysical Chemistry*, 7, 256–319.
- IBSF. (2019). *Track Rules*. https://www.ibsf.org/images/documents/downloads/Rules/2019_2020/IBSF_Track_Rules_am2019.pdf
- IBSF. (2023c). *IBSF | Athletes*. https://www.ibsf.org/en/athletes?sport_bob=1&nationality=ZIM
- IBSF. (2022a). *IBSF | Bobsleigh History*. <https://www.ibsf.org/en/our-sports/bobsleigh-history>
- IBSF. (2023a). *IBSF | Races & Results*. https://www.ibsf.org/en/races-results?sport_bob=1&session=WC&page_number=1
- IBSF. (2023b). *IBSF | Tracks*. <https://www.ibsf.org/en/tracks>
- IBSF. (2022b). *IBSF International Rules Bobsleigh*. https://www.ibsf.org/images/federation/Rules_and_Regulations/2022_International_Rules_BOB_SLEIGH_Web.pdf
- IOC. (2018). *PyeongChang 2018 Two-man Results—Olympic bobsleigh*. Olympics.Com. <https://olympics.com/en/olympic-games/pyeongchang-2018/results/bobsleigh/mens-two-man>

- IOC. (2022b). *Beijing 2022 4-man Results—Olympic bobsleigh*. Olympics.Com. <https://olympics.com/en/olympic-games/beijing-2022/results/bobsleigh/4-man>
- IOC. (2022a). *What is the Olympic motto*. International Olympic Committee. <https://olympics.com/ioc/faq/olympic-symbol-and-identity/what-is-the-olympic-motto>
- Jamar, A., Vries, S. D., & Hesselink, M. (2015). Pedaling Patterns of Professional Cyclists during a Grand Tour. *Journal of Science and Cycling*, 4(2), Article 2. <https://jsc-journal.com/index.php/JSC/article/view/217>
- Janicijevic, D., Knezevic, O. M., Mirkov, D. M., Pérez-Castilla, A., Petrovic, M., Samozino, P., & Garcia-Ramos, A. (2020). Assessment of the force-velocity relationship during vertical jumps: Influence of the starting position, analysis procedures and number of loads. *European Journal of Sport Science*, 20(5), 614–623. <https://doi.org/10.1080/17461391.2019.1645886>
- Jaric, S. (2016). Two-Load Method for Distinguishing Between Muscle Force, Velocity, and Power-Producing Capacities. *Sports Medicine*, 46(11), 1585–1589. <https://doi.org/10.1007/s40279-016-0531-z>
- Jimenez-Reyes, P., Samozino, P., Cuadrado, V., Conceicao, F., González-Badillo, J., & Morin, J.-B. (2014). Effect of countermovement on power-force-velocity profile. *Arbeitsphysiologie*, 114. <https://doi.org/10.1007/s00421-014-2947-1>
- Jiménez-Reyes, P., Samozino, P., Cuadrado-Peñafiel, V., Conceição, F., González-Badillo, J. J., & Morin, J.-B. (2014). Effect of countermovement on power–force–velocity profile. *European Journal of Applied Physiology*, 114(11), 2281–2288. <https://doi.org/10.1007/s00421-014-2947-1>
- Jones, E. J., Bishop, P. A., Woods, A. K., & Green, J. M. (2008). Cross-Sectional Area and Muscular Strength. *Sports Medicine*, 38(12), 987–994. <https://doi.org/10.2165/00007256-200838120-00003>
- Kamba, M., Naito, H., Ozaki, H., Machida, S., & Katamoto, S. (2023). Effect of Gear Ratio and Cadence on Gross Efficiency and Pedal Force Effectiveness during Multistage Graded Cycling Test Using a Road Racing Bicycle. *Sports*, 11(1), Article 1. <https://doi.org/10.3390/sports11010005>
- Katz, B. (1939). The relation between force and speed in muscular contraction. *The Journal of Physiology*, 96(1), 45–64. <https://doi.org/10.1113/jphysiol.1939.sp003756>
- Kautz, S. A., & Hull, M. L. (1993). A theoretical basis for interpreting the force applied to the pedal in cycling. *Journal of Biomechanics*, 26(2), 155–165. [https://doi.org/10.1016/0021-9290\(93\)90046-H](https://doi.org/10.1016/0021-9290(93)90046-H)
- Kautz, S., Feltner, M., Coyle, E., & Baylor, A. (1991). The Pedaling Technique of Elite Endurance Cyclists: Changes with Increasing Workload at Constant Cadence. *International Journal of Sport Biomechanics*, 7, 29–53. <https://doi.org/10.1123/ijsb.7.1.29>

- Kawamori, N., Newton, R., & Nosaka, K. (2014). Effects of weighted sled towing on ground reaction force during the acceleration phase of sprint running. *Journal of Sports Sciences*, 32(12), 1139–1145. <https://doi.org/10.1080/02640414.2014.886129>
- Kaya, M., Leonard, T. R., & Herzog, W. (2006). Control of ground reaction forces by hindlimb muscles during cat locomotion. *Journal of Biomechanics*, 39(15), 2752–2766. <https://doi.org/10.1016/j.jbiomech.2005.10.012>
- Kaya, M., Leonard, T. R., & Herzog, W. (2008). Premature deactivation of soleus during the propulsive phase of cat jumping. *Journal of the Royal Society, Interface*, 5(21), 415–426. <https://doi.org/10.1098/rsif.2007.1158>
- Kistemaker, D. A., Terwiel, T. M., Reuvers, E. D. H. M., & Bobbert, M. F. (2023). Limiting radial pedal forces greatly reduces maximal power output and efficiency in sprint cycling; an optimal control study. *Journal of Applied Physiology*, 134(4), 980–991. <https://doi.org/10.1152/japplphysiol.00733.2021>
- Korff, T., Romer, L. M., Mayhew, I., & Martin, J. C. (2007). Effect of Pedaling Technique on Mechanical Effectiveness and Efficiency in Cyclists. *Medicine & Science in Sports & Exercise*, 39(6), 991–995. <https://doi.org/10.1249/mss.0b013e318043a235>
- Kristensen, G. O., Van Den Tillaar, R., & Ettema, G. J. C. (2006). VELOCITY SPECIFICITY IN EARLY-PHASE SPRINT TRAINING. *The Journal of Strength & Conditioning Research*, 20(4), 833.
- Kulig, K., Andrews, J. G., & Hay, J. G. (1984). Human Strength Curves. *Exercise and Sport Sciences Reviews*, 12(1), 417–466.
- Kuo, A. D., & Zajac, F. E. (1993). A biomechanical analysis of muscle strength as a limiting factor in standing posture. *Journal of Biomechanics*, 26, 137–150. [https://doi.org/10.1016/0021-9290\(93\)90085-S](https://doi.org/10.1016/0021-9290(93)90085-S)
- Lafortune, M. A., & Cavanagh, P. R. (1983). Effectiveness and efficiency during bicycle riding. *Biomechanics VIII-B*, 928–936.
- Lakie, M., & Campbell, K. S. (2019). Muscle thixotropy—Where are we now? *Journal of Applied Physiology*, 126(6), 1790–1799. <https://doi.org/10.1152/japplphysiol.00788.2018>
- Lakie, M., Walsh, E. G., & Wright, G. W. (1984). Resonance at the wrist demonstrated by the use of a torque motor: An instrumental analysis of muscle tone in man. *The Journal of Physiology*, 353(1), 265–285. <https://doi.org/10.1113/jphysiol.1984.sp015335>
- Lee, S., Kim, T., Lee, S., Kil, S., & Hong, S. (2015). Development of force measurement system of bobsled for practice of push-off phase. *Proceedings of the Institution of Mechanical Engineers, Part P: Journal of Sports Engineering and Technology*, 229(3), 192–198. <https://doi.org/10.1177/1754337114565383>
- Legwold, G. (1984). Can Biomechanics Produce Olympic Medals? *The Physician and Sportsmedicine*, 12(1), 187–191. <https://doi.org/10.1080/00913847.1984.11701755>

- Leirdal, S., & Ettema, G. (2011). The relationship between cadence, pedalling technique and gross efficiency in cycling. *European Journal of Applied Physiology*, 111(12), 2885–2893. <https://doi.org/10.1007/s00421-011-1914-3>
- Leonardi, L. M., Cecioni, N., Dal Monte, A., & Komor, A. (1985). Push-off phase influence on bobsled result. A theoretical approach. *Journal of Biomechanics*, 18(7), 551.
- Lieber, R. L. (2002). *Skeletal muscle structure, function & plasticity: The physiological basis of rehabilitation* (2nd ed). Lippincott Williams & Wilkins.
- Lindberg, K., Solberg, P., Bjørnsen, T., Helland, C., Rønnestad, B., Thorsen Frank, M., Haugen, T., Østerås, S., Kristoffersen, M., Midttun, M., Sæland, F., & Paulsen, G. (2021). Force-velocity profiling in athletes: Reliability and agreement across methods. *PLoS ONE*, 16(2), e0245791. <https://doi.org/10.1371/journal.pone.0245791>
- Lockie, R. G., Murphy, A. J., Schultz, A. B., Jeffriess, M. D., & Callaghan, S. J. (2013). Influence of Sprint Acceleration Stance Kinetics on Velocity and Step Kinematics in Field Sport Athletes. *The Journal of Strength & Conditioning Research*, 27(9), 2494. <https://doi.org/10.1519/JSC.0b013e31827f5103>
- Lockie, R. G., Murphy, A. J., & Spinks, C. D. (2003). Effects of resisted sled towing on sprint kinematics in field-sport athletes. *Journal of Strength and Conditioning Research*, 17(4), 760–767.
- Lopes, A. D., & Alouche, S. R. (2016). Two-Man Bobsled Push Start Analysis. *Journal of Human Kinetics*, 50(1), 63–70. <https://doi.org/10.1515/hukin-2015-0143>
- Lorås, H., Ettema, G., & Leirdal, S. (2009). The Muscle Force Component in Pedaling Retains Constant Direction across Pedaling Rates. *Journal of Applied Biomechanics*, 25(1), 85–92. <https://doi.org/10.1123/jab.25.1.85>
- Markovic, G., & Jaric, S. (2007). Positive and Negative Loading and Mechanical Output in Maximum Vertical Jumping: *Medicine & Science in Sports & Exercise*, 39(10), 1757–1764. <https://doi.org/10.1249/mss.0b013e31811ece35>
- Martin, J. C., & Spirduso, W. W. (2001). Determinants of maximal cycling power: Crank length, pedaling rate and pedal speed. *European Journal of Applied Physiology*, 84(5), 413–418. <https://doi.org/10.1007/s004210100400>
- McKay, J. L., & Ting, L. H. (2008). Functional muscle synergies constrain force production during postural tasks. *Journal of Biomechanics*, 41(2), 299–306. <https://doi.org/10.1016/j.jbiomech.2007.09.012>
- McMaster, D. T., Gill, N. D., Cronin, J. B., & McGuigan, M. R. (2016). Force-Velocity-Power Assessment in Semiprofessional Rugby Union Players. *Journal of Strength and Conditioning Research*, 30(4), 1118–1126. <https://doi.org/10.1519/JSC.0b013e3182a1da46>

- Menard, M., Domalain, M., Decatoire, A., & Lacouture, P. (2016). Influence of saddle setback on pedalling technique effectiveness in cycling. *Sports Biomechanics*, 15(4), 462–472. <https://doi.org/10.1080/14763141.2016.1176244>
- Mero, A., Komi, P. V., & Gregor, R. J. (1992). Biomechanics of Sprint Running. *Sports Medicine*, 13(6), 376–392. <https://doi.org/10.2165/00007256-199213060-00002>
- Morin, J.-B., Edouard, P., & Samozino, P. (2011). Technical ability of force application as a determinant factor of sprint performance. *Medicine and Science in Sports and Exercise*, 43(9), 1680–1688. <https://doi.org/10.1249/MSS.0b013e318216ea37>
- Morlock, M., & Zatsiorsky, V. (1989). Factors Influencing Performance in Bobsledding: I: Influences of the Bobsled Crew and the Environment. *International Journal of Sport Biomechanics*, 5, 208–221. <https://doi.org/10.1123/ijsb.5.2.208>
- Mornieux, G., Stapelfeldt, B., Gollhofer, A., & Belli, A. (2008). Effects of Pedal Type and Pull-Up Action during Cycling. *International Journal of Sports Medicine*, 29(10), 817–822. <https://doi.org/10.1055/s-2008-1038374>
- Morris, C. G., Weber, J. A., & Netto, K. J. (2022). Relationship Between Mechanical Effectiveness in Sprint Running and Force-Velocity Characteristics of a Countermovement Jump in Australian Rules Football Athletes. *The Journal of Strength & Conditioning Research*, 36(3), e59. <https://doi.org/10.1519/JSC.00000000000003583>
- Nikolaidis, P. T., & Knechtle, B. (2020). Force–velocity characteristics and maximal anaerobic power in male recreational marathon runners. *Research in Sports Medicine*, 28(1), 99–110. <https://doi.org/10.1080/15438627.2019.1608993>
- Noble, M. (1992). Enhancement of mechanical performance of striated muscle by stretch during contraction. *Experimental Physiology*, 77(4), 539–552. <https://doi.org/10.1113/expphysiol.1992.sp003618>
- Onasch, F., Sawatsky, A., Stano, A., & Herzog, W. (2023). Development of the instrumentation of a 4-man bobsled. *Journal of Biomechanics*, 152, 111578. <https://doi.org/10.1016/j.jbiomech.2023.111578>
- Osbeck, J. S., Maiorca, S. N., & Rundell, K. W. (1996). Validity of Field Testing to Bobsled Start Performance. *The Journal of Strength & Conditioning Research*, 10(4), 239.
- Østerås, H., Helgerud, J., & Hoff, J. (2002). Maximal strength-training effects on force-velocity and force-power relationships explain increases in aerobic performance in humans. *European Journal of Applied Physiology*, 88(3), 255–263. <https://doi.org/10.1007/s00421-002-0717-y>
- Park, S., Lee, K., Kim, D., Yoo, J., Jung, J., & Park, K. (2017a). Biomechanical Analysis at the Start of Bobsleigh Run in Preparation for the 2018 Pyeongchang Winter Olympics. *Korean Journal of Sport Biomechanics*, 27(4), 239–245.
- Park, S., Lee, K., Kim, D., Yoo, J., Jung, J., & Park, K. (2017b). Effects of Factors on Response Variables Lap Time and Lower Extremity Range of Motion in Bobsleigh Start using Bobsleigh

- Shoes for the 2018 PyeongChang Winter Olympics. *Korean Journal of Sport Biomechanics*, 27(3), 219–227. <https://doi.org/10.5103/KJSB.2017.27.3.219>
- Park, S., Lee, K., Kim, D., Yoo, J., Jung, J., & Park, K. (2017b). Biomechanical Analysis at the Start of Bobsleigh Run in Preparation for the 2018 Pyeongchang Winter Olympics. *Korean Journal of Applied Biomechanics*, 27(4), 239–245. <https://doi.org/10.5103/KJSB.2017.27.4.239>
- Park, S., Lee, K., Kim, D., Yoo, J., Jung, J., Park, K., Park, S., & Kim, J. (2017a). Bobsleigh start interval times and three-dimensional motion analysis of the lower limb joints in preparation for the 2018 Pyeongchang Winter Olympics. *ISBS Proceedings Archive*, 35(1). <https://commons.nmu.edu/isbs/vol35/iss1/45>
- Park, S., Lee, K., Kim, D., Yoo, J., Jung, J., Park, K., Park, S., & Kim, J. (2017c). Effects of the toe spring angle of bobsleigh shoes on bobsleigh start time and forefoot bending angle in preparation for the 2018 Pyeongchang Winter Olympics. *Footwear Science*, 9(sup1), S104–S106. <https://doi.org/10.1080/19424280.2017.1314363>
- Park, S.-H., Lim, S.-T., & Kim, T.-W. (2018). Measurement of electromyography during bobsleigh push-start: A comparison with world top-ranked athletes. *Science & Sports*. <https://doi.org/10.1016/j.scispo.2018.06.004>
- Park, S.-H., Lim, S.-T., & Kim, T.-W. (2019). Measurement of electromyography during bobsleigh push-start: A comparison with world top-ranked athletes. *Science & Sports*, 34(1), e25–e30. <https://doi.org/10.1016/j.scispo.2018.06.004>
- Peeters, T., Van de Velde, M., Haring, E., Vleugels, J., Beyers, K., Garimella, R., Truijen, S., & Verwulgen, S. (2019). A Test Setting to Enhance Bobsled Performance at Start Phase. In R. H. M. Goossens (Ed.), *Advances in Social and Occupational Ergonomics* (pp. 294–302). Springer International Publishing. https://doi.org/10.1007/978-3-319-94000-7_30
- Perez, J., Guilhem, G., & Brocherie, F. (2022). Ice Hockey Forward Skating Force-Velocity Profiling Using Single Unloaded vs. Multiple Loaded Methods. *The Journal of Strength & Conditioning Research*, 36(11), 3229. <https://doi.org/10.1519/JSC.0000000000004078>
- Poirier, L. (2011). *Ice friction in the sport of bobsleigh* [University of Calgary]. <https://prism.ucalgary.ca/items/3bf0a396-a3b3-4b80-8ce4-0d6f47d14974>
- Poirier, L., Lozowski, E. P., Maw, S., Stefanyshyn, D. J., & Thompson, R. I. (2011). Experimental analysis of ice friction in the sport of bobsleigh. *Sports Engineering*, 14(2), 67–72. <https://doi.org/10.1007/s12283-011-0077-0>
- Poirier, L., Lozowski, E. P., & Thompson, R. I. (2011). Ice hardness in winter sports. *Cold Regions Science and Technology*, 67(3), 129–134. <https://doi.org/10.1016/j.coldregions.2011.02.005>
- Rabita, G., Dorel, S., Slawinski, J., Sàez-de-Villarreal, E., Couturier, A., Samozino, P., & Morin, J.-B. (2015). Sprint mechanics in world-class athletes: A new insight into the limits of human

- locomotion. *Scandinavian Journal of Medicine & Science in Sports*, 25(5), 583–594.
<https://doi.org/10.1111/sms.12389>
- Rahmani, A., Viale, F., Dalleau, G., & Lacour, J.-R. (2001). Force/velocity and power/velocity relationships in squat exercise. *European Journal of Applied Physiology*, 84(3), 227–232.
<https://doi.org/10.1007/PL00007956>
- Rankin, J. W., Kwarciak, A. M., Richter, W. M., & Neptune, R. R. (2010). The Influence of Altering Push Force Effectiveness on Upper Extremity Demand during Wheelchair Propulsion. *Journal of Biomechanics*, 43(14), 2771–2779. <https://doi.org/10.1016/j.jbiomech.2010.06.020>
- Rebula, J. R., Ojeda, L. V., Adamczyk, P. G., & Kuo, A. D. (2013). Measurement of foot placement and its variability with inertial sensors. *Gait & Posture*, 38(4), 974–980.
<https://doi.org/10.1016/j.gaitpost.2013.05.012>
- Riviere, J. R., Morin, J.-B., Bowen, M., Cross, M., Messonnier, L., & Samozino, P. (2023). Exploring the Low Force-High Velocity Domain of the Force-Velocity Relationship in Acyclic Lower-Limb Extensions. *Sports Medicine - Open*, 9. <https://doi.org/10.1186/s40798-023-00598-0>
- Roeleveld, K., Lute, E., Veeger, D., Woude, L. van der, & Gwinn, T. (1994). Power Output and Technique of Wheelchair Athletes. *Adapted Physical Activity Quarterly*, 11(1), 71–85.
<https://doi.org/10.1123/apaq.11.1.71>
- Rossato, M., Bini, R. R., Carpes, F. P., Diefenthaler, F., & Moro, A. R. P. (2008). Cadence and Workload Effects on Pedaling Technique of Well-Trained Cyclists. *International Journal of Sports Medicine*, 29(9), 746–752. <https://doi.org/10.1055/s-2008-1038375>
- Rudsits, B. L., Hopkins, W. G., Hautier, C. A., & Rouffet, D. M. (2018). Force-velocity test on a stationary cycle ergometer: Methodological recommendations. *Journal of Applied Physiology*, 124(4), 831–839. <https://doi.org/10.1152/jappphysiol.00719.2017>
- Samozino, P., Morin, J.-B., Hintzy, F., & Belli, A. (2010). Jumping ability: A theoretical integrative approach. *Journal of Theoretical Biology*, 264(1), 11–18.
<https://doi.org/10.1016/j.jtbi.2010.01.021>
- Samozino, P., Rabita, G., Dorel, S., Slawinski, J., Peyrot, N., Saez de Villarreal, E., & Morin, J.-B. (2016). A simple method for measuring power, force, velocity properties, and mechanical effectiveness in sprint running. *Scandinavian Journal of Medicine & Science in Sports*, 26(6), 648–658. <https://doi.org/10.1111/sms.12490>
- Samozino, P., Rejc, E., Di Prampero, P. E., Belli, A., & Morin, J.-B. (2012). Optimal force-velocity profile in ballistic movements--altius: Citius or fortius? *Medicine and Science in Sports and Exercise*, 44(2), 313–322. <https://doi.org/10.1249/mss.0b013e31822d757a>
- Samozino, P., Rejc, E., Prampero, P., Belli, A., & Morin, J.-B. (2011). Optimal Force–Velocity Profile in Ballistic Movements—Altius. *Medicine and Science in Sports and Exercise*, 44, 313–322. <https://doi.org/10.1249/MSS.0b013e31822d757a>

- Sanderson, D. J. (1991). The influence of cadence and power output on the biomechanics of force application during steady-rate cycling in competitive and recreational cyclists. *Journal of Sports Sciences*, 9(2), 191–203. <https://doi.org/10.1080/02640419108729880>
- Schache, A. G., Brown, N. A. T., & Pandy, M. G. (2015). Modulation of work and power by the human lower-limb joints with increasing steady-state locomotion speed. *Journal of Experimental Biology*, 218(15), 2472–2481. <https://doi.org/10.1242/jeb.119156>
- Shapiro, S. S., & Wilk, M. B. (1965). An Analysis of Variance Test for Normality (Complete Samples). *Biometrika*, 52(3/4), 591–611. <https://doi.org/10.2307/2333709>
- Smith, S. L., Kivi, D., Camus, H., Pickels, R., & Sands, W. (2006). *Kinematic analysis of men bobsled push starts*. 297–300.
- Smyth, A., & Wu, M. (2007). Multi-rate Kalman filtering for the data fusion of displacement and acceleration response measurements in dynamic system monitoring. *Mechanical Systems and Signal Processing*, 21(2), 706–723. <https://doi.org/10.1016/j.ymssp.2006.03.005>
- Spearman, C. (1904). The Proof and Measurement of Association between Two Things. *The American Journal of Psychology*, 15(1), 72–101. <https://doi.org/10.2307/1412159>
- Stavridis, I., Smilios, I., Tsopanidou, A., Economou, T., & Paradisis, G. (2019). Differences in the Force Velocity Mechanical Profile and the Effectiveness of Force Application During Sprint-Acceleration Between Sprinters and Hurdles. *Frontiers in Sports and Active Living*, 1, 26. <https://doi.org/10.3389/fspor.2019.00026>
- Stenroth, L., Vartiainen, P., & Karjalainen, P. A. (2020). Force-velocity profiling in ice hockey skating: Reliability and validity of a simple, low-cost field method. *Sports Biomechanics*, 1–16. <https://doi.org/10.1080/14763141.2020.1770321>
- Stone, M. H., Hornsby, W. G., Suarez, D. G., Duca, M., & Pierce, K. C. (2022). Training Specificity for Athletes: Emphasis on Strength-Power Training: A Narrative Review. *Journal of Functional Morphology and Kinesiology*, 7(4), Article 4. <https://doi.org/10.3390/jfmk7040102>
- Team USA. (2022). *Combine Test Protocol*. Team USA. <https://www.teamusa.org/443/USA-Bobsled-Skeleton/Recruitment/Combine-Test-Protocol-and-Scoring-Table>
- Tomasevicz, C. L., Ransone, J. W., & Bach, C. W. (2020). Predicting Bobsled Pushing Ability From Various Combine Testing Events. *The Journal of Strength & Conditioning Research*, 34(9), 2618–2626. <https://doi.org/10.1519/JSC.0000000000002489>
- Toussaint, H. M., & Beek, P. J. (1992). Biomechanics of Competitive Front Crawl Swimming. *Sports Medicine*, 13(1), 8–24. <https://doi.org/10.2165/00007256-199213010-00002>
- Valero-Cuevas, F. J., Zajac, F. E., & Bugar, C. G. (1998). Large index-fingertip forces are produced by subject-independent patterns of muscle excitation. *Journal of Biomechanics*, 31(8), 693–703. [https://doi.org/10.1016/S0021-9290\(98\)00082-7](https://doi.org/10.1016/S0021-9290(98)00082-7)

van Ingen Schenau, G. J., Boots, P. J. M., de Groot, G., Snackers, R. J., & van Woensel, W. W. L. M. (1992). The constrained control of force and position in multi-joint movements. *Neuroscience*, 46(1), 197–207. [https://doi.org/10.1016/0306-4522\(92\)90019-X](https://doi.org/10.1016/0306-4522(92)90019-X)

van Ingen Schenau, G. J., Dorssers, W. M., Welter, T. G., Beelen, A., de Groot, G., & Jacobs, R. (1995). The control of mono-articular muscles in multijoint leg extensions in man. *The Journal of Physiology*, 484(Pt 1), 247–254.

Vandewalle, H., Peres, G., Heller, J., Panel, J., & Monod, H. (1987). Force-velocity relationship and maximal power on a cycle ergometer—Correlation with the height of a vertical jump. *European Journal of Applied Physiology and Occupational Physiology*, 56, 650–656. <https://doi.org/10.1007/BF00424805>

Vanlandewijck, Y., Theisen, D., & Daly, D. (2001). Wheelchair propulsion biomechanics: Implications for wheelchair sports. *Sports Medicine (Auckland, N.Z.)*, 31, 339–367.

Veeger, H. E. J., & van der Woude, L. H. V. (1994). Force generation in manual wheelchair propulsion. *XIII Southern Biomedical Engineering Conference*, 779–782.

Veeger, H. E. J., Van Der Woude, L. H. V., & Rozendal, R. H. (1992). Effect of handrim velocity on mechanical efficiency in wheelchair propulsion. *Medicine & Science in Sports & Exercise*, 24(1), 100.

Wickiewicz, T. L., Roy, R. R., Powell, P. L., & Edgerton, V. R. (1983). Muscle Architecture of the Human Lower Limb. *Clinical Orthopaedics and Related Research*®, 179, 275.

Wiemann, K., & Tidow, G. (1995). Relative activity of hip and knee extensors in sprinting—implications for training. *New Studies in Athletics*, 10, 29–49.

Winters, T. M., Takahashi, M., Lieber, R. L., & Ward, S. R. (2011). Whole muscle length-tension relationships are accurately modeled as scaled sarcomeres in rabbit hindlimb muscles. *Journal of Biomechanics*, 44(1), 109–115. <https://doi.org/10.1016/j.jbiomech.2010.08.033>

Wulf, G., Dufek, J. S., Lozano, L., & Pettigrew, C. (2010). Increased jump height and reduced EMG activity with an external focus. *Human Movement Science*, 29(3), 440–448. <https://doi.org/10.1016/j.humov.2009.11.008>

Zameziati, K., Mornieux, G., Rouffet, D., & Belli, A. (2006). Relationship between the increase of effectiveness indexes and the increase of muscular efficiency with cycling power. *European Journal of Applied Physiology*, 96(3), 274–281. <https://doi.org/10.1007/s00421-005-0077-5>

Zimmerman, D. W., & Zumbo, B. D. (1993). Relative Power of the Wilcoxon Test, the Friedman Test, and Repeated-Measures ANOVA on Ranks. *The Journal of Experimental Education*, 62(1), 75–86. <https://doi.org/10.1080/00220973.1993.9943832>

Appendix

1. Detailed calculation of force based on two separate strain sensors p. 165
2. Functional push force-velocity relationships: hyperbolic fits and comparison with linear approximations p. 166
3. Copyright permissions with signatures blacked out
 - a) Permission granted by Andrew Sawatsky p. 169
 - b) Permission granted by Andrzej Stano p. 170
 - c) Permission granted by Walter Herzog p. 171
4. Permission to use published manuscripts in thesis
 - Elsevier Publishing – Journal of Biomechanics p. 172

1. Detailed calculation of force based on two separate strain sensors

The voltage output from the sensors, associated with deformation of the sensors due to a force applied to the push bar, is used to calculate the moments acting about each sensor. The resulting moments can then be used to calculate the applied force, based on

$$M = F \cdot d \quad [A.1]$$

with M = the moment about the location of a strain gauge, F = push force, and d = the associated moment arm. Using one sensor that way would mean that, to calculate the push force, the point of force application would still need to be known. However, using two sensors placed at a known distance from each other (e.g., A-I & A-II, **Figure 3-6**), and their output differential, allows the calculation of push force without any knowledge of the exact point of force application:

$$M_1 = F \cdot d_1 \text{ \& } M_2 = F \cdot d_2 \quad [A.2 \text{ \& } A.3]$$

Assuming sensor 1 is further away from the point of force application than sensor 2, we can modify equation 2 as follows:

$$M_1 = F \cdot (d_2 + x) \quad [A.4]$$

with x = the known distance between the two sensors. F is the same in both equations, which means that

$$\frac{M_1}{(d_2 + x)} = \frac{M_2}{d_2} \quad [A.5]$$

Solving for d_2 and then substituting in $F = \frac{M_2}{d_2}$ (for example), shows that push force can be calculated as

$$F = \frac{(M_1 - M_2)}{x} \quad [\text{A.6}]$$

2. Functional push force-velocity relationships: hyperbolic fits and comparison with linear approximations

Below is the code that was used to fit functional sled push force-velocity profiles (Chapter 4) with hyperbolic functions:

```
%% PART A
% select data (force and velocity) for given test
    if n < length(testdays)
        P          = data4fit(2:end-1,5); % horizontal push
                                   force
        V          = data4fit(2:end-1,7); % sled velocity
    elseif n == length(testdays)
        P          = data4fit(3:end,5); % horizontal push
                                   force
        V          = data4fit(3:end,7); % sled velocity
    end

% sort V from lowest to highest - and then re-order P
accordingly
    [V_prime,I_V]  = sort(V);
    P_prime        = P(I_V);
    V_tmp          = V;
    P_tmp          = P;
    V              = V_prime;
    P              = P_prime;
```

% run this first, then use a, b, P0 as start points for fit below. This part of the code was found on stack exchange, shared by Alan Stevens:

<https://www.mathworks.com/matlabcentral/answers/626148-inverse-hyperbolic-fit-to-data>

```
M = [V P -ones(size(V))];
C = -P.*V;
X = M\C;
a = X(1);
b = X(2);
P0 = X(3)/b;

% PART B
% use start conditions (coefficients from PART A) for the fit
function below:
hff = fittype('c-
X*a)/(X+b)', 'ind', {'X'}, 'dep', {'Y'});
options = fitoptions(hff);
options.Lower = [-Inf 0 0];
options.StartPoint = [a b P0];

[hf,gofhf,outhf] = fit(V,P,hff,options);
```

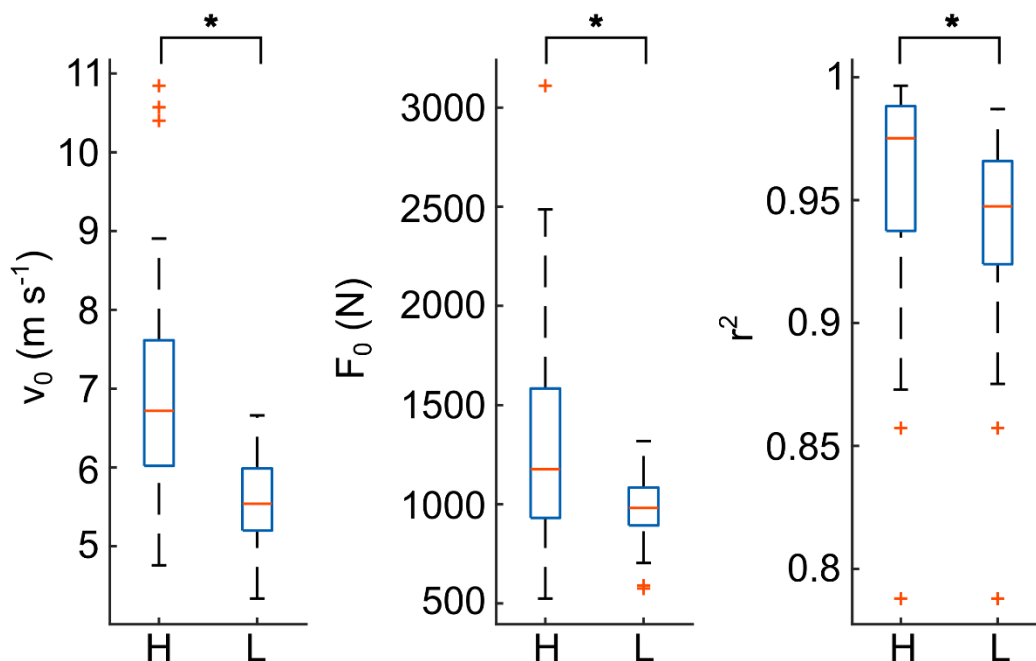


Figure A- 1: Box-and-whiskers plots representing the extrapolated axis intercepts V_0 and F_0 as derived from hyperbolic (H) and linear (L) fits of the functional push force-velocity relationships in Chapter 4, as well as the respective coefficients of determination (r^2) as measures of goodness of fit. Wilcoxon's paired group comparisons were run resulting in significant differences ($p < .01$) for all three variables.

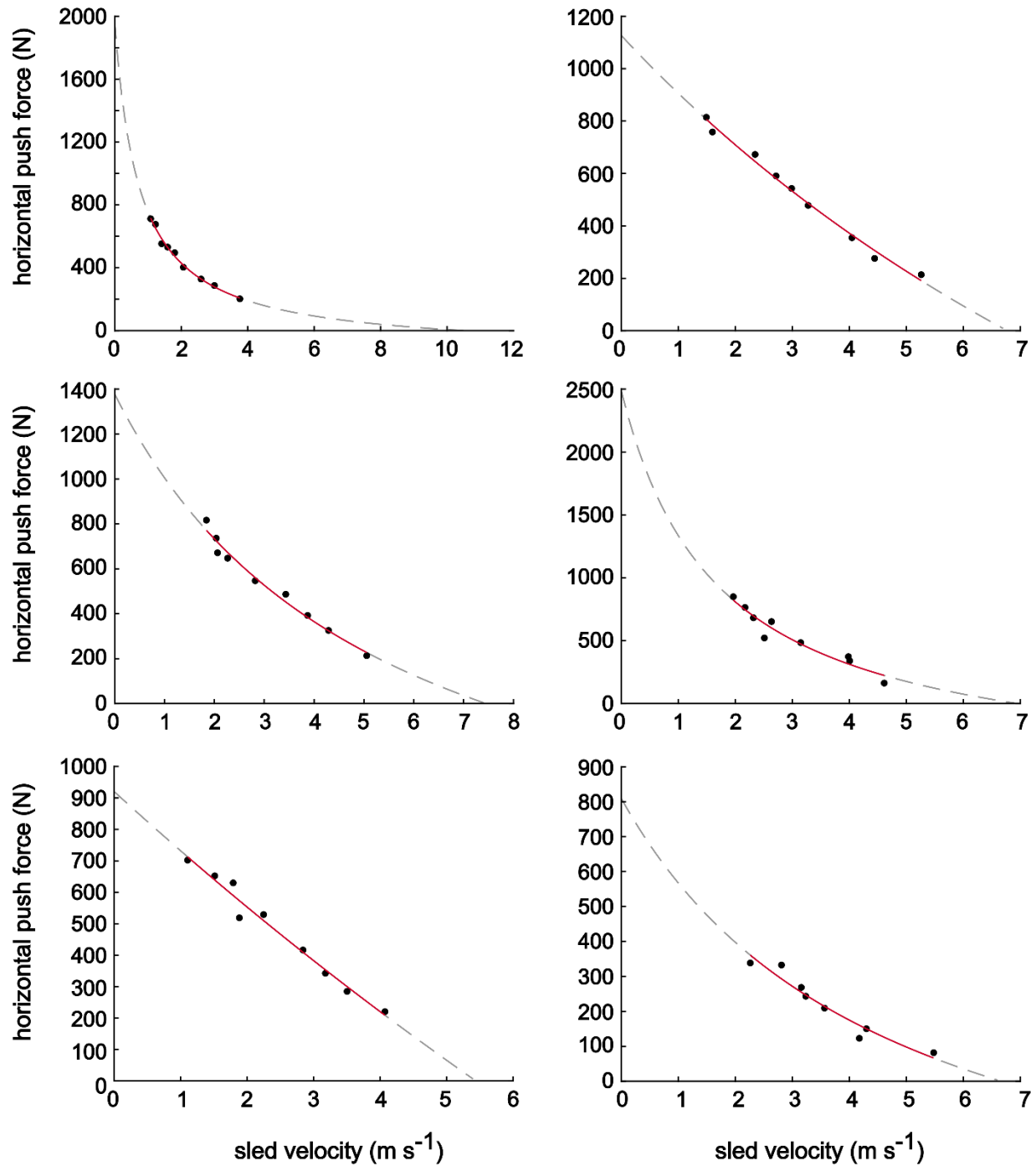


Figure A- 2: Examples of fitting the functional push force-velocity profiles using Matlab's fit function, with a hyperbola based on Hill's equation (Hill, 1938) as the target function, as described above. The black dots are the individual data points for a participant during their test session. The fit of the data points is represented by the red solid lines, and the dashed grey lines are the extrapolated graphs of the fitted functions.

3. Copyright permissions with signatures blacked out

Letter of permission for Franziska Onasch

To whom it may concern,

This is to confirm that I give permission to Franziska Onasch to include the manuscripts below, for which I am a co-author, in her thesis titled Pushing for Gold. On Force Application in Bobsleigh and Cycling.

Onasch, F., Sawatsky, A., Stano, A. & Herzog W. (2023). Development of the Instrumentation of a 4-man Bobsled. *Journal of Biomechanics* 152, 111578. DOI: 10.1016/j.jbiomech.2023.11578

Onasch F., Sawatsky, A. & Herzog, W. Functional Sled Push Force-Velocity Profiling for Bobsled Athletes; Like Taking Snow to Canada or a Pit Stop on the Way to Taking Home Medals? *In Preparation for Submission*

Signature: _____

Name: Andrew Sawatsky

Letter of permission for Franziska Onasch

To whom it may concern,

This is to confirm that I give permission to Franziska Onasch to include the manuscript below, for which I am a co-author, in her thesis titled Pushing for Gold. On Force Application in Bobsleigh and Cycling.

Onasch, F., Sawatsky, A., Stano, A. & Herzog W. (2023). Development of the Instrumentation of a 4-man Bobsled. *Journal of Biomechanics* 152, 111578. DOI: 10.1016/j.jbiomech.2023.11578

Signature: _____

Name: Andrzej Stano

Letter of permission for Franziska Onasch

To whom it may concern,

This is to confirm that I give permission to Franziska Onasch to include the manuscript(s) below, for which I am a co-author, in her thesis titled Pushing for Gold. On Force Application in Bobsleigh and Cycling.

Onasch, F., Sawatsky, A., Stano, A. & Herzog W. (2023). Development of the Instrumentation of a 4-man Bobsled. *Journal of Biomechanics* 152, 111578. DOI: 10.1016/j.jbiomech.2023.11578

Onasch F., Sawatsky, A. & Herzog, W. Functional Sled Push Force-Velocity Profiling for Bobsled Athletes; Like Taking Snow to Canada or a Pit Stop on the Way to Taking Home Medals? *In Preparation for Submission*

Onasch, F. & Herzog, W. (2023). Active Control of Static Pedal Force Direction Results in Decreased Maximum Isometric Force Output. *In Revision with the Journal of Biomechanics*.

Signature: _____

A black rectangular box redacting the signature of Dr. Walter Herzog.

Name: Dr. Walter Herzog

4. Permission to use published manuscripts in thesis

<https://www.elsevier.com/about/policies/copyright>

2023-07024 11:25 am

Copyright

[Overview](#) [Author rights](#) [Institution rights](#) [Government rights](#) [Find out more](#)

Overview

In order for Elsevier to publish and disseminate research articles, we need certain publishing rights from authors, which are determined by a publishing agreement between the author and Elsevier.

For articles published open access, the authors license exclusive rights in their article to Elsevier where a CC BY-NC-ND end user license is selected, and license non-exclusive rights where a CC BY end user license is selected.

For articles published under the subscription model, the authors typically transfer copyright to Elsevier. In some circumstances, authors may instead grant us (or the learned society for whom we publish) an exclusive license to publish and disseminate their work.

Regardless of whether they choose to publish open access or subscription with Elsevier, authors have many of the same rights under our publishing agreement, which support their need to share, disseminate and maximize the impact of their research.

For open access articles, authors will also have additional rights, depending on the Creative Commons end user license that they select. This Creative Commons license sets out the rights that readers (as well as the authors) have to re-use and share the article: please see [here](#) for more information on how articles can be re-used and shared under these licenses.

This page aims to summarise authors' rights when publishing with Elsevier; these are explained in more detail in the publishing agreement between the author and Elsevier.

Irrespective of how an article is published, Elsevier is committed to protect and defend authors' works and their reputation. We take allegations of infringement, plagiarism, ethical disputes, and fraud very seriously.

Author rights

The below table explains the rights that authors have when they publish with Elsevier, for authors who choose to publish either open access or subscription. These apply to the corresponding author and all co-authors.

Author rights in Elsevier's proprietary journals	Published open access	Published subscription
Retain patent and trademark rights	✓	✓
Retain the rights to use their research data freely without any restriction	✓	✓
Receive proper attribution and credit for their published work	✓	✓
Re-use their own material in new works without permission or payment (with full acknowledgement of the original article): 1. Extend an article to book length 2. Include an article in a subsequent compilation of their own work 3. Re-use portions, excerpts, and their own figures or tables in other works.	✓	✓
Use and share their works for scholarly purposes (with full acknowledgement of the original article): 1. In their own classroom teaching. Electronic and physical distribution of copies is permitted 2. If an author is speaking at a conference, they can present the article and distribute copies to the attendees 3. Distribute the article, including by email, to their students and to research colleagues who they know for their personal use 4. Share and publicize the article via Share Links, which offers 50 days' free access for anyone, without signup or registration 5. Include in a thesis or dissertation (provided this is not published commercially) 6. Share copies of their article privately as part of an invitation-only work group on commercial sites with which the publisher has a hosting agreement	✓	✓
Publicly share the preprint on any website or repository at any time.	✓	✓